Atomistic Etching Mechanism and Surface Structure of Silicon in Aqueous Solutions

by

Hirokazu Fukidome

Department of Chemistry
Graduate School of Engineering Science
Osaka University

2000

Contents

Chapter 1

General Introduction

1.1 Background of This Thesis

Significance of the control of surface and interface structure of crystalline silicon

The precise control of surface and interface structures is important for many industrial processes of semiconductors, for instance, the production of integrated circuits.[1] This is because the mechanical, chemical, even electronic properties of nanoscale structures are strongly influenced by their surface and interface morphologies. For example, atomic-scale roughness of the Si/SiO_2 interface in a metal-oxide-semiconductor field-effect transistor gate affects the mobility of electrons in the channel by a factor of 4.[2] A recent XPS study showed that the interface state density for the atomically smooth interface is lower than that for the rough interface.[3] Hence, the method to prepare atomically smooth surface or interface is a central topic in the fields of physics and chemistry of semiconductor.

Characteristics of hydrogen-terminated Si surface

Hydrogen-termination of Si surface is a promising method to realize its ideal surface. There are two ways to hydrogen-terminate Si surface; wet-chemical treatments, and exposure of clean surface of silicon to hydrogen under ultra high vacuum (UHV) condition.[4] Extensive researches about the hydrogen-termination by wet etching and under UHV condition have been done, due to the interesting characteristics as listed below[4] ;

1) Hydrogen-termination of Si surface reduces the surface state density of Si surface.

2) Hydrogen-termination of Si surface can passivate Si surface from oxidation.

3) Hydrogen-termination of Si surface can produce a variety of reconstructed surfaces.

4) Hydrogen-termination of Si surface affects the metal deposition and the epitaxy on Si surface.

The hydrogen-termination by wet etching has some points superior to the UHV process. First, the hydrogen-termination of Si surface by wet etching is a low-cost and easy method to prepare hydrogen-terminated Si surfaces.[1] Second,the hydrogen-termination of Si surface by wet etching can suppress the oxidation of surface more efficiently than that formed under UHV conditions.[4] Third, for Si(111), the unreconstructed, ideally hydrogen-terminated surface (hereafter, H/Si(111) (1x1) surface) can be easily prepared by wet etching,[1] while it can hardly be obtained under UHV conditions.[4] These are the reasons many researchers have studied wet etching of Si surface.

Early works of Si surface treated with HF solutions

Wet etching of Si surface in HF solutions has long been used in semiconductor fabrication for more than 30 years.[1] It has been also one of central topics in semiconductor electrochemistry.[5] However, the surface structure of Si surface in HF solutions was unclear before 1986.[1] Until then, it had been widely believed that silicon surface was fluorine-terminated by HF treatments, although some researchers insisted that silicon surface was covered with hydrogen. The year 1986 was the turning point in the H- vs. F- termination debate. This debate was clearly settled by the works by Yablonovitch et al.,[6] Grunthaner et al.,[7,8] and Grunder et al.[9] Their results by the use of XPS, FTIR and EELS demonstrated that Si surface is mostly covered with H, while the concentration of F and/or O is below 0.1 %.

Atomically flattened Si(111) surface by wet etching

Following the discovery of H-termination of Si surface, it was revealed that the morphology of Si surface could be controlled on an atomic scale by the treatments with NH_4F solutions,[10] boiling water,[11] and alkaline solutions.[12]

Flattening of Si(111) in 40% NH_4F solution

H/Si(111) (1x1) surface was first obtained by 40% NH_4F.[1] Chabal and coworkers discovered by the use of FTIR that Si(111) can be atomically flattened in 40% NH_4F solution, while Si(100) cannot be atomically flattened by the treatment with either dilute HF or high pH HF solution (NH_4F solution).[13] Jakob et al. investigated the pH dependence of the morphology of Si(111) surface, and found that the flatness of Si(111) surface is improved in the solution of pH > 6 from the results of FTIR and HREELS measurements.[14,15] Their results were supported by AFM/STM observations.[16-18]

Flattening of Si(111) in boiling water

Watanabe et al. demonstrated for the first time that Si(111) can be atomically flattened in boiling water.[11] They revealed that the dissolved oxygen concentration (DOC) is a critical parameter for the flattening of Si(111) in water.[19] It was clarified that the flattening of Si can proceed when DOC is below 5 ppb. Si(111) surface treated in oxygen-free water was also observed by STM and AFM.[20,21] These observations showed that Si(111) surface was atomically flattened, but etch pits and meandering steps were formed on the surface.

Flattening of Si(111) in alkaline solutions

Allongue et al. investigated the etching process of Si(111) in NaOH solution by the use of in situ STM.[12), 22)] They revealed that, contrary to in NH_4F solution and water, at open circuit potential Si(111) cannot be atomically flattened, while Si(111) can be atomically flattened (ideally hydrogen-terminated) under cathodic polarization.[12)] They also revealed that etching rate and the selectivity of the etching critically depend on the applied bias.[12)] In addition, it was observed that in alkaline solutions Si-OH bonds are present on terraces and the density of the Si-OH bonds is dependent on the applied bias.[23)] They analyzed their results in detail by Monte Carlo simulation,[24)] and clarified that the etching rate of terrace largely depends on the applied potential, while the etching rates of the steps and kinks do not depend on the applied potential.

Step strutures formed on the atomically flattened Si(111) surface

Attention was also paid to the structures of atomic steps formed on atomically flattened Si(111) surfaces. There are two kinds of steps formed on H/Si(111) (1x1), depending on the orientation of the miscut of the wafer, monohydride steps and dihydride steps as shown in Fig. 1. On the wafers misoriented in the direction of $<11\bar{2}>$, monohydride steps should appear when the surface is ideally hydrogen-terminated.[14)] On the wafers misoriented in the direction of $<\bar{1}\bar{1}2>$, straight dihydride steps are expected to be formed when the surface is ideally hydrogen-terminated.[14)]

The steps structures formed on the atomically flattened surface treated with 40% NH_4F were investigated by the use of FTIR,[14), 15), 25), 26)] STM,[16), 17)] Raman spectroscopy,[27), 28)] and theoretical calculation.[29)]

On the wafers misoriented in the direction of $<11\bar{2}>$, it was shown that straight monohydride steps appeared on this stepped wafers, as expected.[17), 26)] This is because the monohydride steps is chemically stable.

On the contrary, on the wafers misoriented in the direction of $<\bar{1}\bar{1}2>$, it was shown that striaght dihydride steps cannot be always formed on the stepped surface. This is because dihydride is chemically unstable . Pietsch et al. showed by the use of STM that zigzag monohydride steps appeared if miscut angle of the wafer is below 2 degrees, while straight dihydride steps appeared if miscut angle of the wafer is more than 2 degrees.[17)] Jakob et al. precisely measured the FTIR spectra of this stepped surface and assigned the features based on theoretical calculations,[29)] and it

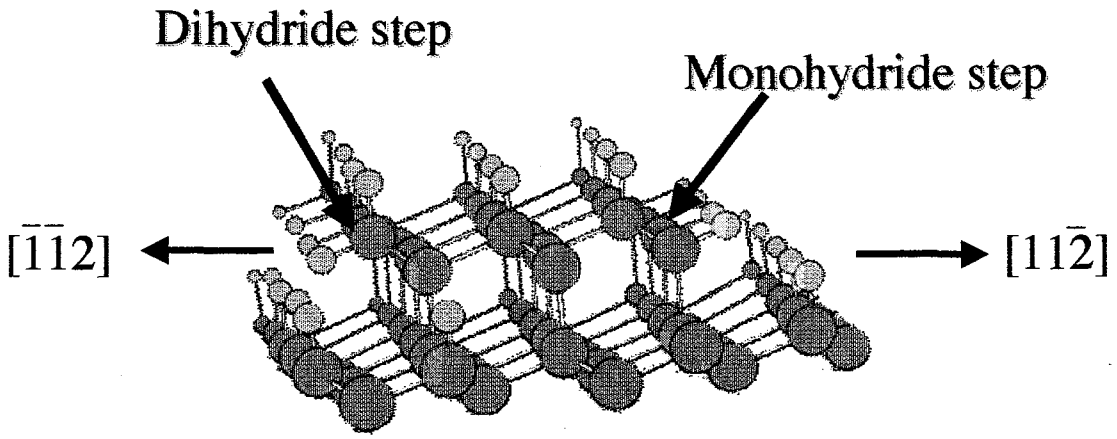

Fig. 1 The relation between the two kinds of the ideal termination of the steps and misorientation angles.

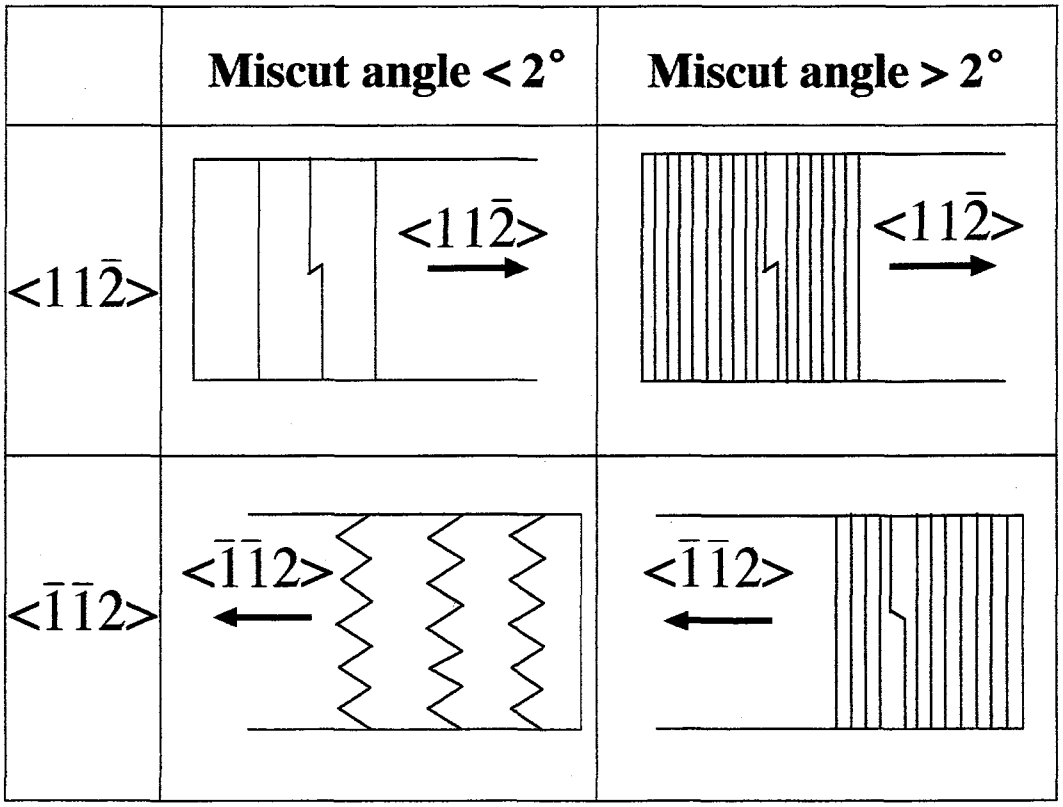

Fig. 2 Change of the step morphology formed in Si(111) surface treated with 40% NH_4F, in relation to the directions and angles of miscut of the wafers.

was confirmed that straight dihydride steps can be formed when the wafer is strongly misoriented in the direction of <$\bar{1}\bar{1}2$> (9 degrees). The results about step morphologies are shown in Fig. 2. In addition, it was clarified that the vertical dihydride formed on the straight steps are relaxed and rotated from bulk-terminated position due to van der Waals repulsion between hydrogen atoms of vertical dihydride and terrace monohydride.[29] The configuration of vertical dihydrides was absolutely determined by angle-resolved Raman spectroscopy.[27), 28)] However, the cause of the change of step structures by the miscut angle of the wafer has not be fully understood yet.

Electrochemistry of Si in HF solutions

In the field of electrochemistry, the properties of Si in HF solutions have attracted much attention.[5)] Recent progress in surface science of Si stated above and the discovery of luminescence of porous silicon stimulated many researchers in the field of electrochemistry of Si.

Before the findings of the hydrogen-termination of Si surface after HF solutions, Matsumura et al. discovered the unique phenomenon that an anodic current starts to flow as the oxide layer is removed when n-Si electrodes with the oxide layer are immersed in a hydrofluoric acid solution.[30)] After passing the maximum value, the current decays and becomes very low at stationary state. At this stage, the bare silicon surface seems to be exposed to the etching solution. The anodic currents observed before reaching the steady state, therefore, are attributed to the chemical reactions of the Si/SiO_2 interfacial species with the HF solution.[30)] Lewerenz and coworkers investigated in detail the relationship between this transient current and surface condition of Si in the light of hydrogen-termination of Si surface. They clarified by the use of FTIR that this transient current is closely related to the hydrogen-termination of Si surface.[31)]

In HF solution, n-Si electrodes at the stationary state show the rectifying properties. Such I-V characteristics are commonly observed for n-type semiconductor electrode in electrolyte solutions.[5)] However, the anodic current density is much larger than expected from the bandgap of silicon.[32), 33)] Gerischer et al.[32), 33)] insisted that this anodic current density can be attributed to the injection of electrons into the conduction band of the substrate in connection with the attack of F^- ions on a Si-Si bond forming new Si-F bonds.[32), 33)] They also showed that the anodic current is very sensitive to pH, concentration, and temperature of the solution.[32-34)]

Another interesting aspect of Si in HF, which was found by Matsumura et al., is that the quan-

tum efficiency of photocurrents of n-Si in HF solution changes with the intensity of light.[35] Under weak illumination the quantum efficiency of photocurrents reached 400%, while under strong illumination it was 200%. This phenomenon must be closely related to the formation of porous silicon. Hence, many papers about this phenomenon have been published.[31]

Etching mechanisms of Si in solutions

One of the main purposes of this thesis is to elucidate the mechanism of Si etching in solutions. The representative reaction mechanisms so far reported in the literatures are summarized below.

1) Hydrogen-termination of Si in HF solutions

The mechanism for the hydrogen-termination of Si surface in HF solutions after removing the oxide on the surface is first proposed by Trucks. et al (Fig. 3).[36] They showed by ab-initio cluster calculation and first principle studies that fliorine-terminated surface is kinetically unstable, while it is thermodynamically stable. The fluorine atom polarizes a Si-Si back bond. As a result, HF molecule further attacks Si-Si backbond and Si surface is hydrogen-terminated.

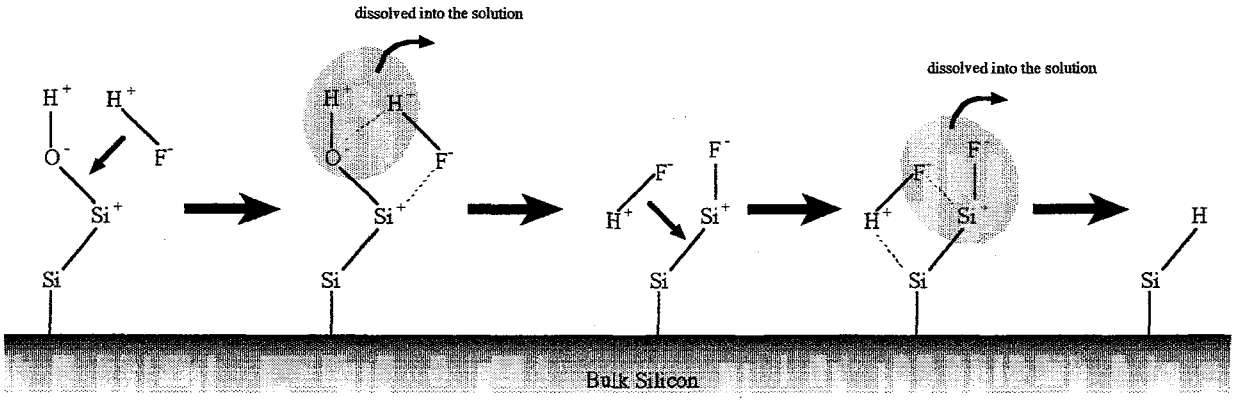

Fig. 3 The hydrogen-termination mechanism of Si in HF solution by Trucks et al.

2) Etching of Si in NH_4F solutions

Most of researchers concluded that OH^- ion is a major etching species for the etching and flattening of Si(111) based on the observations of Si(111) surface by FTIR and STM.[1] On the other hand, Allongue et al.[32] showed that fluorine species in NH_4F solution play a role in the etching process of Si in NH_4F solutions. However, in their mechanisms for the etching of Si, the direct attack of fluorine-related species such as F^-, HF_2^-, HF to the surface are not involved in the rate determining steps.

Representative mechanisms are as follows :

(a) Etching mechanism for Si(111) in NH_4F solutions by Jakob. et al (Fig. 4).[14]

They proposed this mechanism based on their FTIR observation of Si(111) surface that with increasing pH the flattening process of Si(111) proceeds.[14] The rate determining steps in their mechanism is the attack of OH^- ion to Si-H bonds on the surface.

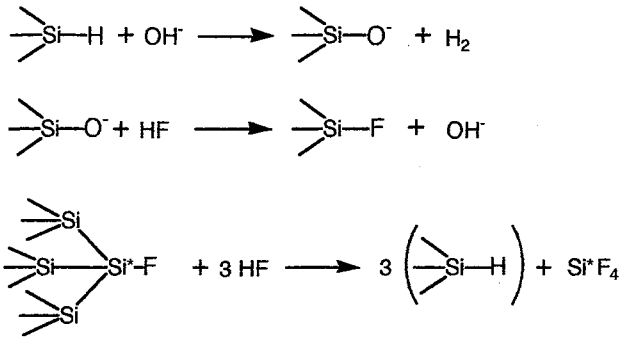

Fig. 4 The etching mechanism for Si(111) in NH_4F solutions by Jakob. et al.

(b) Etching mechanism for Si(111) in NH_4F solutions by Flidr. et al. (Fig. 5).[37]

Flidr. et al. proposed a model,[37] which is similar to the mechanism proposed by Jakob et al.[14] They also insisted that the rate determining steps is the attack of OH^- to Si-H bond.

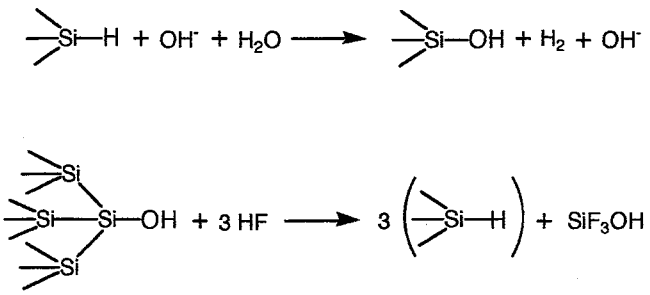

Fig. 5 The etching mechanism for Si(111) in NH_4F solutions by Flidr. et al.

(c) Etching and flattening mechanism for Si(111) by Allongue et al. (Fig. 6).[34]

In the mechanism proposed by Allongue et al., the hydrolysis of SiH to SiOH is the rate determining step. However, contrary to the above two proposals, F^- ion is considered to participate in Si etching. They propsoed that Si-OH is rapidly converted into Si-F, and this Si-F enhances the etching rate of Si.

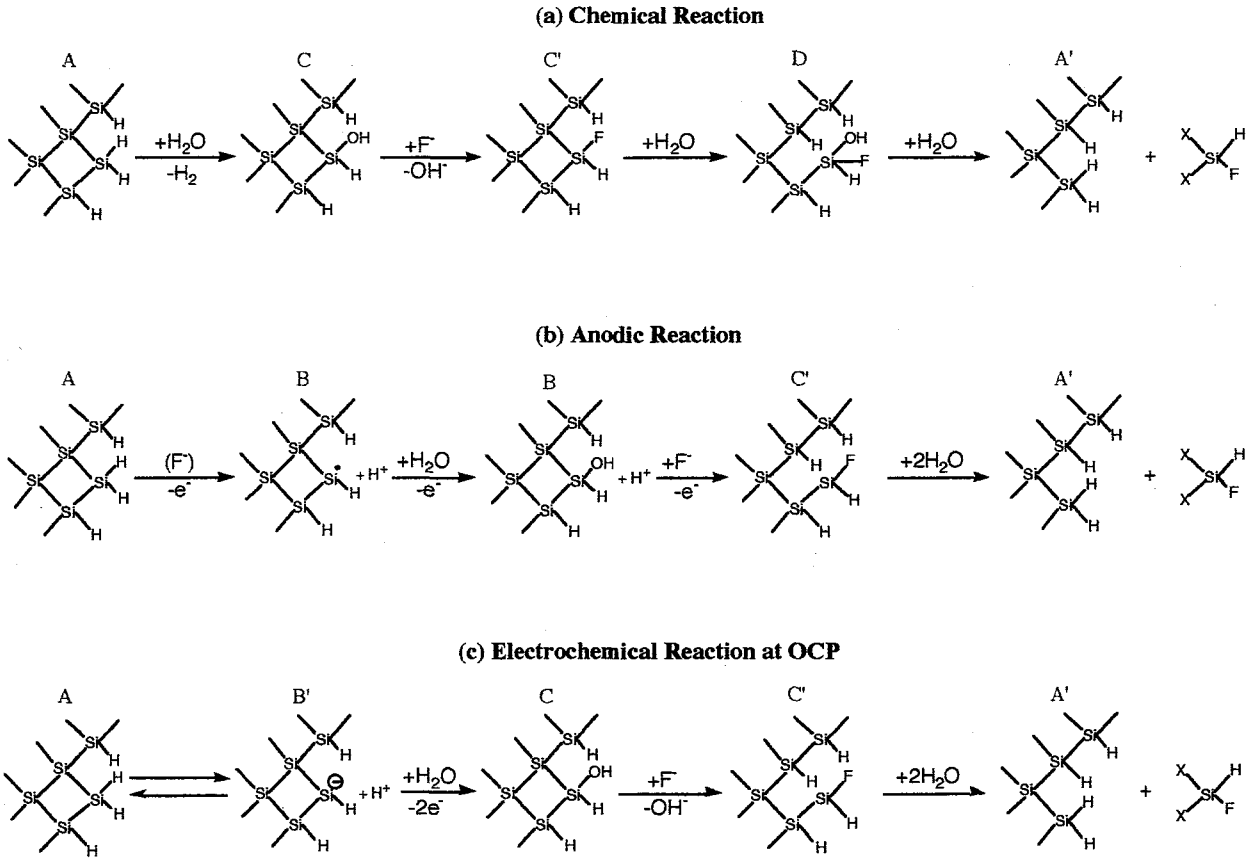

Fig. 6 The etching mechanism for Si(111) in NH_4F solutions by Allongue et al.

3) Etching of Si in water

For the etching of Si in water, there is a debate for the etching mechanism about the main etching species, OH^- or H_2O. The debate has not been settled yet. Two representative mechanisms are described below;

(a) Etching mechanism by Watanabe et al. (Fig. 7).[19]

In the mechanism proposed by Watanabe et al., the main reactant is H_2O. The initial attack of H_2O molecule is a hydrolysis of Si-H. The hydrolysis can be a rate determining steps.

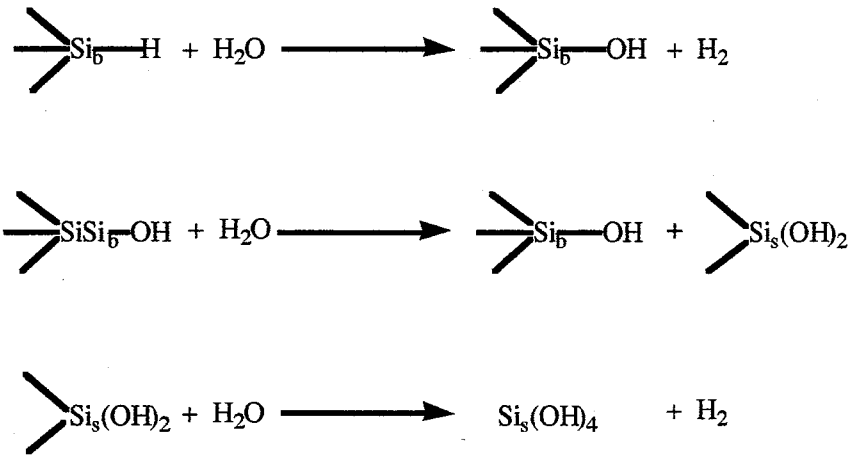

Fig. 7 The etching mechanism of Si in oxygen-free water by Watanabe et al.

(b) Etching mechanism by the research group at Bell Laboratories (Fig. 8).[38]

The etching of hydrogen-terminated Si surface in water is considered to be initiated by the insertion of an oxygen atom into Si-Si back bond, which is followed by the attack of OH^- ion.

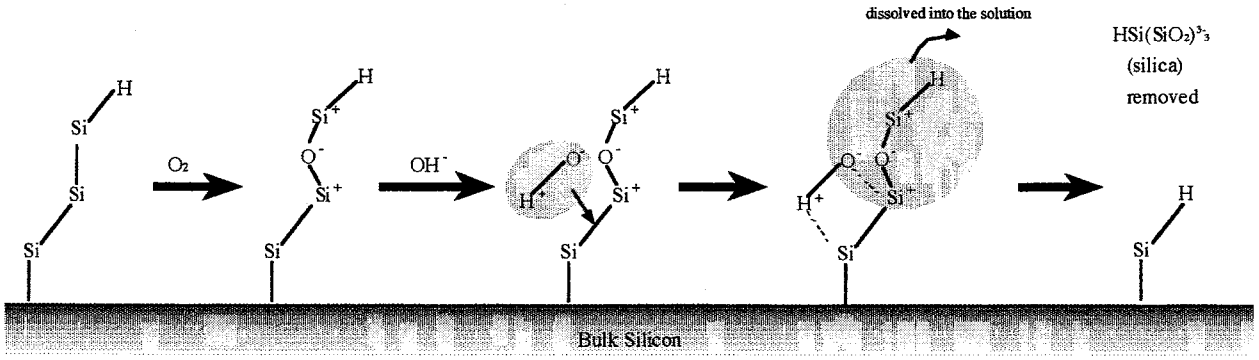

Fig. 8 The etching mechanism in water by Raghavachari et al.

4) Etching mechanisms of Si in alkaline solutions

For the etching of Si in alkaline solution, it is widely accepted that the dissolution of Si begins by the hydrolysis of Si-H into Si-OH.[39] However, the main reactant in alkaline etching has not been determined. Two representative mechanisms are shown below;

(a) Etching mechanism of Si in alkaline solutions by Allongue et al. (Fig. 9).[24]

In this mechanism, they supposed that two kinds of reaction mechanisms exist; chemical dissolution mechanism (upper route in Fig. 9) and the electrochemical dissolution mechanism (lower route in Fig. 9). In the chemical dissolution process, the hydrolysis of Si-H is caused mainly by H_2O (A to C in Fig. 9). On the contrary, in the electrochemical mechanism, OH^- assists the the hydrolysis of Si-H by a kind of acid-base reaction (A to B in Fig. 9). They concluded that the chemial dissolution mechanism predominately proceeds, and the electrochemical dissolution mechanism is a minor path.

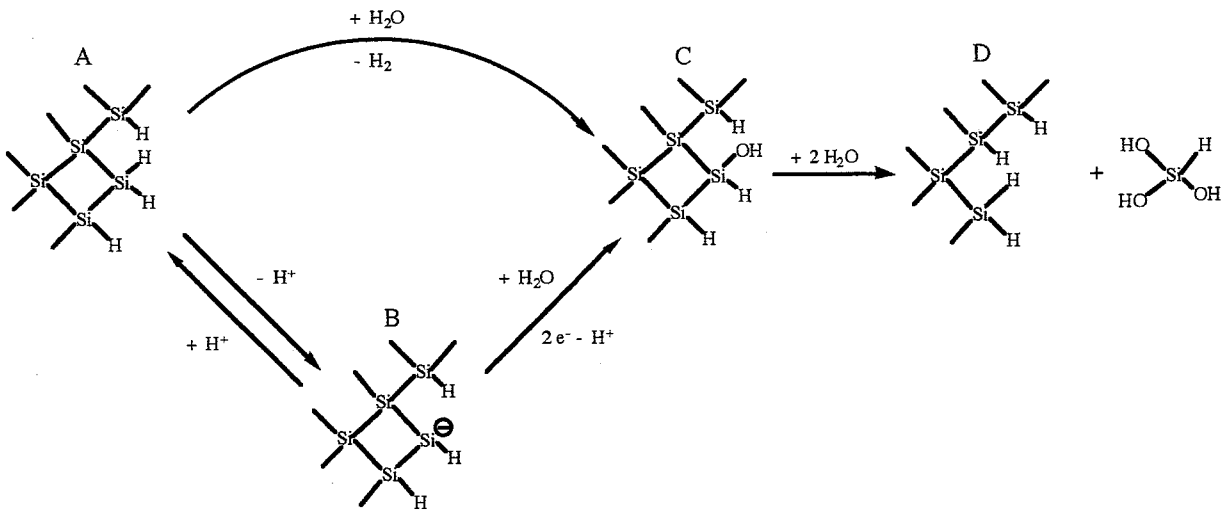

Fig. 9 The etching mechanism of Si in alkaline solutions by Allongue et al.

(b) Etching mechanism of Si in alkaline solutions by Baum et al. (Fig. 10).[40]

Baum et al. investigated the etching mechanisms of Si in alkaline solutions by measuring the H/D-kinetic isotope effect on the dissolution rate.[40] They found that in 2M KOH + H_2O the etching rate was appoximately twice as large as that in 2M KOD + D_2O. This experimental fact indicates that the clevage of Si-H bond represents the rate determining steps in silicon etching. Based on the results, they proposed the reaction mechanism as follows (Fig. 10)[40];

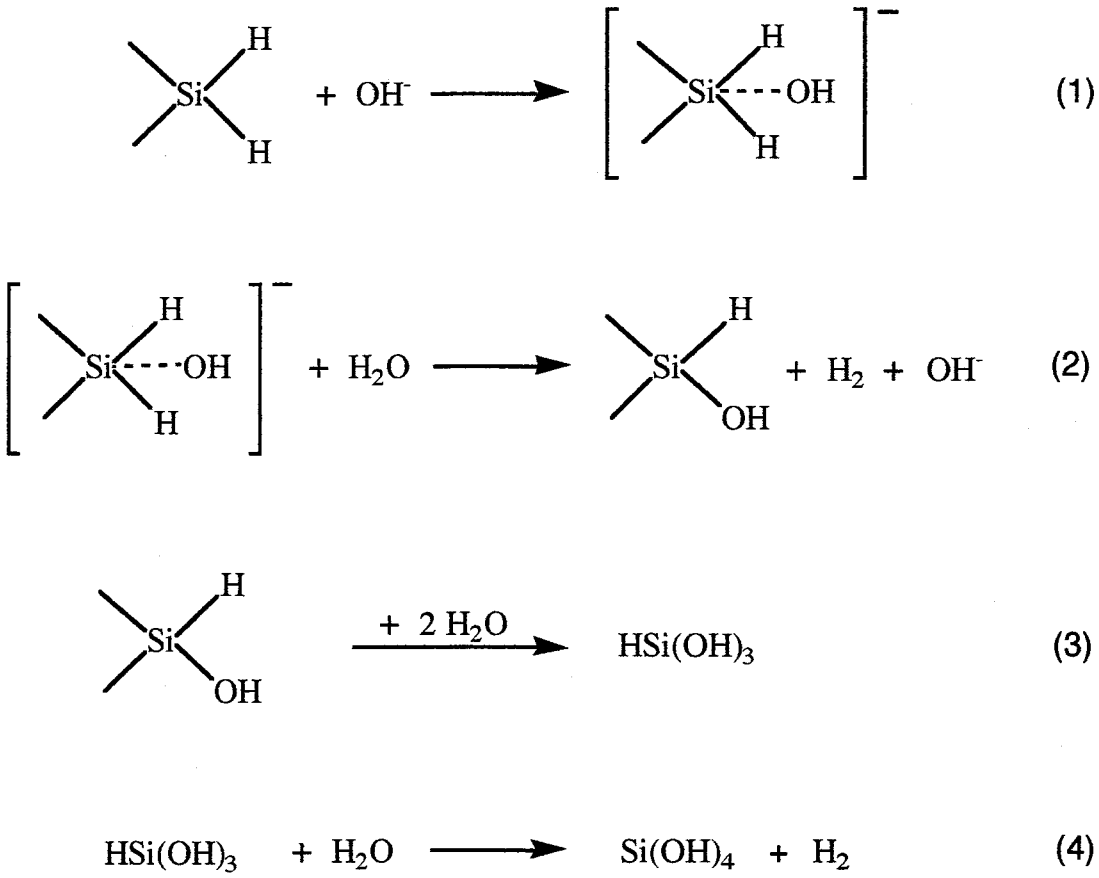

Fig. 10 The etching mechanism for Si etching in alkaline solutions by Baum et al.

They proposed that OH^- attack hydrogen-terminated Si surface, and that simultaneously Si-H bond is broken in RDS (reaction (1) and (2) in Fig. 10). After the RDS, H_2O molecules quickly attack the Si-Si back bond (reaction (3) in Fig. 10). Then, the silicon atoms on the suface are dissolved into the solution as $HSi(OH)_3$. $HSi(OH)_3$ molecule reacts with H_2O in the solution, and $Si(OH)_4$ and hydrogen molecule are produced (reaction (4) in Fig. 10).

1.2 Survey of This Thesis

In this thesis, it will be shown that the electrochemical anodic current is a very useful means to investigate the dissolution process of Si as well as the flattening process of Si(111). Besides the measurements of the anodic currents, surface analysis tools are used to relate the etching process to the change on the surface structures.

Following General Introduction (Chapter 1), the experimental results shall be presented and discussed in Chapter 2, 3, and 4 as follows;

In Chapter 2, the dissolution mechanism of Si in NH_4F solutions is presented. The unique pH dependence of Si etching in 1M NH_4F solution was found for the first time. The measurements of anodic currents and weight loss during Si etching showed that the etching rate of Si in the solutions sharply increases around pH 6.4 . This pH dependence of the etching rate cannot be explained the previous proposals for Si etching in the solution that OH^- ion etches Si surface in the solution. To explain this unique pH dependence, a new mechanism for etching of Si in NH_4F solutions is presented. In this mechanism, HF_2^- is supposed to be a major etching species, and Si-F bonds on the surface to play an important role in the etching of Si. It is also concluded that the etching of Si(111) surface by this mechanism leads to the surface flattened on an atomica scale. By the use of anodic currents and gas chromatography to meausre the etching rate of Si, NH_4F concentration dependence of the etching rate of Si was investigated. The result supported that HF_2^- is the major etching species of Si etching in NH_4F solutions. XPS and Zeta-potential measurements were done to investigate the composition of Si surface after the treatment with 1M NH_4F solutions. The results indicated that the composition of Si surface dramatically changes when the pH of the solution was around pH 6.4, which is consistent with the proposed etching mechanism.

In Chapter 3, the control of the surface morphology of Si (111) in NH_4F solutions is presented. First, the effect of dissolved oxygen onto flattening process of Si (111) is examined. AFM and anodic current measurements clarified that dissolved oxygen impedes both the flattening and dissolution rate of Si(111) in 40% NH_4F solution, and that dissolved oxygen initiates the formation of etch pits and lowers the etching rate of atomic steps. Second, special attention was directed at dihydride steps formed on atomicailly flat Si(111) surface. The parameters to control the formation of dihydride steps on the surface are the pH of the solution, dissolved oxygen concentration, polar-

ity of the substrate, and illumination during the etching. By increasing the pH of the solution from 6.6 to 7.8, dihydride steps become extended straightforwardly. At pH 7.8 (pure 40% NH_4F), almost straight dihydride steps are formed on p-Si(111) surface. When dissolved oxygen is removed, zigzag monohydride steps are predominately formed on the surface, while straight dihydride steps are formed in the solution containing dissolved oxygen. For n-Si(111), straight dihydride steps cannot be formed. The effect of photo-irradiation during the etching was also investigated. Under weak illumination (room light) during the etching in 40% NH_4F solution with oxygen, the formation of dihydride steps on p-Si(111) is enhanced. On the contrary, in the dark, some hillocks are present on the steps. Under strong illumination, jagged steps are formed, and many etch pits are present on terraces.

In Chapter 4, the etching processes of Si(111) in oxygen-free water and in alkaline solution are presented. AFM and FTIR observations of surfaces after the treatment with water and with alkaline solutions were carried out. The effects of pH and dissolved oxygen are the points of the study. It is shown in this chapter that in the pH range from 6 to 10 Si(111) can be hydrogen-terminated and atomically flattened in the absence of dissolved oxygen. In the pH range from 10 to 12, Si(111) can be atomically flattened whether or not dissolved oxygen was present, although the homogeneity of the surface is reduced by the presence of dissolved oxygen. On the other hand, in the pH range above 12, the Si(111) surface is partially oxidized, and many etch pits composed of both monohydride steps and dihydride steps are present on the surface. To clarify the etching process of Si(111), in-situ AFM observation of Si(111) in chemically deoxygenated water were carried out. We could observe staircase structure in the solution, and the step flow rate was estimated to be 8 nm/min from this observation. To examine in detail the etching processes in these solution, the etching rate was investigated by the use of gas chromatography. As a result, the unique pH dependence of etching rate of Si was obtained. This pH dependence shows that H_2O is the major etching species in neutral solution ($6<pH<10$), while OH^- is the major etching species in the pH range above 12. Based on the above results, new mechanisms for the etching of Si in water and alkaline solutions are presented.

Reference

1) G. S. Higashi and Y. J. Chabal: Handbook of Semiconductor Wafer Cleaning Technology, ed. W. Kern (Noyes Publications, New Jersey, 1993), p. 433.

2) T. Ohmi, K. Kotani, A. Teramoto, and M. Miyashita, IEEE Electron Device Lett. **12** (1991) 652.

3) Y. Yamashita, Y. Nakato, H. Kato, Y. Nishioka, and H. Kobayashi, Appl. Surf. Sci. **117/118** (1997) 176.

4) K. Oura, V.G. Lifshits, A.A. Saranin, A.V. Zotov, M. Katayama, Surf. Sci. Rep. **35** (1999) 1, and the references therein.

5) P. C. Searson: Advances in Electrochemical Science and Engineering, Vol. 4, ed. H. Gerischer and C. W. Tobias (VCH, Weinheim, 1995), p. 67.

6) E. Yablonovitch, D. L. Allara, C. C. Chang, T. Gmitter, and T. B. Bright, Phys. Rev. Lett. **57** (1986) 249.

7) F. J. Grunthaner and P. J. Grunthaner, Mat. Sci. Reports **1** (1986) 65.

8) P. J. Grunthaner, F. J. Grunthaner, R. W. Fathauer, T. L. Lin, M. H. Hecht, L. D. Bell, W. J. Kaiser, F. D. Schowengerdt, and J. H. Mazur, Thin Solid Films **183** (1986) 197.

9) M. Grundner and H. Jacob, J. Appl. Phys. A **39** (1986) 73.

10) G.S. Higashi, Y.J. Chabal, G. W. Trucks and K. Raghavachari, Appl. Phys. Lett. **56** (1990) 656.

11) S. Watanabe, N. Nakayama, and T. Ito, Appl. Phys. Lett. **59** (1991) 1458.

12) P. Allongue, V. Costa-Kieling, and H. Gerischer, J. Electrochem. Soc. **140** (1993) 1009.

13) P. Dumas, Y. J. Chabal, and P. Jakob, Surf. Sci. **269/270** (1992) 867.

14) P. Jakob and Y. J. Chabal, J. Chem. Phys. **95** (1991) 2897.

15) P. Jakob, Y. J. Chabal, K. Raghavachari, R. S. Becker, A. J. Becker, Surf. Sci. **275** (1992) 407 .

16) H. E. Hessel, A. Feltz, M. Reiter, U. Memmert and R. J. Behm, Chem. Phys. Lett. **186** (1991) 275.

17) G. J. Pietsch, U. Kohler, and M. Henzler, J. Appl. Phys. **73** (1993) 4797.

18) U. Neuwald, H. E. Hessel, A. Feltz, U. Memmert, and R. J. Behm, Surf. Sci. Lett. **296** (1991) L8.

19) S. Watanabe, Y. Sugita, Surf. Sci. **327** (1995) 1.

20) G. J. Pietsch, U. Kohler, and M. Henzler, Chem. Phys. Lett. **197** (1993) 346.

21) K. Usuda and K. Yamada: J. Electrochem. Soc. **144** (1997) 3204.

22) P. Allongue, H. Brune, and H. Gerischer, Surf. Sci. **275** (1992) 414.

23) P. Allongue, Phys. Rev. Lett. **77** (1996) 1986.

24) J. Kasparian, M. Elwenspoek, P. Allongue, Surf. Sci. **388** (1992) 50.

25) P. Jakob, Y. J. Chabal, K. Raghavachari, and S. B. Christman, Phys. Rev. B **47** (1993) 6839.

26) P. Jakob, Y.J. Chabal, K. Kuhnke, S.B. Christman, Surf. Sci. **302** (1994) 49.

27) M. A. Hines, Y. J. Chabal, T. D. Harris, and A. J. Harris, Phys. Rev. Lett. **71** (1993) 2280.

28) M. A. Hines, Y. J. Chabal, T. D. Harris, and A. J. Harris, J. Chem. Phys. **101** (1993) 8055.

29) K. Raghavachari, P. Jakob, and Y. J. Chabal, Chem. Phys. Lett. **206** (1991) 156.

30) M. Matsumura and S.R. Morrison, J. Electroanal. Chem. **147** (1983) 157.

31) H. J. Lewerenz and H. Jungblut: Semiconductor Micromachining, Vol. 1, ed. S. A. Campbell and H. J. Lewerenz (John Wiley & Sons Ltd., Chichester, 1998), p. 217.

32) H. Gerischer and M. Lübke, Ber. Bunsenges. Phys. Chem., **91** (1987) 394.

33) H. Gerischer, P. Allongue, and V. Costa-Kieling, Ber. Bunsenges. Phys. Chem., **97** (1993) 753.

34) P. Allongue, V. Kieling, and H. Gerischer, Electrochim. Acta **40** (1995) 1353.

35) M. Matsumura and S.R. Morrison, J. Electroanal. Chem. **144** (1983) 113.

36) G.W. Trucks, K. Raghavachari, G.S. Higashi, and Y.J. Chabal, Phys. Rev. Lett. **65** (1990) 504.

37) Y.-C. Huang, J. Flidr, T. A. Newton, and M. A. Hines, Phys. Rev. Lett. **80** (1998) 4462.

38) Raghavachari, G.S. Higashi, and Y.J. Chabal, and G. W. trucks, Mat. Res. Soc. Symp. Proc. **315** (1993) 437.

39) S. A. Campbell, S. N. Port, and D. J. Schiffrin: Semiconductor Micromachining, Vol. 2, ed. S. A. Campbell and H. J. Lewerenz (John Wiley & Sons Ltd., Chichester, 1998), p. 1.

40) T. Baum and D. J. Schiffrin, J. Electroanal. Chem. **436** (1997) 239.

Chapter 2

Dissolution Process of Si in Aqueous Fluoride-Containing Solutions

2.1 Introdcution

The etching mechanism of Si surface in fluoride-containing solutions has not been fully understood yet. The poor understanding of etching mechanism may arise from rwo points as stated below;

1) The main species responsible for the etching has not been determined. Many researchers with a physical viewpoint insisted that OH^- is a common main etchant of Si in fluoride-containing solutions, alkaline solutions and water.[1] The reason for this is that, in 40% NH_4F solutions (pH =7.8), Si(111) can be atomically flattened, while Si(111) surface is atomically rough in HF solutions. However, this proposal is not plausible from a chemical viewpoint. It cannot explain experimental facts, including our results (*vide infra*).
2) To elucidate the dissoluion mechanism, indispensable is the measurements of dissolution rate in the solutions with diifferent pH's and concentrations of fluoride ion. However, there has been only one report about dissolution rate measurements.[2] In addition, the results in the paper are not so precise.

To clarify the etching mechanism of Si in fluoride-containing solutions, I have combined the (electro) chemical methods and surface analytical methods. In this chapter, the work related to the etching mechanism of Si in fluoride-containing solutions will be presented. The unique pH dependence of the etching of silicon in 1M NH_4F will be presented first. Based on the result, new etching mechanism will be proposed. In the later part of this chapter, the verification of our mechanism will be done. First, NH_4F-concentration dependence of the etching of Si will be presented. Second, XPS and Zeta-potential measurements of silicon surface treated in 1M NH_4F will be presented. These will clarify the relation between etching mechanism and silicon surface condition.

2.2 Experimental

(Electrochemical measurements)

We used (111) and (100) oriented silicon wafers obtained from Shin-Etsu Semiconductor Industry. They were both n-type, and had the resistivity of 2.4 to 4.0 and 4.0 to 5.0 Ω cm, respectively. For the electrochemical measuremetns, the wafers were cut into pieces with a size of about 1 × 1 cm^2. Before the measurements, these samples were cleaned with acetone in an ultrasonication bath and rinsed with deionized water. They were mounted in a Teflon holder and sealed with a fluorocarobon-rubber packing, so that only the testing area of the samples (0.25 cm^2) was brought into contact with the fluoride-containing solutions. The back electric contact to the silicon samples was made via In-Ga alloy with copper wires. The electrochemical measurements were carried out in a Teflon beaker equipped with a platinum conterelectrode and an Ag/AgCl reference electrode. The electrode potential of the silicon samples was controlled with a potentiostat (Nikkou-keisoku NPOT2501). Aqueous solution of 1 mol dm^{-3} NH_4F was used as the electrolyte solution. The pH of the solution was adjusted by adding small amounts of aqueous solutions of sulfuric acid, phosphoric acid, and sodium hydroxide. Before measurements, the oxygen in the solutions was removed by bubbling high purity nitrogen gas.

(XPS and Zeta potential measurements)

The pretreatment of samples is the same procedure in electrochemical measurements. After the treatment, the specimens were rinsed by sonication in ethanol for 1 minute, and ethanol was blown off from the surface to avoid the chemical reactions during a rinse in water. Oxygen in aqueous solutions, which were used for the treatment of silicon, was removed by bubbling high-purity nitrogen gas for 30 minutes at a rate of 100 ml min^{-1} before the treatments. Nitrogen gas was kept bubbling during the treatments. On the other hand, ethanol used in the rinsing process was not bubbled with nitrogen, because silicon surfaces are stable in ethanol.

Surface analyses were carried out immediately after the above treatments. XPS measurements were carried out using a Shimadzu ESCA-1000 with a Mg Ka excitation source. All XPS spectra were collected with a pass energy of 78.750 eV and measured with a photoelectron take-off angle of 90°. Under the conditions, the FWHM of the Si 2p band of silicon substrate was about 1.8 eV. Zeta potentials of silicon surfaces were measured using an electrophoretic light

scattering photometer (Otsuka, ELS-800). In the measurements, polystyrene-latex suspended in a stream of aqueous solution of 0.01 mol dm^{-3} sodium chloride were used as the light scattering particles.

(Etching rate measurement of Si)

For the determination of the etching rates, the weight loss of the silicon wafers was measured with a Metler UMTs microbalance using the silicon wafers with the surface area of 1 cm^2. The etching solutions were bubbled with nitrogen gas during the etching process.

The etching rate was also determined from the quanititative analysis of hydrogen evolved as Si dissolved. Both side-polished Cz p-type Si(111) wafers whose resistivity is 10 Ω cm (0.15 mm thick) were used as the samples. Prior to the measurements, these samples were cleaned with RCA cleaning, followed by 1min immersion in 5% HF to remove chemical oxides on the surfaces. Dissolved oxygen in the solutions was removed by the addition of sulfite ion. For the hydorgen evolution measurement (i. e. etching rate measurements), GC-14B (Shimadzu co. ltd.) were used.

2.3 Results and Discussions

2.3.1 Unique pH dependence of anodic currents of Si electrode in NH_4F

The pH dependence of the anodic current of Si in 1 mol l^{-1} NH_4F was measured to elucidate dissolution mechanism of Si in fluoride-containing solutions. The anodic currents were measued at 0.0 V vs Ag/AgCl. The current densities reached a constant value at 0.0 V vs Ag/AgCl. The results are shown in Figs. 1 and 2. One can find that the anodic current shows a very sharp peak at pH 6.4 for both the (111) and (100) wafers.[3)]

Close examination of the currents for the (111) and (100) wafers showed that the current densities for the (100) wafers were higher than those of (111) wafers by a factor of 1.3. The higher anodic current densities of Si(100) indicate that the etching rate of Si(100) is higher than that of (111). This is in good agreement with the experimental fact that Si(100) can be more easily dissolved in NH_4F solutions.[4), 5)]

The anomalous pH dependences of the anodic dark currents shown in Figs. 1 and 2 represent the specific pH dependences of the reactions on silicon surface in fluoride containing solutions. Gerischer et al. also investigated the pH dependence of the anodic current in the fluoride-containing solution.[6)] They, however, missed out the unique pH dependence.

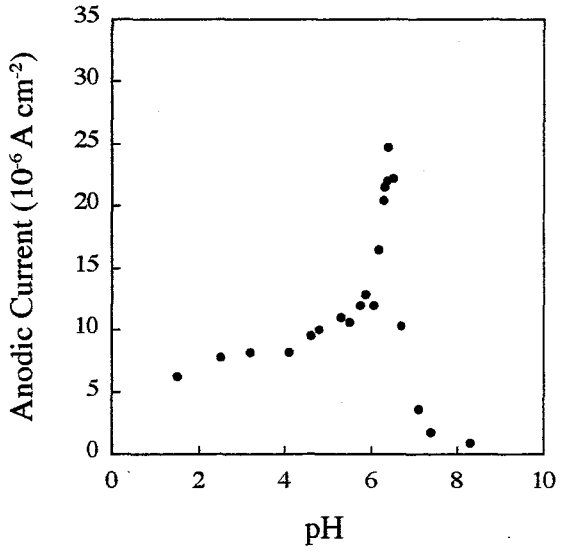

Fig. 1 pH dependence of the anodic current of Si(111) in 1 moll^{-1} NH_4F.

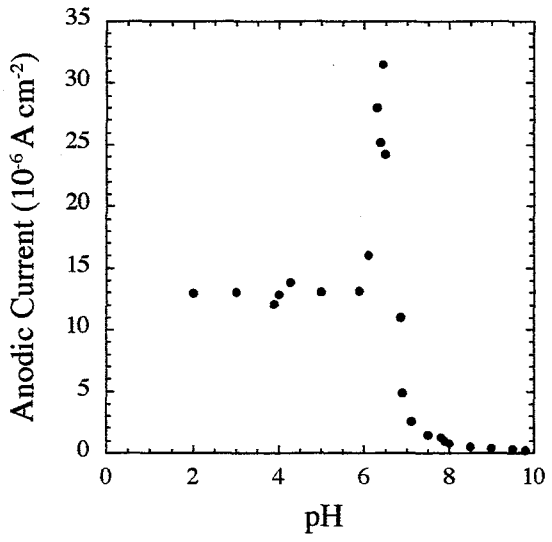

Fig. 2 pH dependence of the anodic current of Si(100) in 1 moll^{-1} NH_4F.

To examine the relationship between the anodic current density and the chemical reaction on the silicon surface, we measured the etching rate of the silicon wafers in the fluoride-containing solutions at various pH values (Fig. 3).[3] The etching rate was obtained from the weight loss of Si(111) immersed in the solutions. This result revealed that the etching rate had the pH dependence quite similar to that of the anodic currents for the (111) wafers. The pH dependence of the etching rate of (100) wafers showed the similar pH dependence, with a little higher etching rate. The etching rates quantitatively correspond to the anodic current densities, if we assume that one silicon atom is oxidatively etched by losing four electrons. These results indicate that the anodic current of silicon is directly related to the etching process. The correspondence of the etching rate and the current density also indicates that silicon is etched oxidatively in the fluoride-containing solutions.

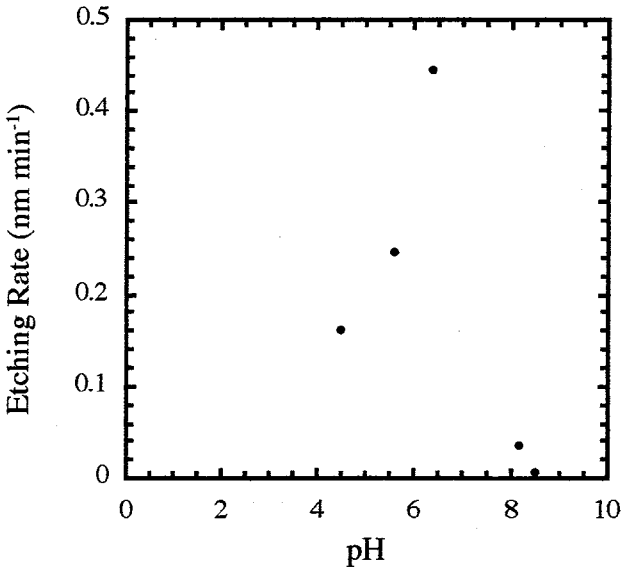

Fig. 3 Etching rate of Si(111) in 1M NH_4F determined by weight-loss measurements.

In the etching process without an external electric circuit, it is supposed that the electrons removed from the silicon atoms during etching in the solutions are consumed by the hydrogen evolution reaction. Two reasons can support this. First, it was alreay reported that hydrogen gas evolved during etching of Si in HF solutions.[1a), 7), 8)] Furthermore, the rest potential of the silicon electrodes in hydrofluoric acid is more negative of the hydrogen evolution potential. It was therefore concluded that electrons are injected into conduction band of bulk silicon, regardless of the electrode potential.

On the basis of the experiments, we proposed the reaction schemes for the anodic dissolution mechanism of n-Si in fluoride-containing solutions, as shown in Fig. 4.[3] In this reaction mechanism, the starting point of the dissolution reaction is the silicon atom where a fluorine atom is bound. Once a fluorine atom is bound to a silicon atom, the silicon atom should be so reactive because the fluorine atom withdraw the electron from the silicon atom.

In the acidic solutions, the concentration of HF in the solutions is high so that the hydrogen

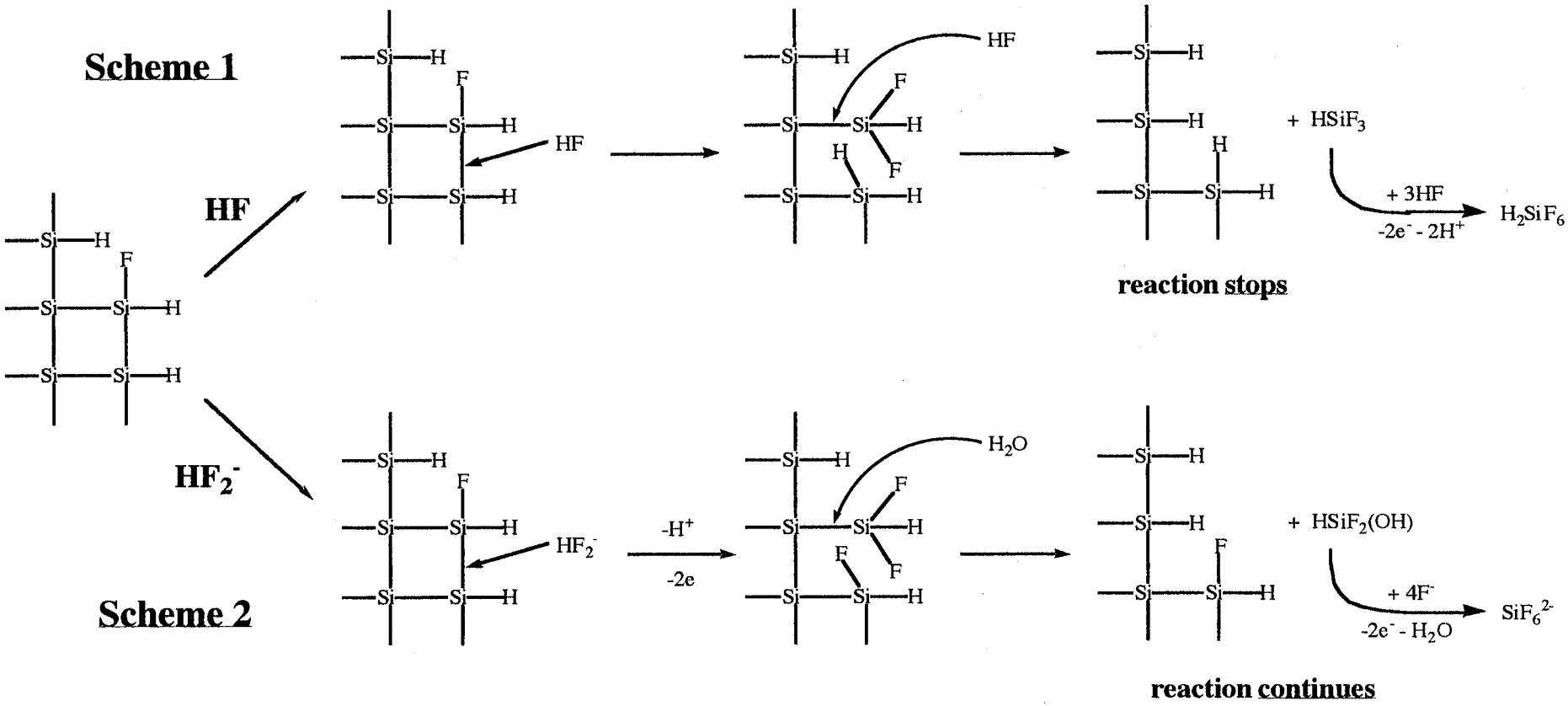

Fig. 4 New proposal for the etcthing mechanism of Si in NH_4F solutions.

termination of Si surface predominately occurs, represented by Scheme 1 in Fig. 4. The similar mechanism has already been proposed by Imura et al.[9] and Trucks et al.[10] At the stationary state, therefore, the etching rate and current density are expected to be low, since the hydrogen-terminated surface is chemically very stable. This is consistent with the results of Figs. 2 and 3.

In Scheme 2, we propose oxidative dissolution of silicon by HF_2^- ions. Etching of silicon oxide by HF_2^- ions has been reported by Judge et al.[11] However, the proposal for the etching of silicon by HF_2^- ions is new, as far as we know. This reaction proceeds competitively with the process of Scheme 1. Scheme 2 cannot be predominant over Scheme 1, if the concentration of HF in the solution is larger than that of HF_2^- to a certain level. This is because HF stabilizes the surface by the hydrogen termination and, thus, inhibits Scheme 2, if the concentration of HF in the solution exceeds a critical value. Figure 5 shows the concentrations of HF, $(HF)_2$, F^-, and HF_2^- in the solution as a function of pH. They were calculated using equilibrium constants as described below[12]:

1) $HF = H^+ + F^-$ $K_1 = 6.85 \times 10^{-4}$

2) $HF + F^- = HF_2^-$ $K_2 = 3.963$

3) $2HF = (HF)_2$ $K_3 = 2.7$

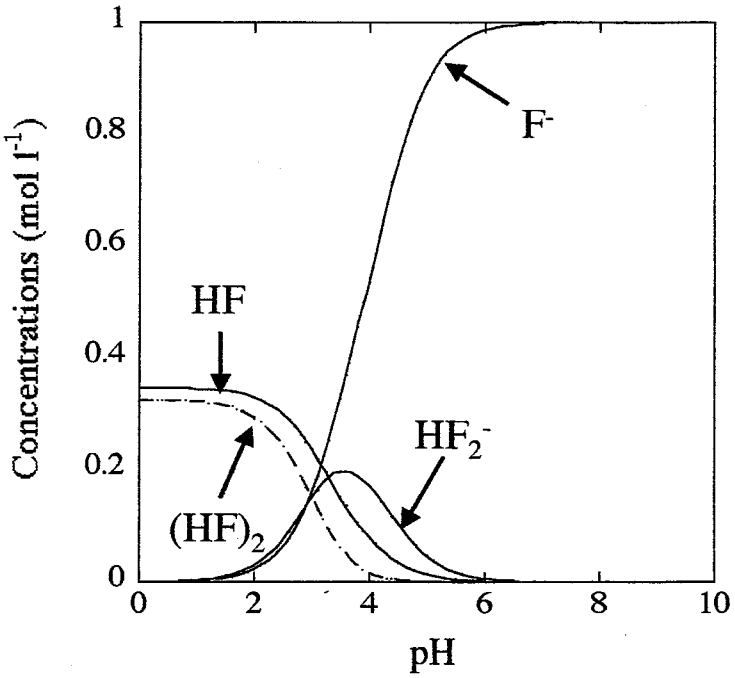

Fig. 5 The concentrations of HF, $(HF)_2$, HF_2^-, and F^- in 1M NH_4F solution.

Experimentally, the anodic current and etching rate increased steeply in the pH region from 6.0 to 6.4, as shown in Fig. 2 and 3. In this pH region, the concentration of HF in the solution is considered to be too low to stabilize the surface by the hydrogen termination. This allows the Scheme 2 to be effective. In more alkaline solution, the concentration of HF_2^- is too low to drive Scheme 2. Therefore, the appearance of the peaks at pH about 6.4 for the etching rate and the anodic current was concluded to be caused by these conditions. Many researchers assigned OH^- ions to the oxidizing species of silicon even in the solutions of neutral and weakly alkaline solutions.[8), 14] However, the pH dependences shown in Fig. 2 and 3 cannot support the etching

mechanism by the OH^- ions at least in the pH region lower than 10.

The energetic driving force of the reaction represented by Scheme 2 is attributable to the formation of very strong Si-F bonds. In addition, this reaction is kinetically favored by the agreement of the lengths of the reactive chemical bonds. Namely, the distance between the two F atoms of HF_2^- ions, which is estimated to be 0.226 nm for KHF_2 in the solid state,[13] matches the length of the Si-Si bond of 0.235 nm very well. As has been described, the etching rate agrees quantitatively with the anodic current density by assuming that one silicon atom is etched by losing four electrons. This result suggests that $HSiF_3$ produced as the result of the reactions Schemes of Fig. 4 injects two electrons into silicon, forming SiF_6^{2-} in the solution.

SEM observation of silicon immersed in the solutions at pH about pH 6.5 showed the surfaces etched anisotropically, as shown in Fig. 6. The surfaces exposed after etching were equivalent to the (111) face irrespective of the original orientations of the wafers, as has been reported by the use of FTIR[4] and STM[5]. This is consistent with the similarities in the pH dependences of the etching rate and the anodic current between (111) and (100) wafers. The slightly higher etching rate and current density for (100) wafers than for (111) wafers are probably due to the larger surface area of anisotropically etched surface of (100) wafers, as seen in Fig. 6.

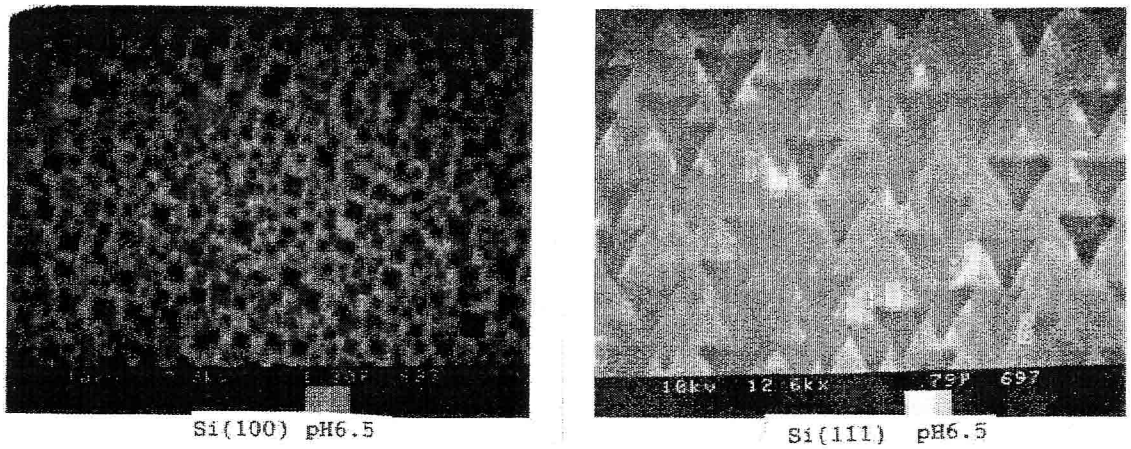

Fig. 6 SEM images of Si(100) and Si(111) surfaces treated in 1M NH_4F (pH = 6.5).
Scan sizes are 10 x 15 μ m^2 for Si(100) , and 6 x 9 μ m^2 for Si(111).

2.3.2 Verification of Our Ecthing Mechanism

Two experimental results are presented here to determine the major etching species of the etching of Si in NH_4F solutions. One is the anodic current measurements to investigate the pH dependence of etching rate of Si in NH_4F solutions with different concentrations. The other is the measurements of hydrogen evolution from Si(111) in NH_4F solution with different concentrations at a given pH where Si(111) can be atomically flattened.

2.3.2.1 Anodic current measurements

The anodic currents measured in 1 mol l^{-1} and 3 mol l^{-1} NH_4F solutions are shown in Fig. 7. This result shows that etching mechanisms change in the two pH range, pH<6, and 6<pH<10.

In the pH range below 6, it is now made clear that the anodic currents show no pH and concentration dependence, as shown in Fig. 7. This result cannot be explained the previous proposal that OH^- is the main etchant of silicon. If the previous proposal is true, the etching rate of Si at pH=2 is larger that that at pH=6, by a factor of 10000. On the contrary, our etching mechanism can explain the experimental fact. According to our etching mechanism, HF stops the etching of Si in the low pH region. HF attack Si-Si backbond of Si-F (active site) and Si-H bond (inactive site). Hence, the etching reaction cannot proceed, although the concentration of HF_2^- increases.

On the other hand, in the pH range from 6 to 10, anodic currents strongly depend on the concentration of NH_4F as shown in Fig. 7. The etching reaction of Si by HF_2^- can efficiently proceed in this pH range. In this pH range, the concentration of HF is so small that Si-F bonds on the surface can be stable. Furthermore, it seems that the anodic currents in this pH range are proportional to the second power of NH_4F concentration, not the first power of NH_4F concentration. This point can be explained as follows: In the pH region around 6, HF_2^- is a major etching species in our etching mechanism. Hence, etching rate of Si at a given pH is expected to be proportional to the second power of fluoride ion. This can be an indirect evidence that HF_2^- is a main etchant of Si in this pH range.

In addition, it should be noticed that the peak shift of the anodic currents with the increase in NH_4F concentration. As NH_4F concentration increases, the pH of the maximal HF_2^- concentration in the solutions shifts to a higher pH, as shown in Fig. 8. This is probably the reason for the pH shift of the maximal anodic current with the concentration of NH_4F

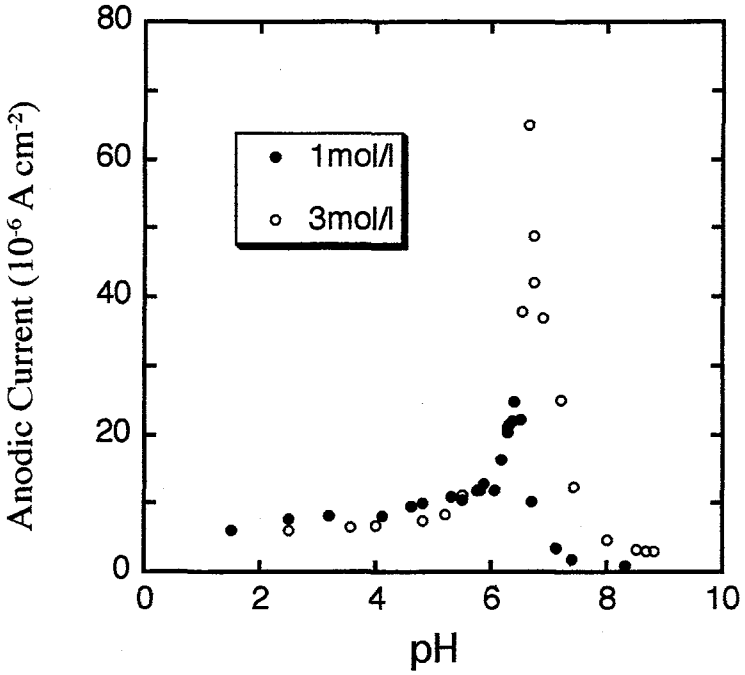

Fig. 7 pH dependences of the anodic currents of Si(111) in 1 mol l^{-1} and 1 mol $l^{-1}NH_4F$ solutions.

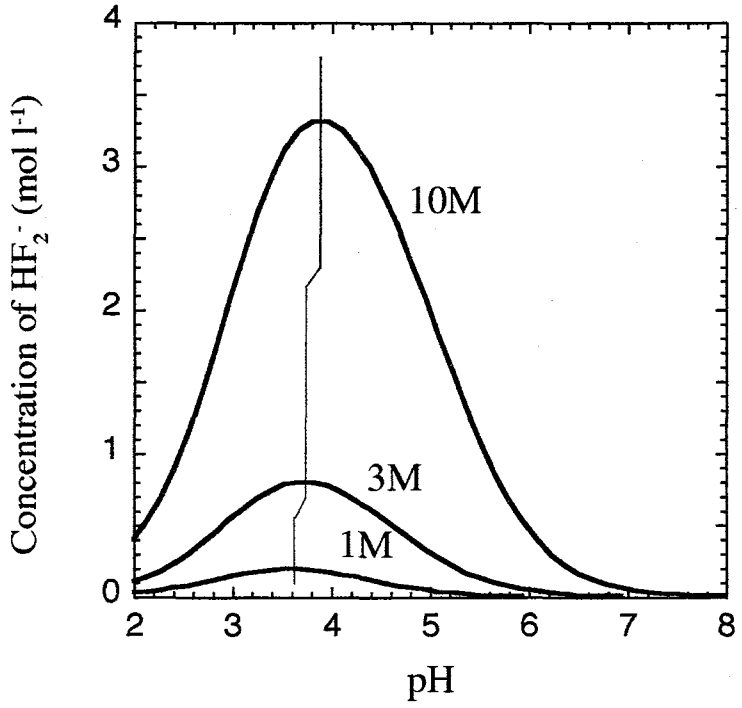

Fig. 8 The concentration of HF_2^- in 1 mol l^{-1}, 3 mol l^{-1}, 10 mol l^{-1} NH_4F solutions.

2.3.2.2 Etching rate measurements by the use of gas chromatography

Hydrogen evolution rate from Si(111) surface during etching was measured to determine the dissolution rate of Si. Four electrons are released during the etching of silicon because the oxidation state of Si atom in the final etching product is +4. These four electrons are compensated by the hydrogen evolution reaction and two hydrogen molecules are evolved. In fact, we confirmed that 2 H_2 molecule are evoled per silcon atom dissolved by the use of gas chromatography measurement and weight loss measurement for Si etching in 40% NH_4F solution at open circuit potential. The etching rate measurements of Si(111) were done in 1-40% NH_4F. The pH's of the solutions was kept constant, and dissolved oxygen was removed prior to the measurements because oxygen in solution affect surface morphology in 40% NH_4F, as will be shown in Chapter 3.

The result of dissolution rate measurements is shown in Fig. 9. It is clearly demonstrated that the etching rate of Si is proportional to the second power of NH_4F concentration, i.e. F^- ion concentration. This result can deny the previous proposal that OH^- ion is a main etchant of Si in NH_4F solutions.

In Fig. 10, the etching rates are plotted against HF_2^- concentration calculted using the equilibrium constant. This figure clearly shows that the etching rate of Si is proportional to the concentration of HF_2^-. A least square fit of the dissolution rate yields the following equation (Fig. 10);

Dissolution rate (nm/min) = 170 $[HF_2^-]$ + 0.343

The value of the intercept of the above equation is very close to the value of the etching rate of Si(111) in water, as will be presented in Chapter 4.

In conclusion, the major etching species of the etching of Si in NH_4F solutions is determined to be HF_2^- ion by measuring dissolution rates. These results support our proposal for the etching of Si in NH_4F solutions.

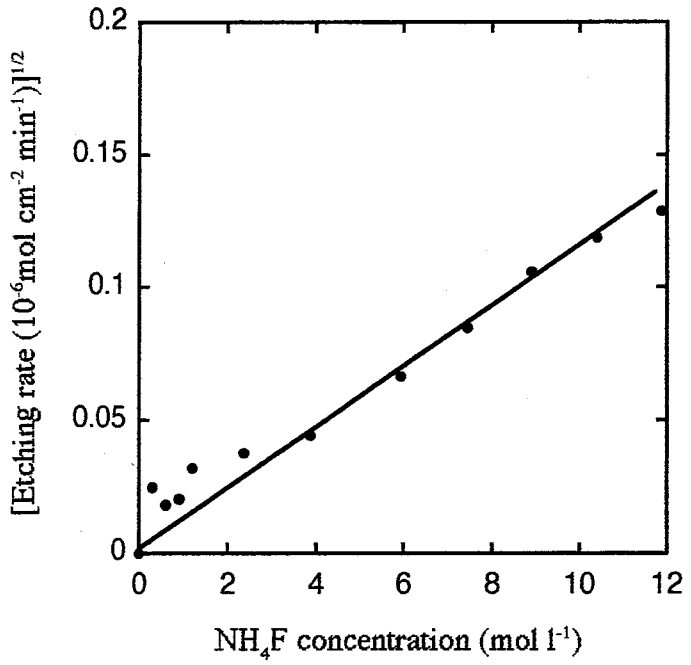

Fig. 9 NH_4F-concentration dependence of the etching rate. The square root of $(R-R_0)$ is plotted against the concentration of NH_4F solution. R is the etching rate in NH_4F solution, and R_0 is the etching rate without NH_4F i.e. the etcthing rate in water.

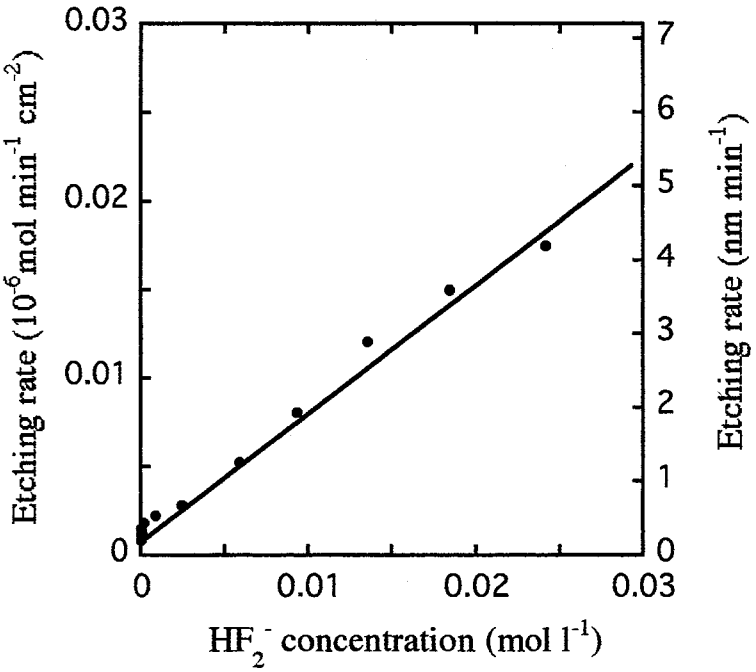

Fig. 10 Etching rates of Si(111) plotted against calculated HF_2^- concentration.

2.3.3 Characterization of Si surface treated in 1M NH_4F by the use of XPS and Zeta potential measuremetns

2.3.3.1 XPS measurements

Detailed information on the surface conditions can be obtained from the XPS spectra. Hence, we used XPS to relate the dissolution mechanism and surface chemistry of Si in 1M NH_4F solution. For the specimens treated with ammonium fluoride solutions at pH's lower than about 7, the F 1s band of the XPS spectra appears at around 687 eV, as seen in Fig. 11. This binding energy agrees with that for the fluorine atoms bound to silicon.[14), 15)] This means that fluorine atoms remaining on the silicon surface after the treatment with these solutions are directly bound to the silicon atoms on the surface. On the other hand, the peak positions for the specimens treated at pH's higher than 7 are located at higher binding energies, as shown in Fig. 11 for the cases treated at pH's of 7.6 and 8.4. We assume that these fluorine atoms are bound to or adsorbed on the oxide layer of silicon, whose existence was indicated by the spectra of the Si 2p band, as will be shown later. When we used the specimens whose native oxide was removed by etching in 5% HF solution before the treatment with ammonium fluoride solutions, the peak position of the F 1s band agreed with that of the fluorine atoms bound directly to silicon atoms irrespective of the pH of solutions. The broken line in Fig. 11 shows the result, as an example, for the treatment at a pH of 7.3.

Figure 12 shows the XPS spectra of the Si 2p region for the same samples as those shown in Fig. 12. The peaks appearing at about 99 and 103 eV have been attributed to the unoxidized and oxidized silicon atoms, respectively.[16)] The other peak in the range 99-103 eV (such as SiFx and SiOx (x = 1-3))were hardly deteceted. This is probably because the full width half maxima of Si 2p of the bulk is too broad and the angle of detection is normal to the surface, hence, the surface sensitivity was not so good. Hence, the results indicate that silicon oxide is present for the samples treated with 1 mol dm^{-3} ammonium fluoride at pH's higher than 7, if they are not pre-treated with 5 wt% HF solution. The oxide is assigned to the native oxide which was present on the silicon wafer. On the basis of this result, the high binding energy of the F 1s band for the sample treated at pH's higher than 7 without etching with 5 % HF, as observed in Fig. 12, is attributed to the fluorine atoms adsorbed on the oxide layer.

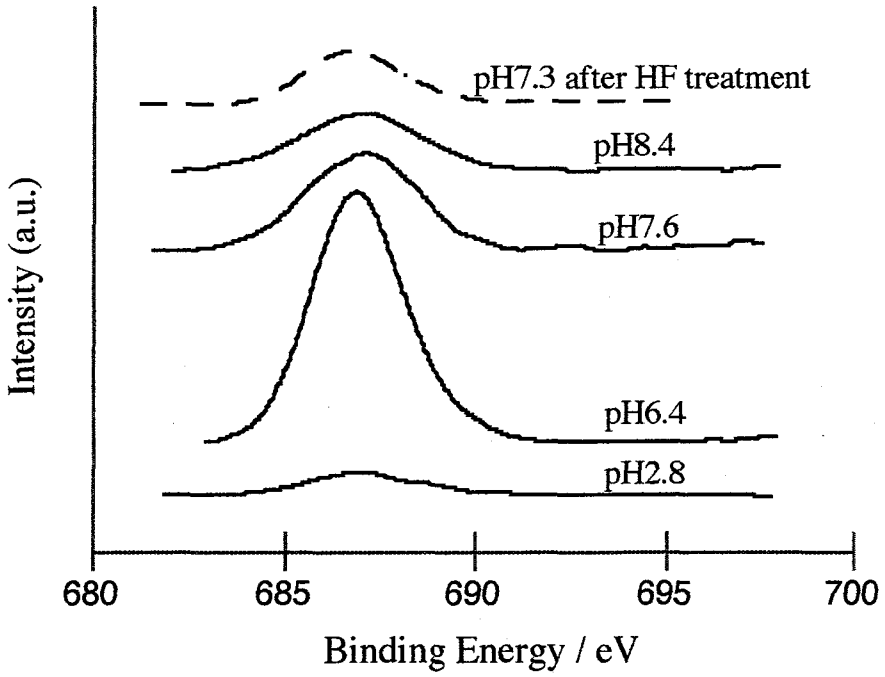

Fig. 11 XPS spectra of the F 1s band of n-type Si (111) surfaces which were treated with 1 mol dm^{-3} ammonium fluoride solutions at different pH's. The broken line is for the specimen pre-treated with 5 wt% HF before the treatment with ammonium fluoride solution at a pH of 7.3.

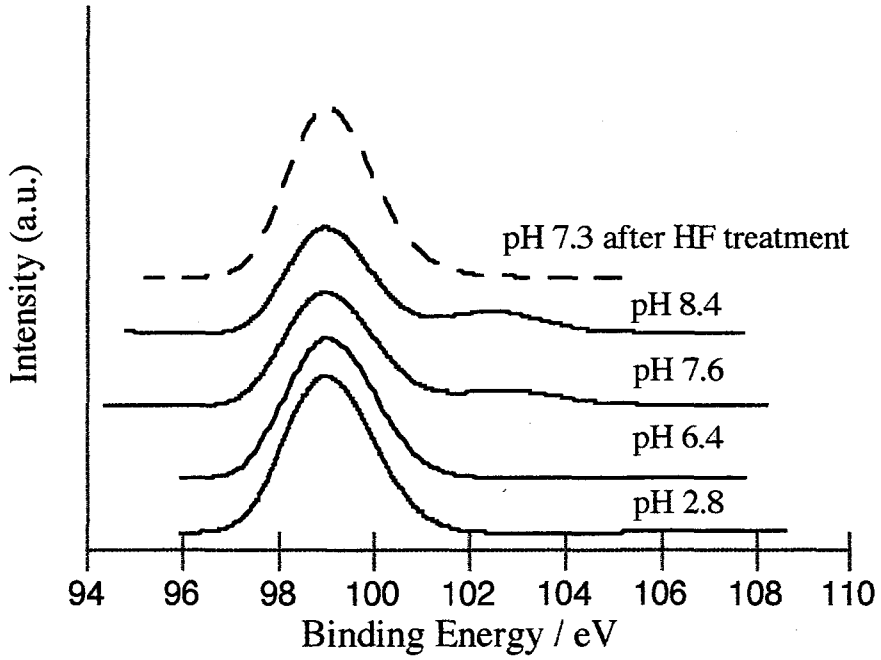

Fig. 12 XPS spectra of the Si 2p band of n-type Si (111) surfaces which were treated with 1 mol dm^{-3} ammonium fluoride solutions at different pH's. The broken line is for the specimen pre-treated with 5 wt% HF before the treatment with ammonium fluoride solution at a pH of 7.3.

We have reported that silicon is inert in the solutions of 1 mol dm^{-3} ammonium fluoride at pH's higher than 7 on the basis of its electrochemical properties.[3] This conclusion is consistent with the results of XPS spectra, which indicate the presence of the oxide layer on the samples treated at this pH region. Seemingly, the oxide layer plays the role of a protector of silicon from the attack of reactive species in solutions. This is consistent with the finding that HF_2^- ions play the role of etchant for silicon oxide.[11), 12), 17)] We have found that bare silicon is also electrochemically inert and the etching rate is low in the solutions of 1 mol dm^{-3} ammonium fluoride at pH's higher than 7.[3] Therefore, it is concluded that both silicon and silicon oxide are inert in the solutions at pH's higher than 7. In strong alkaline solutions, for instance at pH's higher than 10, the situation is different, because OH^- ions play the role of the etchant for the oxide layer, as will be discussed in Chapter 4.

Even by the treatment at a pH of 7.8, no oxide was observed on the silicon specimens when they were treated with 11.8 mol dm^{-3} ammonium fluoride solutions (40 wt%). This result indicates that the etching rate of silicon oxide in the ammonium fluoride solution is strongly dependent on the concentration as well as the pH. It should therefore be noted that our study was carried out mostly in solutions of ammonium fluoride at the concentration of 1 mol dm^{-3} (3.6 wt %). Different results are expected if the concentration of ammonium fluoride is altered.

Using the fractional monolayer model (in this case, the surface is partly covered with fluorine layer (monolayer thichness) and the rest part of the surface is not.),[18), 19)] we tried to quantify the amounts of fluorine atoms remaining on the silicon surface after the treatment with solutions of 1 mol dm^{-3} ammonium fluoride. On the basis of this model, the intensities of F 1s and Si 2p bands, which are symbolized by I_F and I_{Si}, are expressed by

$$\frac{I_0}{I_{Si}} = \frac{I_0^{\infty}}{I_{Si}^{\infty}} \phi \left[1 - \exp\left(- \frac{a_0}{\lambda (E_F)\cos\theta} \right) \right] \Big/ \left[1 - \phi + \phi \exp\left(- \frac{a_0}{\lambda (E_F)\cos\theta} \right) \right]$$

$$\fallingdotseq \frac{I_0^{\infty}}{I_{Si}^{\infty}} \left[\frac{a_0}{\lambda (E_F)\cos\theta} \right] \left[1 - \frac{a_0 \phi}{\lambda (E_F)\cos\theta} \right]^{-1}$$

where I_F^{∞} and I_{si}^{∞} are the intensities for pure F and Si atoms, respectively, a_0 the monolayer thickness, ϕ the fractional monolayer coverage, I(F) and I(Si) the mean free paths of electrons in F and Si, respectively, and θ the take-off angle relative to the surface normal. a_0 is assumed to be the length of the Si-F bond of 0.16 nm. λ (Si) is chosen to be 0.23 nm,[20] and λ (F) is estimated to be 0.14 nm from the reported relationship of $\lambda_0(E_F)/\lambda_0(E_{Si}) \fallingdotseq (E_F/E_{Si})^{0.7}=0.6$.[21] θ is zero in our measurements. By substituting these values and experimental results to the parameters of Eq. (1), we obtained f values for the specimens treated at different pH's. The results are shown in Fig. 13, which indicates that the amount of Si-F species reaches a maximum at a pH of about 6.4. Again at the pH, where the anodic current, etching rate show the peculiar behavior.

The fluorine atoms observed on the specimens treated at pH's higher than 7 are mostly attributed to those bound to and/or adsorbed on the oxide layer if they were not pretreated with 5 % HF, as discussed above. For the specimens pretreated with 5 % HF before the treatment with ammonium fluoride solutions, the coverage of silicon surfaces by fluorine atoms was much lower, as shown by the open circle in Fig. 13. This result indicates that high density of Si-F bonds are formed peculiarly in the narrow pH region around 6.4.

The very large amount of fluorine atoms observed for the specimens treated at a pH of about 6.4 indicates that solutions of this region have unique reactivity with silicon surfaces. On the basis of this result and those obtained previously,[3] we propose that HF_2^- ions oxidatively attack silicon atoms on the surface, as shown in Fig. 14(a). The reaction leaves Si-F bonds, two electrons, and a proton. The electrons are monitored as the anodic current in the electrochemical measurements and are used for the hydrogen evolution in the chemical etching process. This reaction is favored by the formation of strong Si-F bonds and by the matching of the length of the Si-Si bond (0.23 nm) and the distance between the F atoms in HF_2^- ions (0.226 nm)[22]. This reaction is expected to take place favorably around the Si atoms where a fluorine atom(s) is (are) bound, because these Si-Si bonds are weakened owing to the withdrawal of bonding electrons by fluorine atoms.[3] The positive polarization of these silicon atoms also leads to the enhancement in the reaction with nucleophiles such as HF_2^- ions. Hence, once the surface concentration of the Si-F bond reaches a certain level, a kind of a chain reaction is triggered. Under such conditions, the amount of surface fluorine atoms becomes extraordinary high, and the etching rate as well as

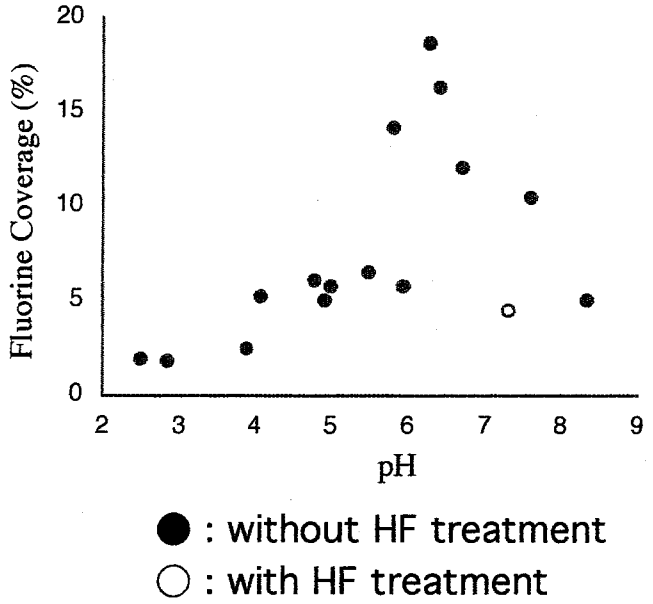

Figure 13 Dependence of fluorine coverage of silicon surfaces on the pH of 1 mol dm^{-3} ammonium fluoride solutions which were used for the surface treatment. The open circle represents the result for the sample which was pretreated with 5 wt% HF to remove the native oxide layer before the treatment with ammonium fluoride solutions.

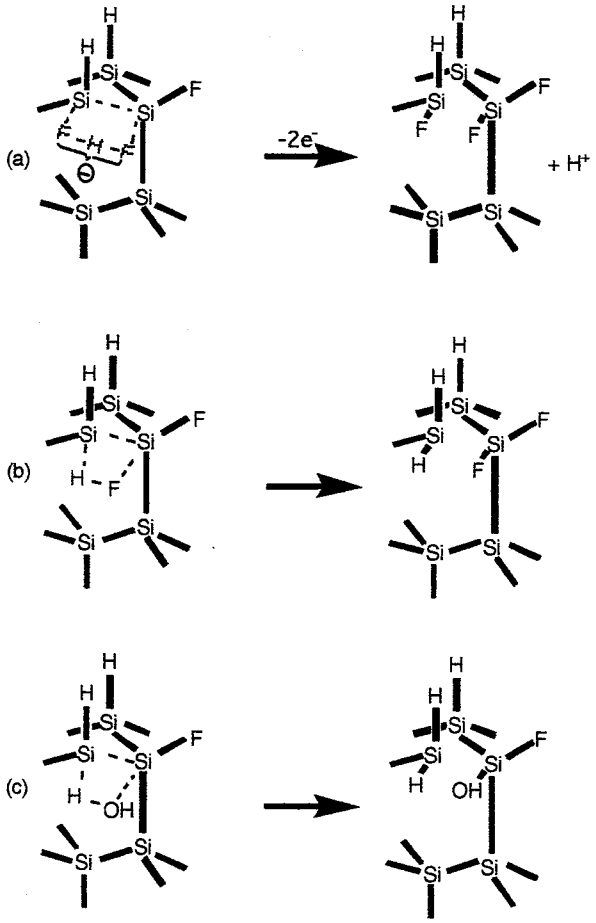

Figure 14 Mechanisms for oxidative Si-Si bond breaking by HF_2^- ion (a), and for chemical Si-Si bond breaking by HF (b) and by water (C).

the anodic current are accelerated, as observed experimentally.[3)]

Hydrogen fluoride is also expected to attack the silicon atoms around the place where a fluorine atom(s) is (are) bound, as shown in Fig. 14(b). By this reaction a new Si-F bond is formed on the silicon atoms on which a fluorine atom(s) is (are) bonded, because of its high electrophilicity. By repeating the reactions, the silicon atoms bonded to a fluorine atom(s) are removed from the surface as SiF_4 (or SiF_6^{2-}), leaving the hydrogen-terminated surface. In acidic solutions this process is considered to become predominant over the reaction with HF_2^- ions (process (b)) , because the concentration of HF is much higher than that of HF_2^- ions.[3)] Since the reaction leaves chemically stable hydrogen-terminated surface, the etching rate is expected to be very slow in acidic solutions. This is in agreement with the experimental results.

The usefulness of boiling water for hydrogen-termination of silicon surface has been reported by Watanabe et al.[23)] Their result suggests that the silicon atoms bonded to fluorine atoms are attacked by water, as shown in Fig. 14(c), because these places are considered to be most reactive. As the case of the attack by HF, the surface will be covered with hydrogen when silicon is immersed in fluoride-containing solutions at pH's higher than 7, as the result of the reaction with water. The inertness and the low fluoride concentration of silicon surfaces after the treatment with solutions at pH's higher than 7 are therefore attributable to the hydrogen-termination of the surfaces by water. If the surface is covered with an oxide layer, the surface is passivated and no reaction proceeds in the solutions, as discussed above.

2.3.3.2 Zeta potential measurement

Zeta potentials of the n-type Si (111) specimens after the treatment with 1 mol dm^{-3} ammonium fluoride solutions of different pH's are shown in Fig. 15. In the measurements, it took 5 minutes to adjust the experimental conditions after the specimens were exposed to the monitor solution. The closed circles are those obtained at the earliest time, i.e. 5 minutes after the specimens were immersed in the monitor solution. The results show that the specimens treated at a pH of about 6.4 have negative zeta potential as low as - 25 mV in contrast to the specimens treated at other pH's, where the potentials are close to zero.

Because of the above time interval needed for the measurement of zeta potentials, the zeta potentials do not give the information of as-treated surfaces. The effects of the surface treatments are nevertheless expected to remain to some extent when the zeta potential was determined. The zeta potentials determined after the specimens were immersed in the monitor solutions for 12 and 19 minutes are represented by the open circles and the crosses in Fig. 15, respectively. The results indicate that the zeta potentials shift positively while the specimens are immersed in the monitor solution. After immersion in the solution for 12 and 19 minutes, the specimens treated at a pH of about 6.4 show the zeta potentials more positive than those treated at other pH's. Presumably, the time dependence of the changes of the zeta potentials reflects the changes in surface conditions of silicon as the result of chemical reactions of the surfaces with water.

Although we cannot acquire the exact information about the chemical conditions of surfaces from the zeta potentials, it is evident that the silicon surface treated with the solution at a pH of about 6.4 has the conditions largely different from those treated at other pH's. We consider that the peculiar property of the zeta potential of the specimens treated at a pH of about 6.4 is related to the large anodic current and the fast etching rate observed in this pH region.[3)]

The sharp peaks appeared at a pH of about 6.4 for the anodic current, the zeta potential, and the content of fluorine atoms on silicon surfaces observed by XPS are all consistent with the competitive processes shown in Fig. 15. The competition gives rise to the reactive silicon surface at a pH of about 6.4, where a large amount of fluorine atoms are bonded to surface silicon atoms as was shown in Fig. 14. The competition of the processes is dependent on the concentrations of HF and HF_2^- in solutions.

In conclusion, the surface condition of Si in 1M NH_4F at around pH 6.4 is very different from that of other pH's. This arises from the change in the dissolution mechanism of Si in the solution with the pH. The relation between the dissolution mechanism and surface microroughness is, however, unclear. This point has been one of the central topics in the science and technology of semiconductor. In the next chapter, this point will be discussed, based on the results by AFM and FTIR.

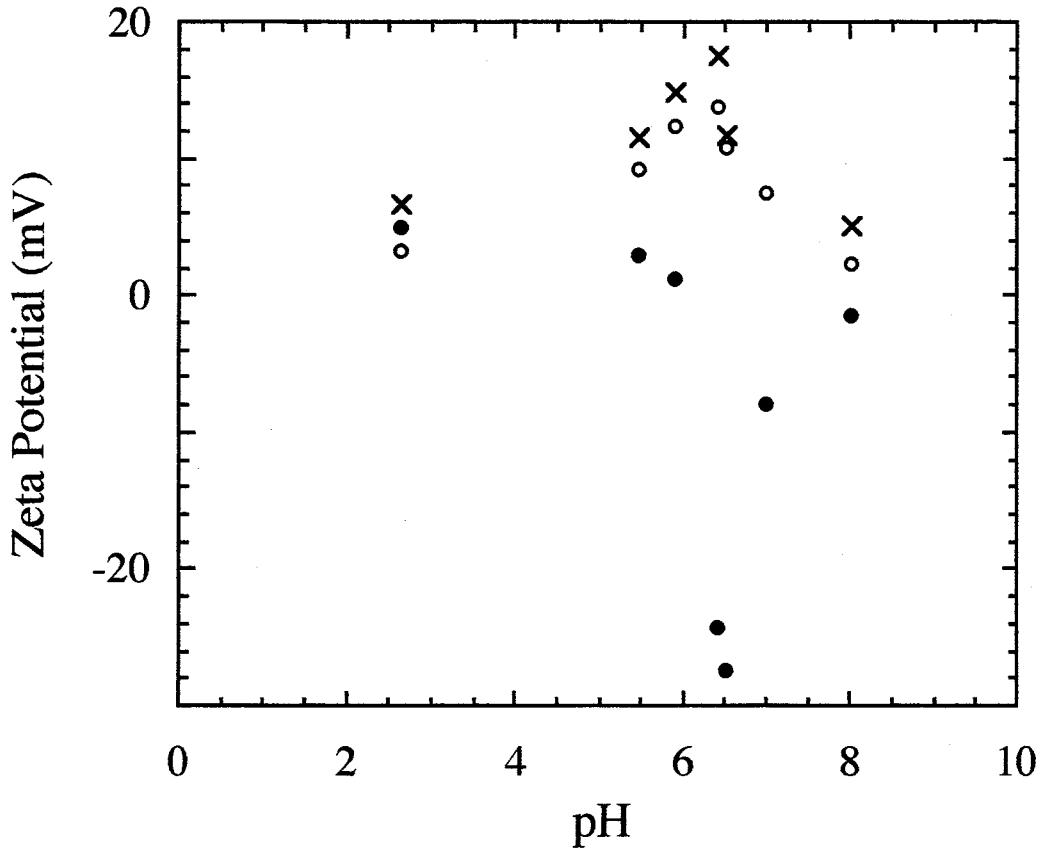

Figure 15. Dependence of the zeta potential of n-type Si (111) surfaces on the pH of the 1 mol dm^{-3} ammonium fluoride solutions which were used for the surface treatment. The potentials were measured 5 minutes (filled cirecle), 12 minutes (open circle), and 19 minutes (cross) after the specimens were immersed in the monitor solution (aqueous solution of 0.01 mol dm^{-3} sodium chloride suspending polystyrene-latex).

2.4 Conclusion

In this chapter, the dissolution process of Si in fluoride-containing solutions has been studied in detail to relate it to the surface chemistry of Si. The finding of the unique pH dependence of Si in 1M NH_4F leads to the newly original proposal for the etching of Si in 1M NH_4F. The proposal is that HF_2^- is a main reactant of the etching of Si in NH_4F solutions. This proposal could be verified by the etching rate measurements by anodic current and gas chromatography. The XPS and Zeta potential study has clarified that the surface chemistry of Si is closely related to the unique pH dependence of Si. Our proposal is also applicable to the flattening process of Si(111) in NH_4F solution.

[Reference]

1) a) P. Jakob and Y.J. Chabal, J. Chem. Phys. 95 (1991) 2897.

b) . Raghavachari, G.S. Higashi, and Y.J. Chabal, and G. W. trucks, Mat. Res. Soc. Symp. Proc. **315** (1993) 437.

c) K. Usuda and K. Yamada, J. Electrochem. Soc. **144** (1997) 3204.

d) Y.-C. Huang, J. Flidr, T. A. Newton, and M. A. Hines, Phys. Rev. Lett. **80** (1990) 4462.

2) P. Allongue, V. Kieling, and H. Gerischer, Electrochim. Acta **40** (1995) 1353.

3) M. Matsumura and H. Fukidome, J. Electrochem. Soc. **143** (1996) 2683.

4) P. Dumas, Y. J. Chabal, and P. Jakob, Surf. Sci. **269/270** (1992) 867

5) U. Neuwald, H. E. Hessel, A. Feltz, U. Memmert, and R. J. Behm, Surf. Sci. **296** (1993) L8.

6) H. Gerischer and M. Lübke, *Ber. Bunsenges. Phys. Chem.*, **91** (1987) 394.

7) G.S. Higashi, Y.J. Chabal, G. W. Trucks and K. Raghavachari, Appl. Phys. Lett. **56** (1990) 656.

8) M. J. Eddowes, J. Electroanl. Chem. **280** (1990) 297

9) T. Imura, K. Mogi, A. Hiraki, S. Nakashima, and A. Mitsushi, Solid. State. Comm. **40** (1981) 161.

10) G.W. Trucks, K. Raghavachari, G.S. Higashi, and Y.J. Chabal, Phys. Rev. Lett. **65** (1990) 504.

11) J. S. Judge, J. Electrochem. Soc. **118** (1993) 1772.

12) S. Verhaverbeke, I. Teerlinck, C. Vinckier, G. Stevens, R. Cartuyvels, and M. M. Heyns, J. Electrochem. Soc. **141** (1993) 2852.

13) F. A. Cottons and G. Wilkinson: Advanced Inorganic Chemistry, A Comprehensive Text, 4th ed., p. 221, Jonh Wiley & Sons, Inc., New York (1980).

14) T. .J. Chang, J. Appl. Phys. **51** (1980) 2614.

15) B.R. Weinberger, G. G. Peterson, T. C. Eschrich, and H. A. Krasinsky, J. Appl. Phys. **60**. (1986) 3232.

16) F.J. Himpsel, F.R. McFeely, A. Taleb-Ibrahimi,and J.A. Yarmoff, G. Hollinger, Phys. Rev., **B38** (1988) 6084.

17) H. Kikuyama, M.Waki, M. Miyashita, T. Yabune, N. Miki, J. Takano, and T. Ohmi, This Journal, **141** (1994) 366.

22) F.A. Cotton, G. Wilkinson, and P.L. Gaus, Basic Inorganic Chemistry, 2nd ed., John Wiley, New York (1987).

18) D. Briggs and M.P. Seah, Practical Surface Analysis, John Wiley, New York (1983).

19) J. Stumper, H.J. Lewerenz, and C. Pettenkofer, Phys. Rev., **B41** (1990) 1592.

20) R. Flitsch and S.I. Raider, J. Vac. Sci. Technol., **12** (1975) 305.

21) J. Szajman, J. Liesegang, J.G. Jenkin, and R.C.G. Leckey, J. Electron Spectrosc. Relat. Phenom., **23** (1980) 97.

22) F.A. Cotton, G. Wilkinson, and P.L. Gaus, Basic Inorganic Chemistry, 2nd ed., John Wiley, New York (1987).

23) S. Watanabe, N. Nakayama, and T. Ito, Appl. Phys. Lett. **59** (1991) 1458.

Chapter 3

Exploration of Parameters Regulating Surface Morphology of Si in NH_4F Solutions

3.1 Introduction

In Chapter 2, the etching mechanism of silicon in fluoride-containing solution was discussed. It was verified that HF_2^- ion is a main species of the etching of silicon in fluoride-containing solutions. However, the relation between the surface morphology on an atomic scale and the etching mechanisms was not fully examined in Chapter 2.

The control of surface and interface morphology on an atomic scale has become one of the central topics in science and technology.[1)] Therefore, many papers have been already published about the surface morphology of materials, especially that of silicon.[1-3)] However, these works are lacking in the chemical viewpoint, while the chemical reactions on the surface must play an important role to control the surface morphology.

Chabal et al. produced the excellent works of surface observation by vibrational spectroscopies for the flattening process of Si(111) in 40% NH_4F.[1), 4-6)] In addition, they also investigates the shape of step structures appeared on the atomically flattened Si(111) by treatment with 40% NH_4F.[5-10)] It was shown that the pH of the solution and the miscut angle of the wafer are the parameters to control the surface morphology. Their results were confirmed by STM observations of these surfaces.[11)] However, they did not obtain clear answers to the relationship between the surface structure and the etching mechanism of silicon.

In this chapter, the parameters to control the surface morphology of Si(111) in 40% NH_4F solution will be examined. Etch pits formation and the shapes of the atomic steps on the surface are the targets in this chapter. In the first part of this chapter, the effects of dissolved oxygen on the flattening process and etch pits formation in 40% NH_4F solution are investigated. It will be shown that dissolved oxygen impedes both flattening and etching rate, while it enhances the etch pit formation. In the latter part, the parameters to affect the shape of dihydride step formed in 40% NH_4F solution will be examined. The critical parameters for the formation of dihydride steps are shown to be pH, dissolved oxygen, the polarity of the substrate, and illumination during the etching.

3.2 Experimental

AFM observation and electrochemical measurements

N-type Si(111) wafers and p-Si(111) wafers with resistivity of about 10 ohm cm were used. N-Si(111) were covered with thermally grown 181-nm-thick oxide to make the Si/SiO_2 interface smooth, while p-Si was not thermally oxidized. Before the measurements of the flattening processes, the wafers were cleaned by the RCA procedure, followed by 5 min dipping into 5% HF aqueous solution to remove the oxide layer. After a short rinse with water, the Si wafers were quickly immersed in a 40% NH_4F solution. To remove oxygen from the solution, two methods were used. One is nitrogen gas bubbling. The other is the addition of sulfite ion (0.05 mol l^{-1}), which is an efficient chemical deoxygenator.

AFM images of Si surfaces were obtained in air using a NanoScope IIIa (Digital Instruments Inc.). Electrochemical measurements of Si electrodes in a 40% NH_4F solution were carried out using a Pt counter electrode and an Ag/AgCl reference electrode. During the measurements, the potential of the Si electrodes was adjusted to 0.0 V vs. Ag/AgCl. The measurements were performed at room temperature (298 K) and at 274 K.

Etching rate of Si(111) measured by the use of gas-chromatography

For dissolution rate measurements by gas chromatography, both side-polished Cz p-type (10 ohm cm) and n-type Fz Si(111) (2-500 ohm cm) wafers were used. These wafers were cleaned by the RCA method, followed by 1 min immersion in 5% HF to remove chemical oxides on the surfaces. Then, the wafers were treated with NH_4F solutions. For the hydorgen evolution measurement (i. e. etching rate measurements), GC-14B (Shimadzu co. ltd.) were used.

3.3 Results and Discussions

3.3.1 Effect of dissolved oxygen on the flattening process: the formation of etch pits and etching of the steps

An AFM image of the Si surface after a 5-min treatment with a 40% NH_4F solution *without oxygen at room temperature* is shown in Fig. 1a. Large terraces and long atomic steps can be seen on the surface. The structure indicates that the Si surface was perfectly flattened at the atomic level after a 5-min treatment in a 40% NH_4F solution without dissolved oxygen. Even after the treatment for 1 min, large terraces appeared on the surface, although the atomic steps meandered a little. On the other hand, when the wafer was treated in a 40% NH_4F solution *with oxygen at room temperature* for 15 min, there were many pimples on the surface, although the surface was basically flattened, as shown in Fig. 1b. After a 1-min treatment in the same solution, there were many triangular etch pits and many irregular steps, and even after a 5-min treatment, many etch pits and many steps remained on the surface. Judging from these results, it is obvious that dissolved oxygen slows down the flattening process in a 40% NH_4F solution at

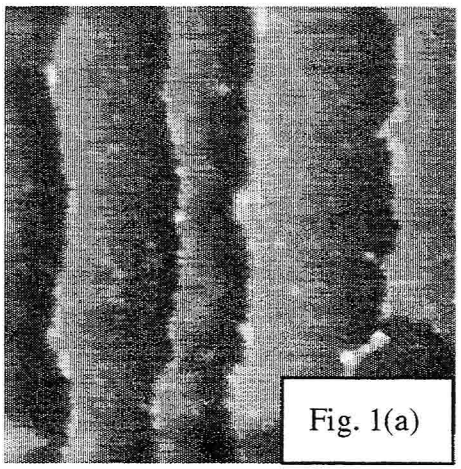

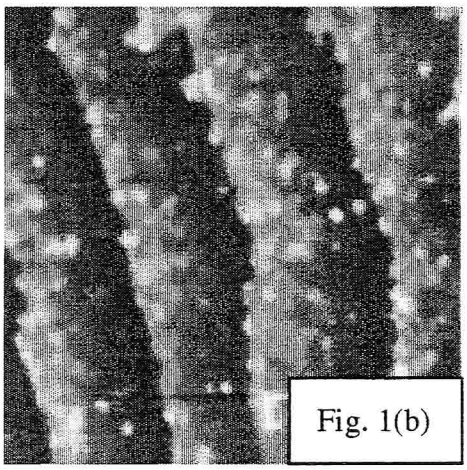

Figure 1

AFM imagesofSi(111) surfaces after treatments at room temperature in 40% NH_4F solutions, (a) without oxygen for 5 min, and (b) with oxygen for 15 min. The AFM scan areas are 500 x 500 nm^2.

room temperature.

At low temperature (274 K), it took longer time to flatten the surface. An AFM image of Si surface after treatment with a 40% NH_4F solution *without oxygen at 274 K* for 10 min is shown in Fig. 2a. Although it takes longer time than at room temperature, the Si surface becomes very flat as the result of the treatment. On the other hand, at low temperature, atomically flat Si surfaces were hardly obtained by the treatment with a 40% NH_4F *with oxygen* even after a 25-min treatment, as shown in Fig. 2b.

From the above results, two conclusions can be deduced about the flatting process of Si. First, dissolved oxygen always hinders the flattening process. Second, a longer time is required to flatten Si surfaces in a 40% NH_4F solution at low temperature, although the final surface

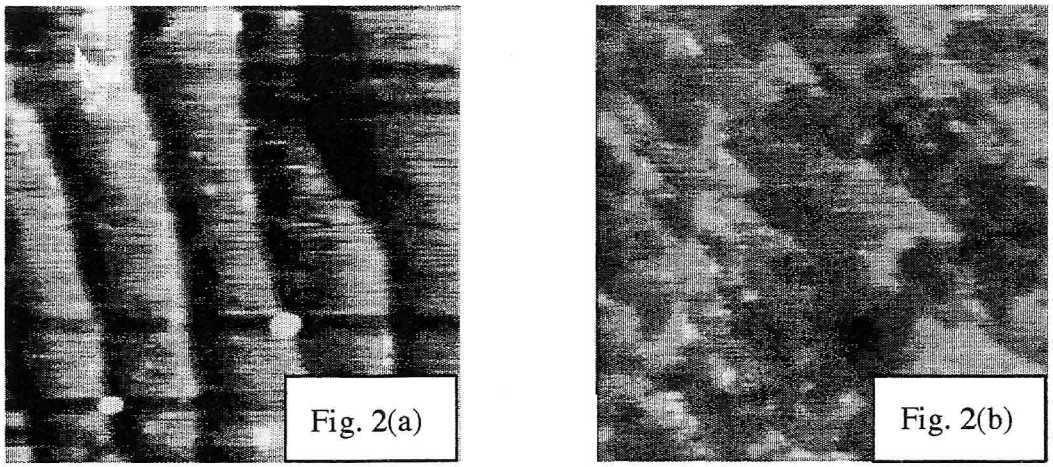

Figure 2

AFM images of Si(111) surfaces after treatments at 274 K in 40% NH_4F solutions, (a) without oxygen for 10 min, and (b) with oxygen for 25 min. The AFM scan areas are 500 x 500 nm^2.

becomes very flat in the absence of oxygen.

Concerning the etching behavior of Si in fluoride containing solutions, we have reported that electrochemical measurements of the anodic current of n-type Si electrodes are very useful.[12), 13)] The characteristics of the anodic currents of Si electrodes are as follows: (1) The current density is independent of potentials in the region above 0.0 V Ag/AgCl, or under the reverse bias condition in the terminology of semiconductor physics. (2) The current density is quantitatively in agreement with the dissolution rate of Si into the solution, if we assume that Si atoms are dissolved into the solution in the form of SiF_6^{2-}. (3) The density of the anodic current (and the dissolution rate) depends on temperature, concentration of fluorine compounds in the solution, and pH of the solution. It is worthwhile to note that the etching rate of Si in strong alkaline solutions is reported to depend on the applied voltage.[14)]

Figure 3 shows the anodic currents of n-Si electrodes measured at room temperature in 40% NH_4F solutions with and without dissolved oxygen. The currents started flowing immediately after the electrodes were immersed in the solution, owing to the chemical dissolution of Si into the solution. Interestingly, the current density was lower in the solution with oxygen than in the solution without oxygen. Another interesting feature is that the current density reached a maximum at about 10 s after immersion into the solution when measured in the solution in the presence of oxygen. The current gradually decayed and leveled off at the densities of about 50 and 80 μ A cm^{-2}, for the measurements in the solutions with and without oxygen, respectively.

When the anodic currents were measured at low temperature (274 K), they showed tendencies similar to those observed at room temperature, but the current density was much lower than that obtained at room temperature, as shown in Fig. 4. Furthermore, at low temperature, the currents drastically decreased with time.

These properties of electrochemical anodic currents are consistent with the morphological changes of the Si surface observed after the treatments. The lower current densities at low temperature correspond to the result that a longer treatment was required to get flat surfaces. The temperature dependence is attributed to the activation energy of the chemical dissolution of Si into the solution. Assuming that the current density directly reflects the rate of dissolution, the activation energy of about 96 kJ mol^{-1} is estimated from the density of the anodic currents in the steady state measured in a 40% NH_4F solution at different temperatures. Gerischer et al. esti-

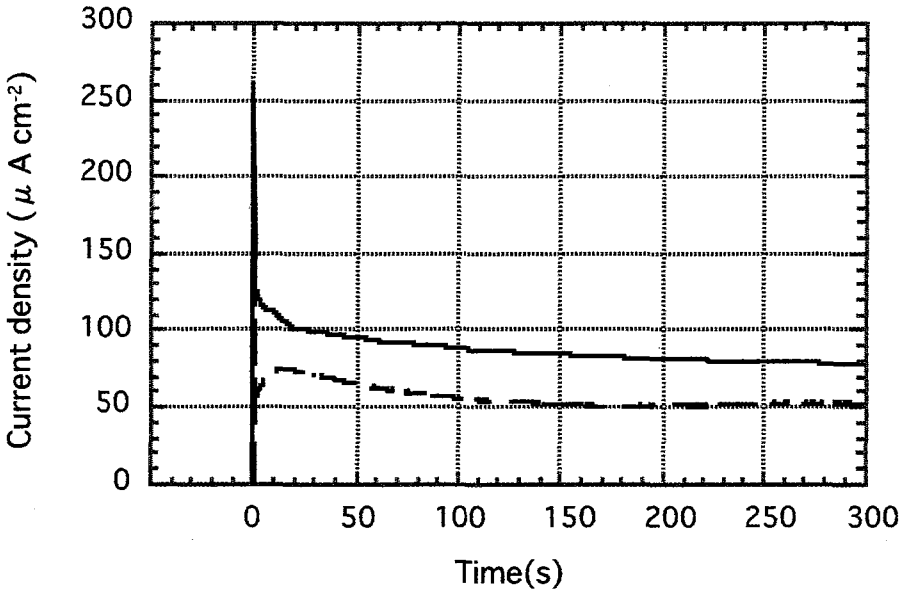

Figure 3. Anodic currents of n-Si electrodes measured at room temperature in 40% NH_4F solutions with oxygen (broken line) and without oxygen (solid line).

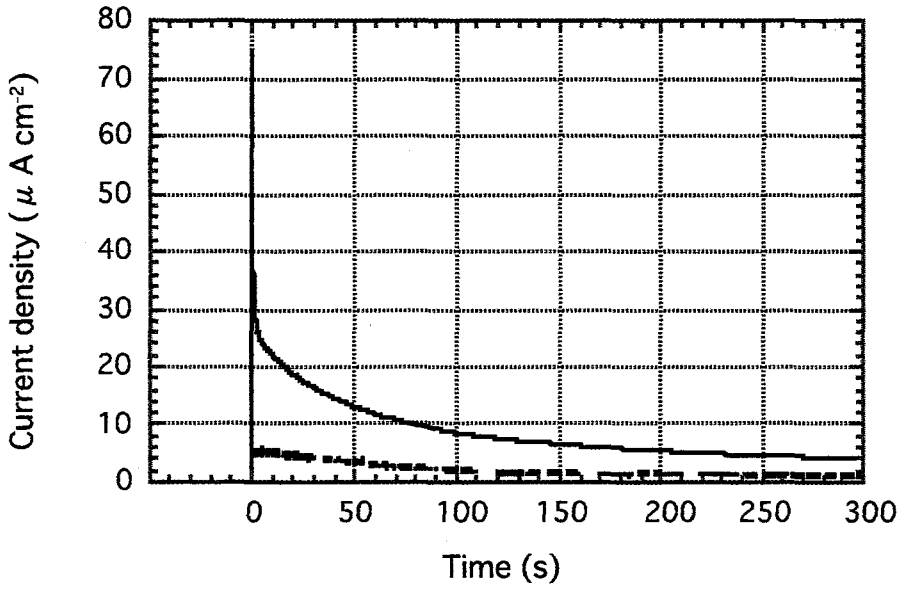

Figure 4 Anodic currents of n-Si electrodes measured at 274K in 40% NH_4F solutions with oxygen (broken line) and without oxygen (solid line).

mated an activation energy of about 53 kJ mol^{-1} for the anodic current of Si wafers in a 1 mol/l NH_4F solution at pH 4.5[15]; their Si surfaces are probably rougher than ours judging from their preparation conditions.

Comparing the results shown in Figs. 1 and 3 for the surfaces treated at room temperature without oxygen, we find that the anodic current of about 80 μ A cm^{-2} kept flowing even at the time when clear steps and large terraces were observed by AFM observation. This result in turn suggests that the steps on the surface were continuously dissolved under these conditions. The activation energy estimated by us is, therefore, related to the dissolution of the step sites by HF_2^- ions.

At low temperature (274 K), the current density decreased to a level as low as 4 μ A cm^{-2} in the solution without oxygen, indicating that the dissolution of Si becomes very slow when the surface is flattened. This low current density indicates that the etching rate of monohydride steps as well as terraces can be hardly etched due to the large acivation energies for the ethcing of these. The drastic decrease of the current for the initial period for about 5 min (see Fig. 4) is, therefore, considered to be related to the flattening processes starting from the surface with many kink sites on the surface. Namely, the current density observed at low temperature should be roughly proportional to the density of kink sites on the surface.

In order to determine the etching rate of Si(111) at open circuit potential, we measured hydrogen gas evolved during Si dissolution by the use of gas chromatography. The details of this etching rate measurements were decribed in Chapter 2. From the result, the etching rate of Si(111) in 40% NH_4F without dissolved oxygen at 298 K was found to be faster than in the solution with dissolved oxygen by a factor of 1.8. This result clearly indicates that dissolved oxygen reduces the etching rate of Si(111) also at open citcuit potential.

When oxygen is present in the solution, it may attack both steps and terraces because of its chemical reactivity. The reactions lead to the formation of etch pits and irregular steps, together with a longer treatment time to get flat surfaces. Besides these effects, oxygen in the solution is found to lower the current densities, as shown in Figs. 3 and 4. Such an effect by oxygen suggests that oxygen retards the flattening reaction at the kink sites. A possible mechanism of this effect is that oxygen protects the kink sites from the attack of HF_2^- ions. We have postulated that the flattening is caused by the attack at the kink sites by HF_2^- ions, which proceeds in a chain

reaction.[12), 13)] On the basis of this mechanism, oxygen is expected to compete with the HF_2^- ions for the kink sites to retard the flattening process by stopping the chain reaction.

In a 40% NH_4F solution containing oxygen, the anodic current started rising when the electrodes were immersed in the solution, and it took about 10 s and 15 s before the currents reachded the maximum, at 295 and 273 K, respectively, as shown in Figs. 3 and 4. These times are probably required to change the bonding of the kink sites to the quasi-equilibrium conditions, at which some of the kink sites form Si-F bonds.[16)] On the other hand, without oxygen in solution, the maximum of the anodic current appeared soon, because the surface is changed to the quasi-equilibrium conditions rapidly. The reason for this is that there is no competition between oxygen and HF_2^- ions for the kink sites.

We demonstrated that flat Si surfaces at an atomic level are obtained by the treatment of Si wafers with a 40% NH_4F solution from which oxygen is removed using sulfite ions as a deoxygenator. From the study of electrochemical anodic currents we think that oxygen hinders the flattening process occurring at the kink sites, leading to a low etching rate. It was also found that the treatment at low temperature in the absence of oxygen was effective to improve the selectivity of the flattening reaction.

3.3.2 Control of the shape of atomic steps: monohydride vs. dihydride steps

In this section, the control of the formation of the dihydride step in NH_4F solutions will be discussed. For the sake of clarity, the parameters to control the shape of the steps will be discussed in the order of 1) pH of the solution, 2) dissolved oxygen, 3) polarity of substrates, and 4) illumination during etching. In all experiments, the concentration of NH_4F solutions is 11.7 mol/l (equal to that of pure 40% NH_4F).

For a better understanding of AFM images of the surface shown in this section, representative surface structures of Si(111) after treatment with NH_4F solution are schematically shown in Fig. 5. When a silicon sample is misoriented in the direction of $<\bar{1}\bar{1}2>$, nominal steps should be di-hydrogenated. However, monohydride steps usually appear on this stepped surface.[5), 6), 11)] The reason for this is that dihydride steps are more easily etched in the solution than monohydride steps. The monohydride steps are oriented at 60 degrees relative to the direction of nominal steps. A hillock (shaded region) is enclosed with two monohydride steps on the nominal steps (dihydride steps). These two monohydride steps of the hillock are crossed with each other at 60 degrees.

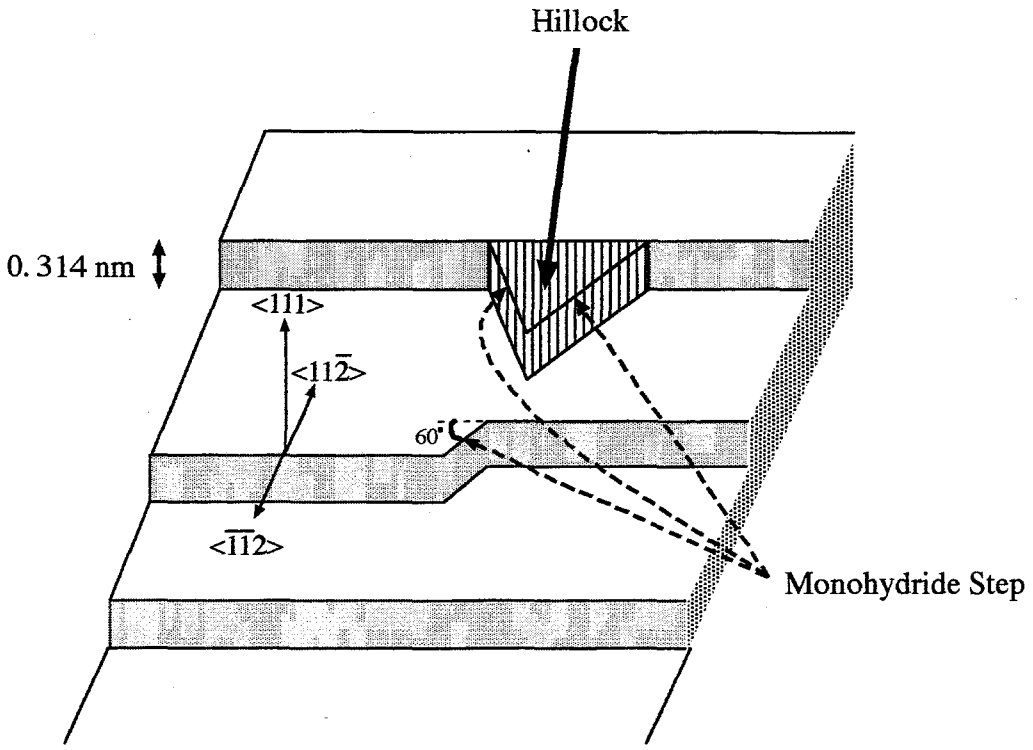

Fig. 5 A schematic picture of Si(111) surface misoriented in the direction of $<\bar{1}\bar{1}2>$. A shaded protrusion on the dihydride steps is called hillock. The steps other than the monohydride steps marked by dashed arrows are dihydride steps.

To consider the microscopic etching rate of the sites on Si(111) surface, the atomic structure of Si(111) surface misoriented in the direction of $[\bar{1}\bar{1}2]$ is shown in Fig. 6. The terraces are seperated by steps which are mono- or di- hydrogenated, and Si atoms on the terraces are mono-hydrogenated. Previous works showed that the microscopic etching rates of the sites in Fig. 6 increase in the order; terrace monohydride < step monohydride < step dihydride.[7), 17), 18)] Besides, it can be assumed that the dihydride at the tip of the hillock should be more easily etched than step dihydride. The reason for this argument is as follows; As for the dihydride at the tip, the adjacent silicon atom is hydrogenated and are positively charged, while, as for the dihydride on the steps, the adjacent silicon atom is not hydrogenated and, therefore, not charged. In conclusion, the microscopic etching rates are in the order; terrace-monohydride < step-monohydride < dihydride at the step < dihydride at the tip of the hillock.

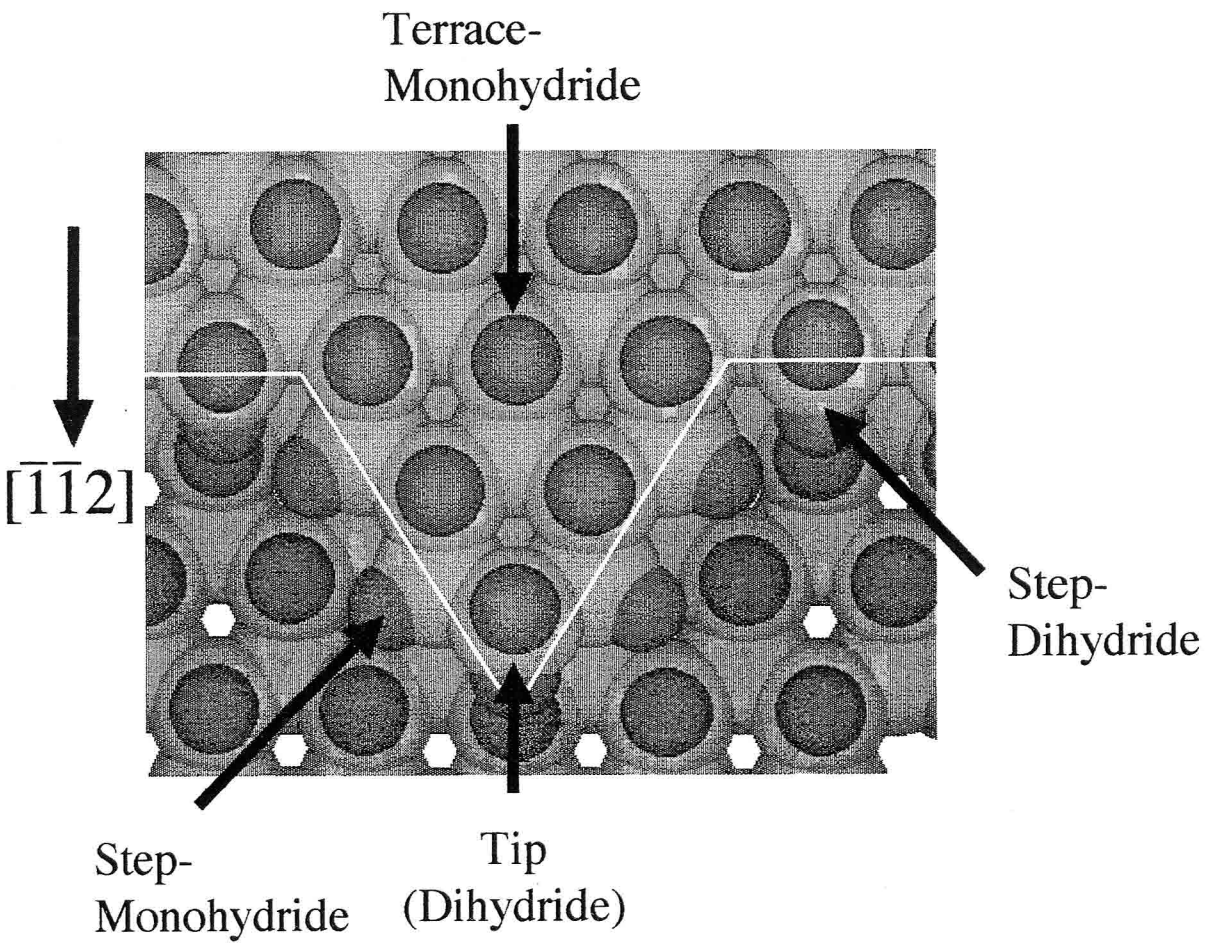

Fig. 6 The atomic structure of Si(111) surface misoriented in the direction of <$\bar{1}\bar{1}$2> (top view). The white line is the guide for eye to see the edge of the upper terrace.

According to the work by Flidr et al., the size of hillock is determined, in part, by a balance between hillock growth and hillock decay, as shown in Fig. 7. Imagine an extended region that contains N_{mono} step-monohydride sites, N_{di} step-dihydride, N_t dihydride sites at the tips of hillocks. The average rate of hillock growth, which is rate-limited by verical dihydride etching, is given by;

$$k_{grow} = N_{di} \times k_{di} \quad (1)$$

Similarly, the average rate of hillock decay will be given by;

$$k_{decay} = N_t \times k_t + N_{mono} \times k_{mono} \quad (2)$$

From equation (1) and (2), the size of hillock, i .e., the shape of dihydride steps can be determined by three microscopic etching rates, k_{di}, k_t and k_{mono}. In what follows, these microscopic etching rates will be discussed by the results of AFM and macroscopic etching rates, based on the arguments here.

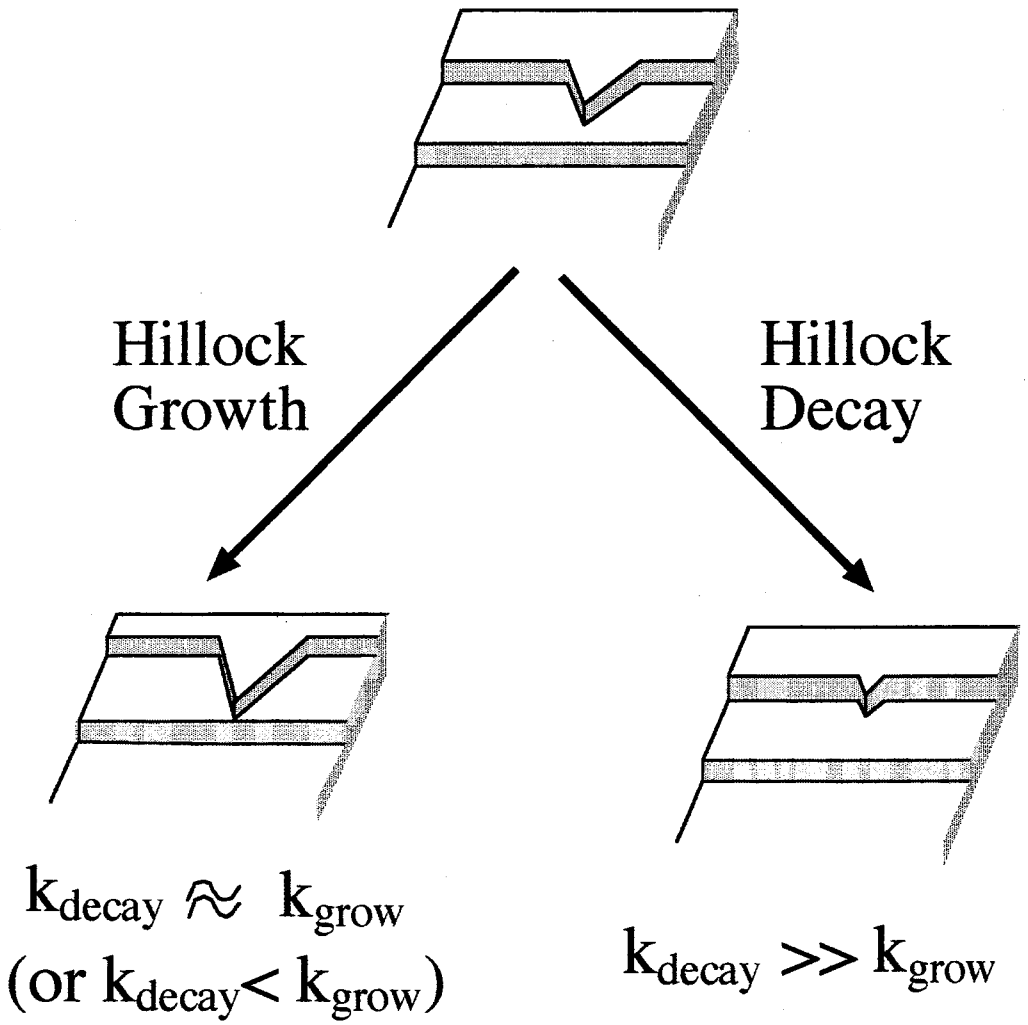

Fig. 7 Hillock size is determined by a balance between growth and decay.

3.3.2.1 Effect of pH of the solution

The wafers used are p-Si(111) misoriented in the direction of $<\bar{1}\bar{1}2>$ at an angle of 0.5 degrees. The pH's of the solutions were 6.6, 7.0, and 7.5 (pure 40% NH_4F). The solutions contained dissolved oxygen (DOC is about 4 ppm). The intensity of illumination (room light) during the treatment was 0.2 mW cm^{-2}.

Fig. 8 shows the AFM images of the surface treated with 40% NH_4F (pH = 7.5). It can be seen that straight dihydride steps are formed, and hillocks and kinks decrease as the etching time elapsed. The result is in contrast with previous papers which reported that zigzag monohydride steps are formed on the wafer slightly misoriented in the direction of $<\bar{1}\bar{1}2>$.[11)]

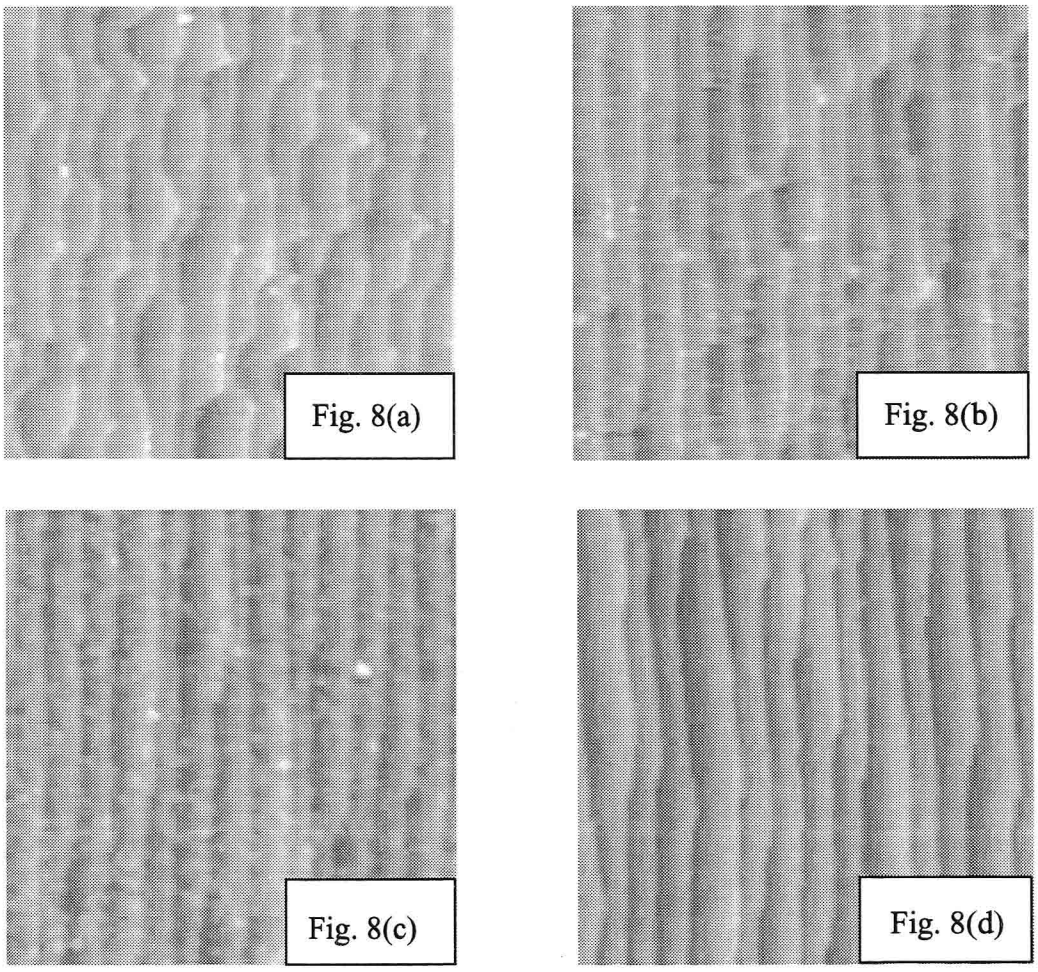

Fig. 8 AFM images of p-Si(111) treated with 40% NH_4F (pH 7.5) with dissolved oxygen (DOC is about 4 ppm). The wafers were misoriented in the direction of $<\bar{1}\bar{1}2>$ at an an angle of 0.5 degrees; (a) 1 min treatment; (a) 3 min treatment;(c) 5 min treatment; (d) 10 min treatment.

Decrease in the pH of the solution leads to the increase in the hillocks formed on the steps, and monohydride steps oriented at 60 degrees relative to dihydride steps increases in number and size (Figs. 9 and 10). At pH 7, although straight dihydride steps appear on the surface, hillocks and monohydride step increase, compared to the surface etched in 40% NH_4F solution (pH 7.5). At pH 6.6, hillocks formed on the surface dramatically increase, as shown in Fig. 10. Hence, it can be said that at pH 6.6 the monohydride steps are predominately formed on the surface, compared to the surfaces treated with the above two solutions (Figs. 8 and 9).

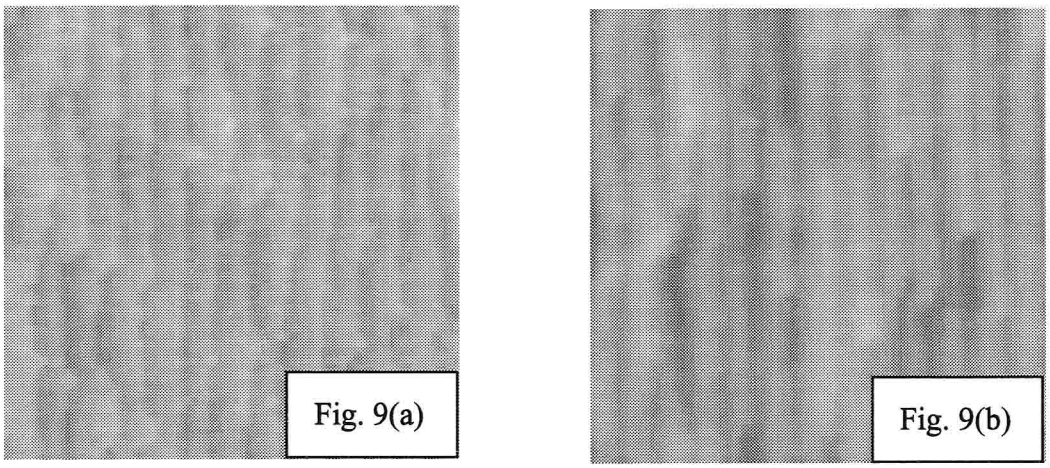

Fig. 9 AFM images of p-Si(111) treated with NH_4F (pH 7.0) with dissolved oxygen. The wafers were misoriented in the direction of $<\bar{1}\bar{1}2>$ at an an angle of 0.5 degrees. (a) 5 min treatment; (a) 10 min treatment.

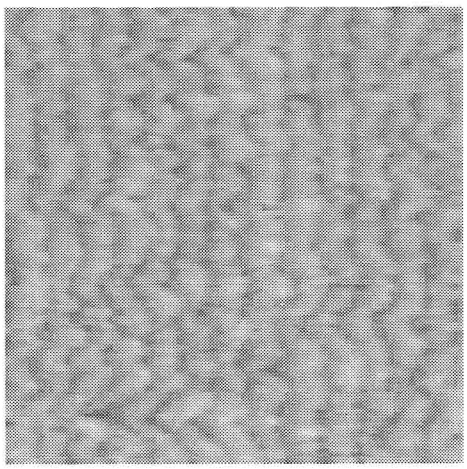

Fig. 10 AFM images of p-Si(111) with NH_4F (pH 6.6) with dissolved oxygen for 10min. The wafer was misoriented in the direction of $<\bar{1}\bar{1}2>$ at an an angle of 0.5 degrees.

To clarify the reason for the change on the shape of the steps on the surfaces, the etching rate of Si in the NH_4F solutions ([NH_4F] = 11.7 mol/l) was investigated, as shown in Fig. 11. The pH range of the measured solutions is 5 to 8. Above pH = 8, etching rate could not be measured, because the ammonium salt of fluoride was precipitated due to its solubility limit. In the pH range from 5 to 6.6, the etching rate is almost constant. On the other hand, above pH 6.6, the etching rate steeply increases. The pH dependence is similar to that observed in 1M NH_4F solution (see Chapter 2), although the etching rate in 40% NH_4F is higher than by a factor of about 10.

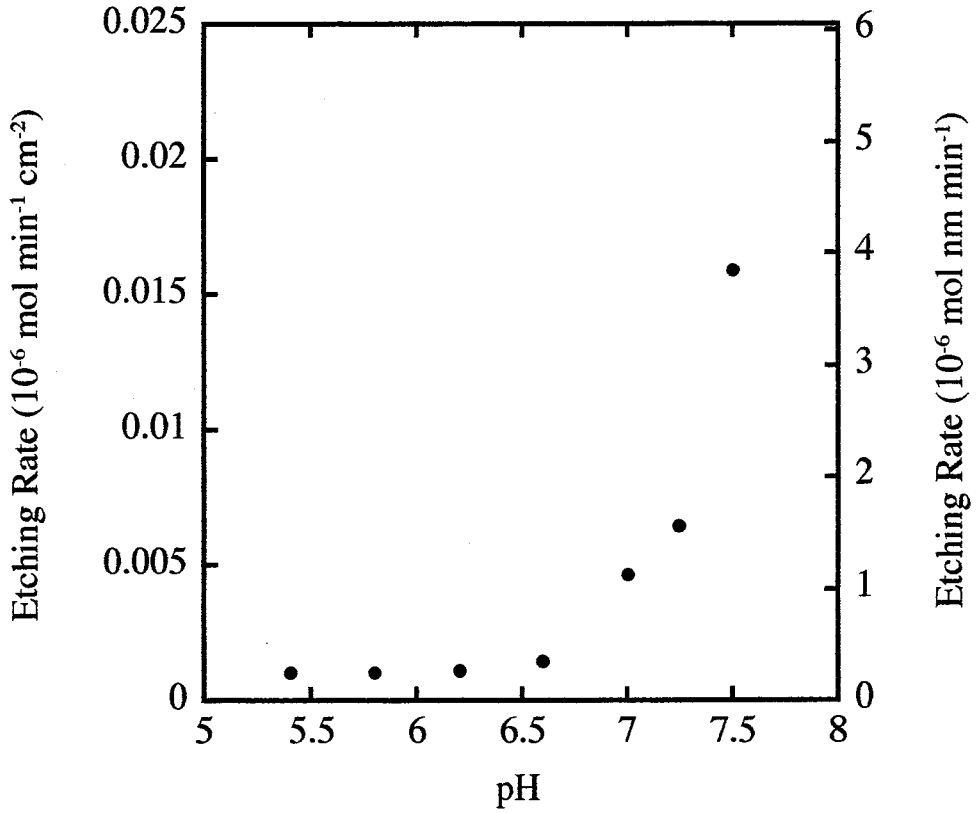

Fig. 11 pH dependence of etching rates of p-Si(111) in 40% NH_4F with dissolved oxygen.

The scenario which was explained before (pp. 52) can be used to examine our results, as follows; To a first approximation, k_{mono} is ignored here because, in general, it should be much smaller than k_{di} and k_t. That is, only k_{di} and k_t are discussed in the arugument below. When pH of the solution increases from 6.6 to 7.5, the hillocks decrease in size and number, and macroscopic etching rate steeply increases. This indicates that the increase in the macroscopic etching rate in this pH range is due to the increase of the microscopic etching rate at the tip of the hillocks. In the pH range below 6.6, the etching rate of the tip of the hillocks is lowered to be comparable to that of straight

dihydride steps. Hence, the zigzag monohydride steps are present on the surface due to the formation and growth of hillocks, as shown in Fig. 11. In conclusion, the increase of pH leads to the change of etching mechanism of the steps, i.e., from the hillock growth mode to the hillock decay mode.

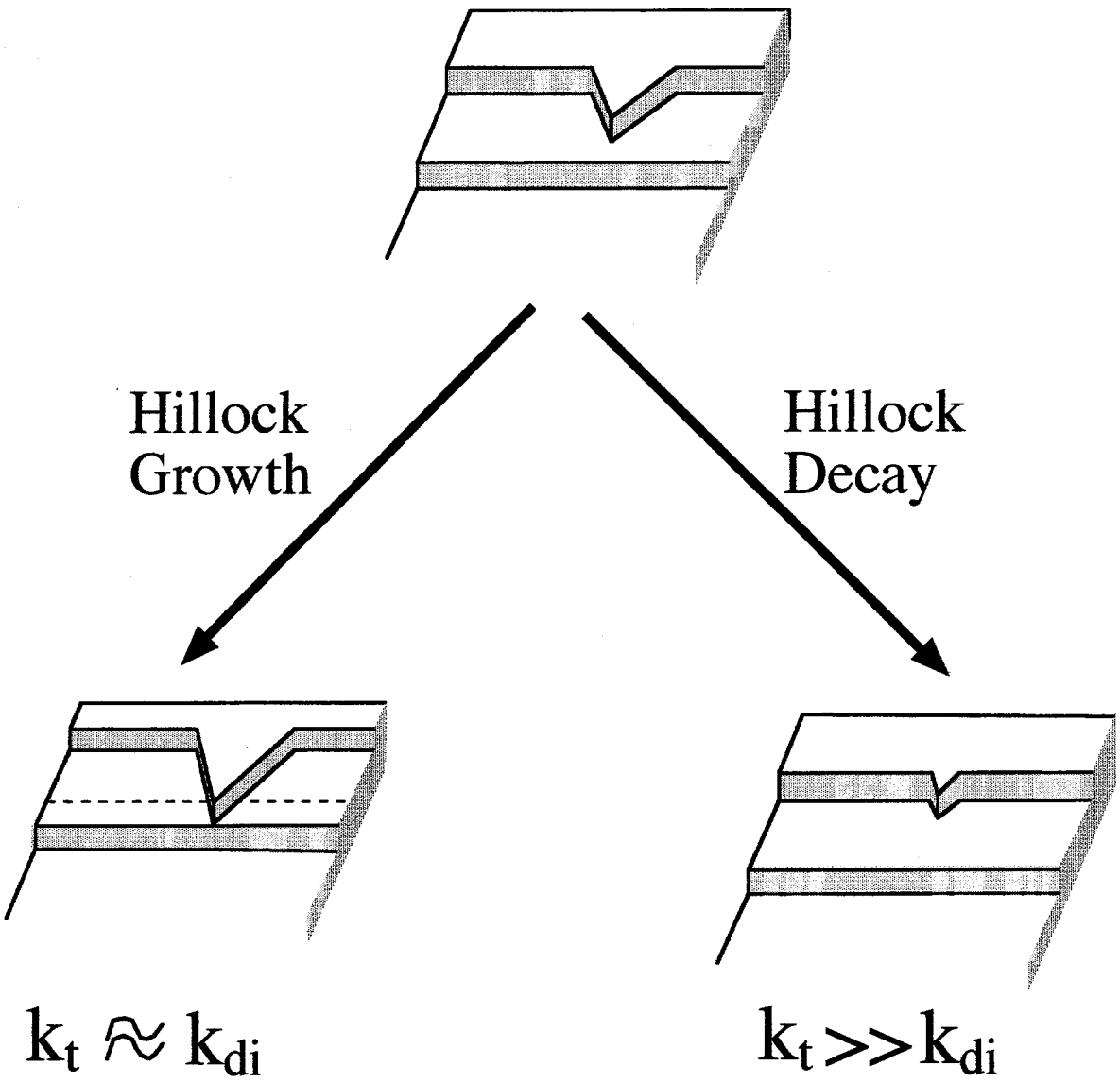

Fig. 12 Hillock size (and the shape of dihydride steps) on the step is determined by k_{di} and k_t.

3.3.2.2 Effect of dissolved oxygen

The effect of dissolved oxygen on the shape of steps on p-Si(111) formed in 40% NH_4F is discussed. In the experiments, the intensity of illumination (room light) during the treatment was 0.2 mW cm^{-2}. Dissolved oxygen was removed by nitrogen gas bubbling or by adding sulfite ion.

Fig. 13(a) shows an AFM image of the p-Si(111) surface after the 10 min treatment with 40% NH_4F where dissolved oxygen was removed by nitrogen gas bubbling (DOC: 50 ppb). The hillocks composed of monohydride steps appeared on the dihydride steps. When dissolved oxygen concentration is decreased to a lower level by the addition of sulfite ion (DOC: 4.1 ppb), larger hillocks appeared and dihydride steps disappeared on the surface (Fig. 13(b)). On the contrary, as has already shown in Fig. 6, straight dihydride steps appeared on the surface when the solution contains dissolved oxygen (DOC is about 4 ppm). These results suggest that dissolved oxygen preferentially passivates the dihydride steps during the etching in 40% NH_4F solutions.

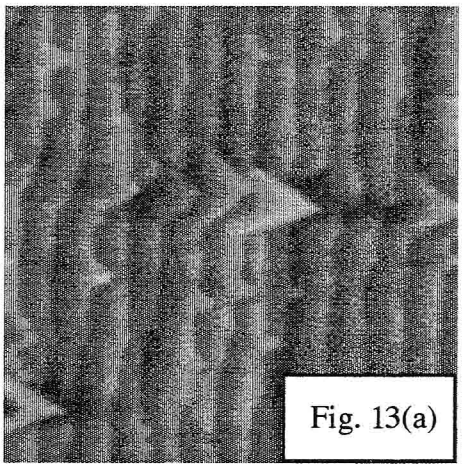

Fig. 13(a)

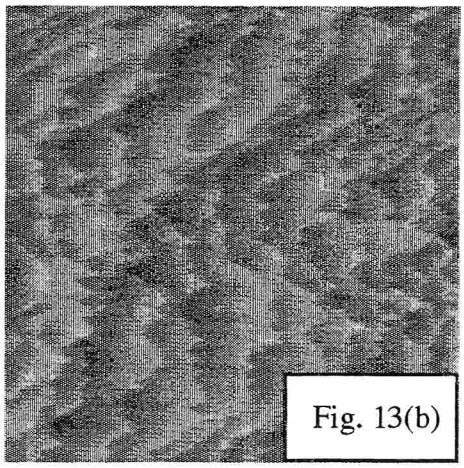

Fig. 13(b)

Fig. 13 AFM images of p-Si(111) treated with 40% NH_4F (pH 7.5) for 10min without dissolved oxygen. The wafers are misoriented in the direction of $<\bar{1}\bar{1}2>$ at an an angle of 0.5 degrees. (a) DOC is 50 ppb (by nitrogen gas bubbling); (b) DOC is about 4 ppb (by the addition of sulfite ion).

To examine the effect of dissolved oxygen in detail, the etching rates of p-Si(111) in 40% NH_4F with (DOC: 3.6 ppm) and without (DOC: 4.1 ppb) dissolved oxygen were measured. As a result, the etching rate of p-Si(111) in the solution without dissolved oxygen was found to be lower than that in the solutions without dissolved oxygen by a factor of about 1.2. Hence, it can be concluded that removal of dissolved oxygen increases k_{di}, that is, dissolved oxygen passivates the striaight dihydride steps.

3.3.2.3 Effect of polarity of the substrate

The polarity of the substrates, i.e., n- and p- types, is also an important factor in the control of the shape of the steps. On n-Si(111) surface, zigzag monohydride steps appeared instead of straight dihydride steps after the treatment with 40% NH_4F solutions with and without dissolved oxygen, as shown in Fig. 14. This is contrast to the case of p-Si(111) surface, which showedstraight dihydride steps on the surface, as was shown in Fig. 6. These results imply that the density of free carriers (electron and/or holes) affects the surface morphology.

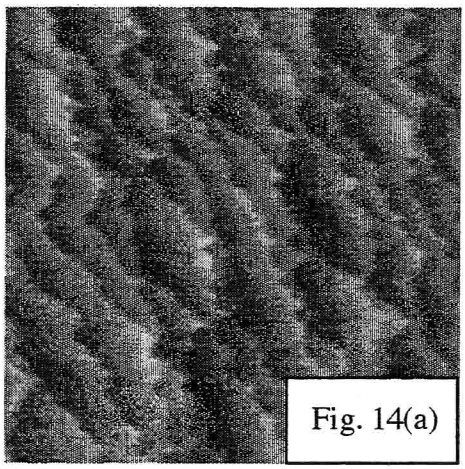

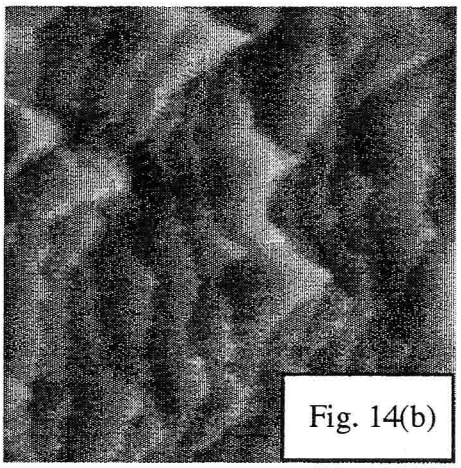

Fig. 14 AFM images of n-Si(111) slightly treated with 40% NH_4F (pH 7.5) for 10 min, with (a) and (b) without dissolved oxygen. The wafers were slightly misoriented in the direction of $<\bar{1}\bar{1}2>$

3.3.2.4 Effect of illumination

Light intensity incident on the wafer during the treatment was also found to be an important factor in controlling the surface morphology. When the p-Si(111) was treated with 40% NH_4F with dissolved oxygen (3.6 ppm) in the dark, small hillocks on the straight dihydride steps are present on the surface (Fig. 15(a)). On the other hand, under weak illumination (0.2 mW cm^{-2}), straight dihydride steps without hillocks are formed on the surface, as shown in Fig. 15 (b). Under strong illumination (2 mW cm^{-2}), many etch pits are formed on the surface, and steps are meandering (Fig. 15(c)).

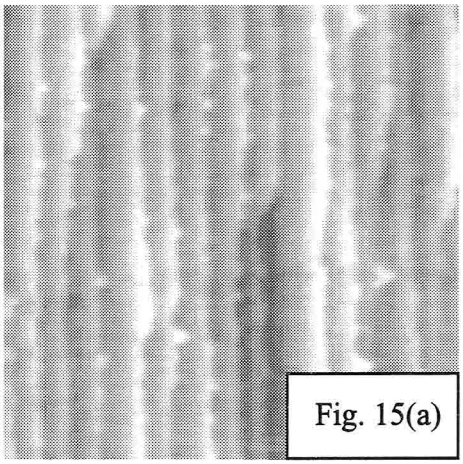

Fig. 15(a)

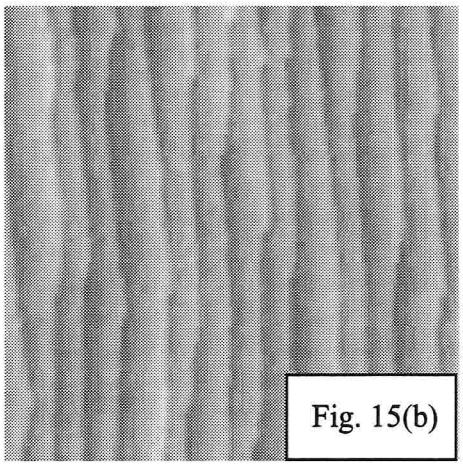

Fig. 15(b)

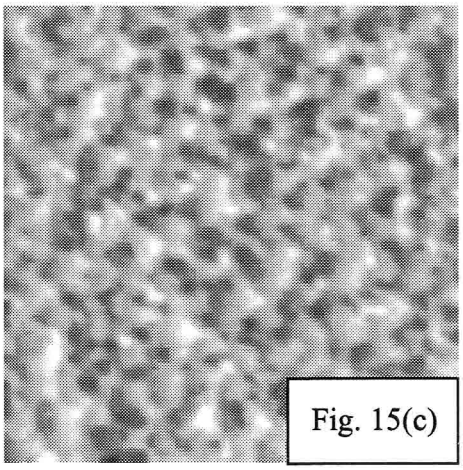

Fig. 15(c)

Fig. 15 AFM images of p-Si(111) misoriented treated with 40% NH_4F (pH 7.5) with dissolved oxygen for 10 min. (a) in the dark; (b) under weak illumination (0.2 mW cm^{-2});(c) under strong illumination (2 mW cm^{-2}). The wafers were misoriented in the direction of $<\bar{1}\bar{1}2>$ at an an angle of 0.5 degrees .

Etching rate measurements showed that weak illumination during the etching enhances the etching rate by a factor of 1.5. This result suggests that dissolution of dihydride steps is enhanced under weak illumination.

The open circuit potential (OCP) of the p-Si wafers was measured in the dark and under illumination. In the dark, the OCP is -0.89 V (vs. Ag/AgCl). It was -0.69 V and -0.35 V under weak illumination and strong illumination, respectively. A flatband potential of Si(111) in 40% NH_4F is reported to be 0.8 V (vs. Ag/AgCl).[19] This anodic shift of open circuit potential leads to the increase in the density of holes at the surface, and this is considered to be the cause of the increased etching rate. In fact, it has been already confirmed that holes can accelarate the etching of silicon,[2] and previous in-situ STM observations clarified that the etching rate of n-Si is increased under anodic bias.[14), 20)]

From the results of AFM observation (Fig. 15), the etching rate measurements and the shift of OCP, it can be supposed that, under weak illumination, hole on the surface increases both k_t and k_{mono}, and that, under strong illumination, hole on the surface increase both k_t and k_{mono} and the etching rate at terrace sites. The reasons for these are as follows; 1) Under weak illumination, the density of hole is limited so that hole concentrates on the tip and/or the monohydride steps of the hillocks. 2) Under strong illumination, the density of hole increases so that hole exists on the terraces as well as at the tip and/or the monohydride steps of the hillocks.

3.4 Conclusion

In this chapter, the etching process of Si(111) surface were microscopically examined in detail by AFM observations and measuring macroscopic etching rate. It was revealed that pH, dissolved oxygen, holes on the surface affect the surface morphology of Si(111) during the etching in NH_4F solution. The results obtained in this chapter may lead to the flattening of Si(100).

[References]

1) G. S. Higashi and Y. J. Chabal: Handbook of Semiconductor Wafer Cleaning Technology, ed. W. Kern (Noyes Publications, New Jersey, 1993), p. 433.

2) P. C. Searson: Advances in Electrochemical Science and Engineering, Vol. 4, ed. H. Gerischer and C. W. Tobias (VCH, Weinheim, 1995), p. 67.

3) K. Oura, V.G. Lifshits, A.A. Saranin, A.V. Zotov, M. Katayama, Surf. Sci. Rep. **35** (1999) 1, and the references therein.

4) G.S. Higashi, Y.J. Chabal, G. W. Trucks and K. Raghavachari, Appl. Phys. Lett. **56** (1990) 656.

5) P. Jakob and Y. J. Chabal, J. Chem. Phys. **95** (1991) 2897.

6) P. Jakob, Y. J. Chabal, K. Raghavachari, R. S. Becker, A. J. Becker, Surf. Sci. **275** (1992) 407 .

7) P. Jakob, Y.J. Chabal, K. Kuhnke, S.B. Christman, Surf. Sci. **302** (1994) 49.

8) M. A. Hines, Y. J. Chabal, T. D. Harris, and A. J. Harris, Phys. Rev. Lett. **71** (1993) 2280.

9) M. A. Hines, Y. J. Chabal, T. D. Harris, and A. J. Harris, J. Chem. Phys. **101** (1993) 8055.

10) K. Raghavachari,P. Jakob, and Y. J. Chabal, Chem. Phys. Lett. **206** (1991) 156.

11) a) G. J. Pietsch, U. Kohler, and M. Henzler, J. Appl. Phys. **73** (1993) 4797.
b) Y. Morita, K. Miki, and H. Tokumoto, Appl. Surf. Sci. **60/61**(1992) 466.

12) M. Matsumura and H. Fukidome, J. Electrochem. Soc. **143** (1996) 2683.

13) H. Fukidome and M. Matsumura, J. Electrochem. Soc. **144** (1997) 679.

14) P. Allongue, V. Costa-Kieling, and H. Gerischer, J. Electrochem. Soc. **140** (1993) 1009.

15) H. Gerischer and M. Lübke, Ber. Bunsenges. Phys. Chem. **91** (1987) 394.

16) From our preliminary XPS measurements on the concentration of F-atoms on Si surfaces, it was found that the concentration reached a maximum after treatment for about 10 s in a 40 % NH_4F solution containing oxygen at 274 K. The time was in agreement with that for the appearance of the peak of the anodic current in the same solution (see Fig. 3).

17) J. Flidr, Y.-C. Huang, T. A. Newton, and M. A. Hines, Chem. Phys. Lett. **302** (1999) 85.

18) J. Flidr, Y.-C. Huang, T. A. Newton, and M. A. Hines, J. Chem. Phys. **111** (1999) 6970.

19) P. Allongue, V. Kieling, and H. Gerischer, Electrochim. Acta **40** (1995) 1353.

20) J. H. Ye, T. H. Bok, J. S. Pan, Sam. F. Y. Li, and J. Y. Lin, J. Phys. Chem. B **103** (1999) 5820.

Chapter 4

Dissolution Processes of Si(111) in water and alkaline solutions

4.1 Introduction

Etching of Si in water and alkaline solution is becoming key processes in semiconductor industry.[1),2)] Following the etching of Si in fluoride-containing solutions,[1)] the atomistic understanding of the etching of Si surface in water and alkaline solutions has also progressed.[1),2)] Watanabe et al. discovered that the Si(111) surfaces can be ideally H-terminated by treatment with boiling water.[3)] They clarified that the concentration of dissolved oxygen is a critical parameter in the hydrogenation of Si in water.[4)] Allongue et al. found that Si(111) can be atomically flattened in 1M NaOH solution under cathodic bias, while at rest potential Si(111) cannot be flattened.[5),6)]

The mechanisms of the etching process of Si in water and alkaline solutions has not been fully established yet, though the surface structures of Si has been well understood. Even the main species of Si etching in the solutions has not been clarified yet. In addition, the effect of pH and dissolved oxygen on the etching mechanism and surface morphology has not been fully understood. Some researchers have pointed out the effect of oxygen in strong alkaline solution, however, there is a room for debate.[2)] Further developments in ULSI and micromachining need the complete understanding of the etching process and surface conditioning.

The purpose of this chapter is to examine the effects of pH and dissolved oxygen on both surface structures and etching mechanism in water and alkaline solutions. The work presented in this chapter are divided into three parts. First, AFM and FTIR observations of Si(111) surface treated in water and alkaline solutions will be presented. The observations were done for Si(111) surface treated in water (pH=7), weakly alkaline solution (pH=12), and strong alkaline solution (pH=14). It will be shown that pH and dissolved oxygen are critical parameters for the morphology and composition of Si(111) surface. Second, in-situ AFM observation of Si(111) in water (pH 7) will be presented. The obervation reveals that the selectivity of the etching of Si(111) in water is higher than in other etchants. Lastly, etching rate measurements of Si(111) in the solutions by the use of gas chromatography will be presented. It will be shown that H_2O is a major etching species in neutral solutions while OH^- is a major etching species of Si in alkaline solutions. The relation between surface morphology and etching mechanisms will be examined in detail.

4.2 Experimental

(Observation of Si(111) treated in water)

We used p-type Si(111) wafers misoriented in the direction of <11$\bar{2}$> at an angle of 0.37° or in the direction of <$\bar{1}\bar{1}$2> at an angle of 0.5° . The resistivity of the wafers was 10-20 ohm cm. The samples (1 x 1 cm^2) cut from the wafers were successively cleaned with acetone and ethanol, followed by a water rinse. Subsequently, they were etched in a 5% HF solution to remove a native oxide layer from the surfaces. The samples thus prepared were treated with water, which contained 0.05 mol dm^{-3} ammonium sulfite as deoxygenator, at room temperature. The content of oxygen in this solution was determined to be 0.9 ppb using an oxygen meter (Orbisphere Lab., Model 3600); hereafter, we call this solution chemically deoxygenated water (CDW). The pH of the solution was about 7. The surfaces of the samples were imaged with a tapping mode atomic force microscopy (AFM) (Digital Instruments, Nanoscope IIIa). FT-IR measurements of the Si(111) surfaces were conducted by the ATR (attenuated total reflection) method, using a germanium prism and a p-polarized light beam.[1)]

(Observation of Si(111) treated in alkaline solutions)

Three kinds of Si(111) wafers were used for the experiments. For atomic force microscopy (AFM) measurements, Cz-n-type Si(111) wafers whose resistivity is 10 ohm cm were used. For FTIR measurements, Fz n-type wafers whose resistivity was 2-500 οημ cm were used. These wafers were cleaned by RCA method, followed by 1 min immersion in 5% HF to remove chemical oxides on the surfaces. Then, the wafers were treated in 2.5% aqueous ammonia with different dissolved oxygen concentrations. Nanoscope IIIa was used for AFM observations. For FTIR measurements, Si wafer itself was used as a prism for multiple internal reflectin, and the short edges is bevelled at 45 degrees in order to couple the radiation in and out for multiple internal reflection. FTS-575C (BIO-RAD Laboratories) was used for FTIR measurements.

(In-situ AFM observation of Si(111) in water)

We used p-type Si(111) wafers slightly misoriented in the direction of <11$\bar{2}$>. The resistivity of the wafers was 10-20 ohm cm. The wafers were cut into 1.8 x 1.8 cm^2 pieces. Prior to experiments, the samples were cleaned sequentially with acetone and ethanol, and etched in a 5% HF solution to remove a native oxide layer from the surface. Oxygen-free water was prepared by

adding ammonium sulfite as a deoxygenator at a concentration of 0.05 mol dm^{-3} to ultra pure water supplied from MINI PURE TW-300RU (Nomura Micro Science). The solution showed a pH of about 7. In-situ contact-mode AFM observations of the Si(111) surface misoriented in the direction of $[1\bar{1}2]$ at an angle of 0.37° in oxygen-free water were performed using a PicoSPM™ (Molecular Imaging). The spring constant of the cantilever was 0.12 N/m. The force between the tip and the sample was minimized by adjusting the operation parameter of setpoint to avoid mechanical damage.

(Etching rate measurements of Si(111) by the use of gas-chromatography)

For dissolution rate measurements by gas chromatography, both-side polished Cz p-type and Fz n-type Si(111) wafers whose resistivity are 10 ohm cm and 2-500 ohm cm, respectively, were used. These wafers were cleaned with RCA method, followed by 1min immersion in 5% HF to remove chemical oxides on the surfaces. Then, the wafers were immersed in the solutions. For dissolution rate measurements, GC-14B(Shimadzu co. ltd.) was used to measure hydrogen evoluiton rate.

4.3 Results and Discussions

4.3.1 Ex-situ observation of Si(111) surface treated with water and alkaline solutions

4.3.1.1 Observation of Si(111) surface treated with chemically deoxygenated water (pH=7)

The AFM images of p-Si(111) misoriented in the direction of **<11$\bar{2}$>** before and after the treatment with chemically deoxygenated water (CDW) for 5 min and 20 min are shown in Fig. 1(a) , (b) and (c), respectively. The surface just after the treatment with a 5% HF solution is atomically rough, as seen from Fig. 1 (a). By contrast, Si(111) was atomically flattened after the treatment with CDW where dissolved oxygen is completely removed (DOC:0.1 ppb), as shown in Fig.1 (b) and (c). On the Si(111) treated with CDW for 5min (Fig. 1(b)), the surface was atomically flattened, although triangular etch pits, composed of monohydride steps, were on the terraces. On the Si(111) treated with CDW for 20 min (Fig. 1(c)), the surface is composed of wide terraces and atomically straight steps. Mean terrace widths separated by the steps are in good agreement with that estimated from the miscut angle of the wafer (48.6 nm). The step height (0.3 nm) indicates that the steps are the bilayer steps[7), 8)], and the miscut-orientation of the surface suggests that they are monohydrogenated.[8-10)]

The flatness of the surface after 20 min treatment (Fig. 1(c)) is comparable to the Si(111) surface treated with a 40% NH_4F solution for 15 min.[7)] The time needed to flatten Si(111) is almost the same as that in 40% NH_4F, while the etching rate of Si(111) in water is smaller than that in 40% NH_4F by more than an order of magnitude. This suggests that the selectivity of the etching of Si(111) in water is higher than in 40% NH_4F. The reason for this selectivity of Si etching in theses two solutions is that the main reactants in these solutions are different. In water, H_2O molecule is the main reactant of Si etching as will be proven in the later section, while HF_2^- is the main reactant of Si etching in NH_4F solutions as shown in Chapter 2. Because H_2O is less reactive than HF_2^-, the etching of Si in CDW is more selective than in 40% NH_4F.

When Si(111) surfaces misoriented in the direction of **<1$\bar{1}\bar{2}$>** were treated with CDW, the surfaces were atomically flattened, and steps appeared with a characteristic zigzag pattern, oriented 60° each other, as shown in Fig. 2. They are also attributed to the monohydride steps.[8)] The average distance between the steps (37 nm) is in good agreement with the miscut angle of

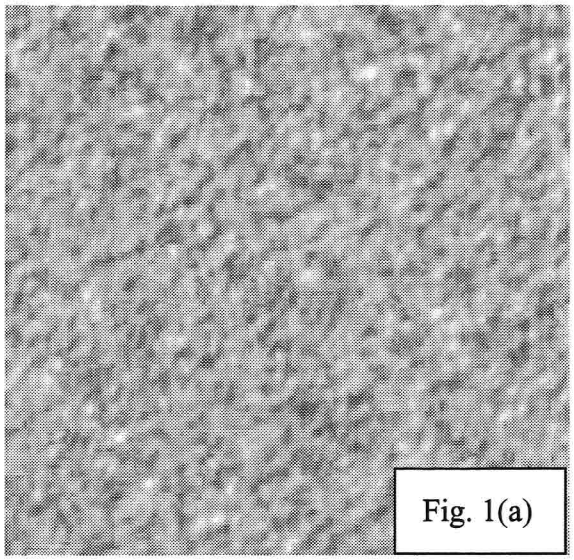

Fig. 1(a)

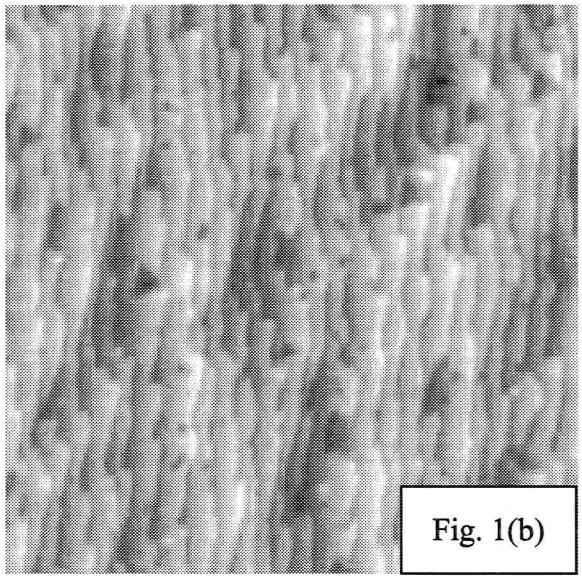

Fig. 1(b)

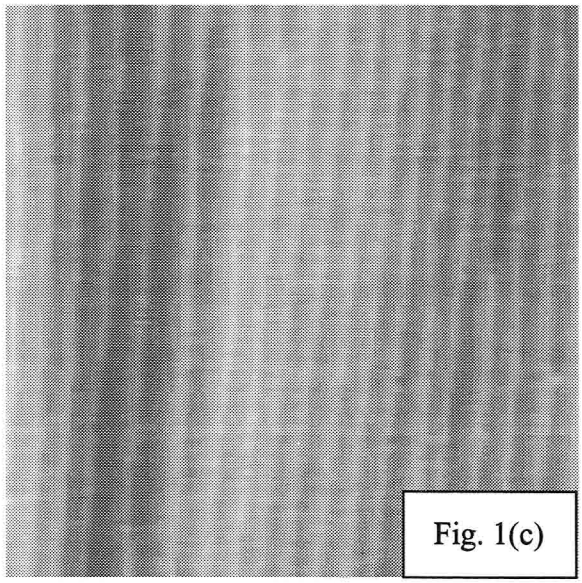

Fig. 1(c)

Fig. 1 AFM images of Si(111) surface before and after the treatment with water : before the treatment in water (a), and after 5 min (b), 20 min (c) treatments. Scan sizes are 1 x 1 μ m^2.

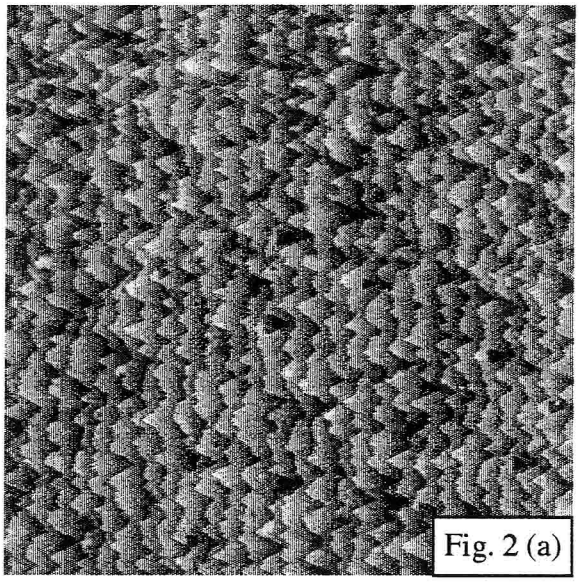

Fig. 2 (a)

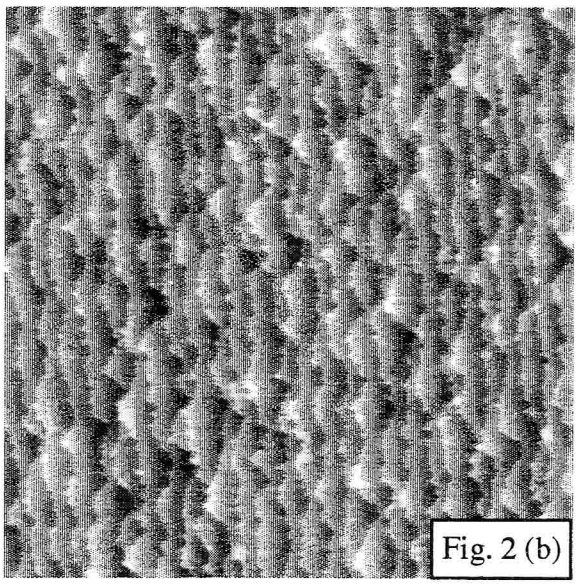

Fig. 2 (b)

Fig. 2 p-Si(111) surface misoriented in the direction of $<\bar{1}\bar{1}2>$ treated with CDW for 1 min (a) and 5 min (b), respecively.Scan sizes are 1 x 1 μ m^2.

the wafer. As the etching time elapsed, etch pits and triangular hillocks (composed of monohydride steps) on the steps decrease in number. Therefore, it can be seen that the ratio of dihydride steps to monohydride steps increases a little with a passage of the treatment time. However, straight steps like Fig. 1(c) has never been obtained. Compared with the treatment with 40% NH_4F without dissolved oxygen, the size of the hillocks is very small. This can be ascribed to the lower etching rate of Si in CDW.

FT-IR measurements of the Si(111) surfaces were done to investigate the termination and flatness of the surface. For the measurements, attenuated total reflection method was adopted, using a germanium prism and a p-polarized light beam.[1)] After the removal of the native oxide layer on the surface with a 5% HF, observed were the absorption bands due to monohydrides on terraces (centered at about 2080 cm^{-1}), coupled monohydrides (centered at about 2070 cm^{-1}), and dihydrides (centered at about 2100 cm^{-1}), as shown by a plain line in Fig. 3. Therefore, Si(111) surface at this stage is hydrogen-terminated but atomically rough . On the other hand, the wafer treated with oxygen-free water for 5 min showed an intense and narrow band due to monohydrides on terraces, as shown by a bold line in Fig. 3. This result indicates that Si(111) is ideally hydrogen-terminated by CDW treatment.

For comparison, when the Si(111) wafers were treated with water bubbled with nitrogen (99.99 pure), no flattened Si(111) surfaces were obtained. By this method, the oxygen concentration in water was lowered to 25 ppb. In fact, Watanabe et al. reported that at room temperature Si(111) cannot be atomically flattened by 30min immersion in water where dissolved oxygen is removed by bubbling with inert gas (DOC is below 5 ppb).[3)] Usuda et al.[11)] reduced the concentration of oxygen in water below 5 ppb by thorough purging with inert gas. Using this water, they obtained a flattened Si(111) surfaces at room temperature after the treatment for 50 h. On their surfaces, however, still many etch pits and kinks were present. The effectiveness of our chemically deoxygenated water to flatten Si(111) surfaces is attributable to the high ability of sulfite ion to reduce dissolved oxygen (DOC: 0.1 ppb). The results obtained suggest that water can be a good etchant of Si even at room temperature, if oxygen is thoroughly removed.

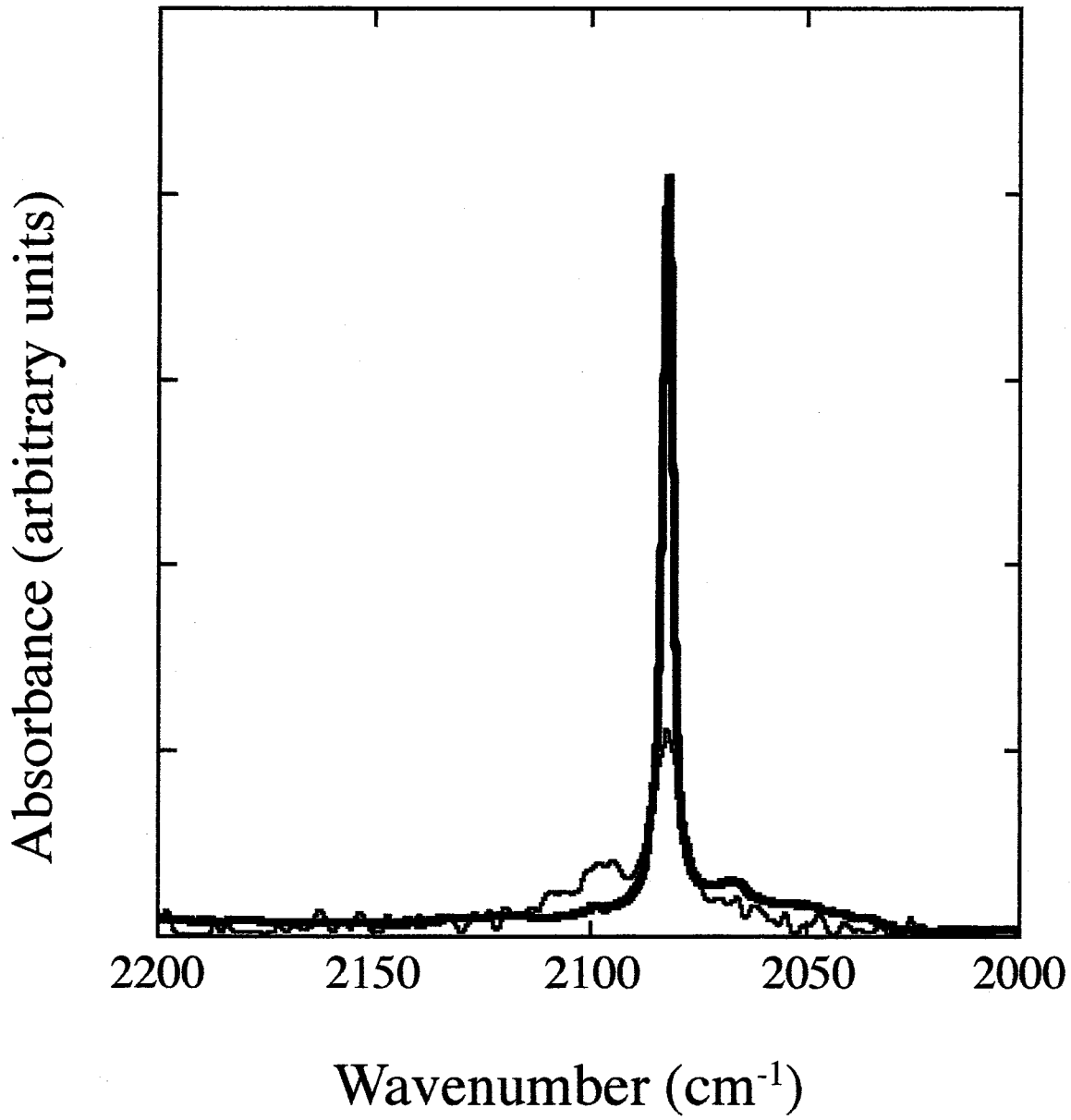

Fig. 3 FTIR spectra of Si(111) before (bold line) and after the treatment in water 5min (plain line). The spectrum shown in this figure are p-polarized.

4.3.1.2 Observation of Si(111) surface treated with weakly alkaline solutions (pH=12)

First, AFM observations of Si(111) surface treated with 2.5% aqueous ammonia (pH=12) with different dissolved oxygen concentrations (DOC) are shown. The wafer is slightly misoriented in the direction of $<11\bar{2}>$. Therefore, straight monohydride steps should appear on the surface of the wafer when the surface is ideally hydrogen-terminated.

On Si(111) surface immersed in air-saturated 2.5% aqueous ammonia (DOC is about **8 ppm**), many etch pits were formed on the surface, as shown in Fig. 4. This is in agreement with previous reports that Si(111) surface cannot be atomically flattened in alkaline solution at open circuit potential.[5), 6), 12), 13)]

The shape of etch pits on these surfaces is triangular or hexagonal, whilst only triangular etch pits were formed after the treatment with 40% NH_4F.[8)] Hence, it can be conculded that the selectivity of the etching in this solution is lower than in 40% NH_4F solution. In fact, the selectivity of the etching can be quantitatively analysed from the shape of etch pits, according to a recent paper of kinetic Monte Carlo simulation for wet etching of Si(111).[14)] Based on the results in this paper, we elucidated the ratio of the etching rate of monohydride steps (k_{mono}) and dihydride steps (k_{di}) in weakly alkaline solutions from Fig. 4 (c). The ratio of the etching rate of monohydride step (k_{mono}) to that of dihydride step (k_{di}) is estimated to be $1/10<k_{mono}/k_{di}<1$. On the other hand, the shape of etch pits formed in 40% NH_4F is trangular.[8)] Accordong to the report, k_{mono}/k_{di} is estimated to be below 1/100 for the etching of Si(111) in 40% NH_4F. Hence, the etching of Si(111) surface in weakly alkaline solutions is less selective than in 40% NH_4F by more than an order of magnitude.

The density of the etch pits increased as the treatment time was exteneded;1.5×10^{10} cm^{-2} for 1 min treatment, 2×10^{10} cm^{-2} for 5 min treatment, 2.5×10^{10} cm^{-2} for 10 min treatment. On the other hand, in 40% NH_4F solution containing dissolved oxygen (DOC: 8 ppm), few etch pits appeared on Si(111) surface.[7), 15), 16)] Hence, it is now clear that dissolved oxygen in weakly alkaline solution can more easily initiate the formation of etch pits than in 40% NH_4F.

Fig. 5 shows AFM images of Si(111) surface treated with 2.5% aqueous ammonia where dissolved oxygen is decreasd by nitrogen gas bubbling (DOC:**25 ppb**). The AFM images show that staircase structures are formed by the treatment with this solution. The height of the steps is 0.3 nm. This means that these steps are bilayer steps.[7), 8)] The density of the etch pits decreases with time; 3×10^{9} cm^{-2} for 1 min treatment, 3×10^{8} cm^{-2} for 10 min treatment. These values are much

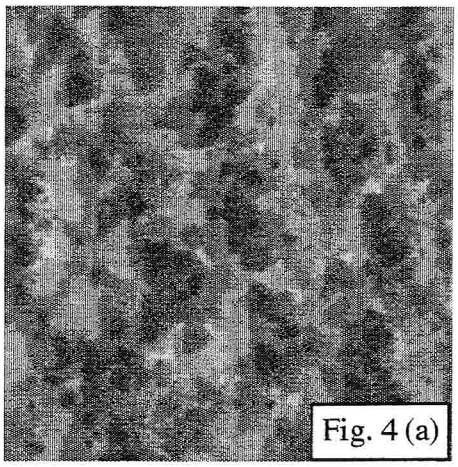

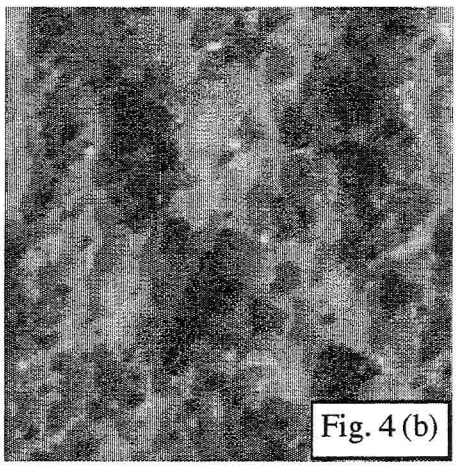

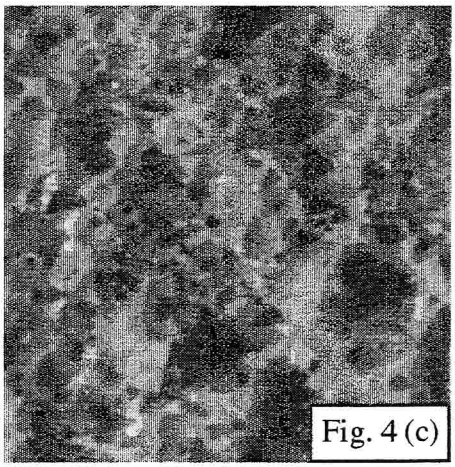

Fig. 4 AFM image of Si(111) treated with 2.5% NH_4OH at room temperature with O_2 (DOC: 9 ppm) for 1min (a), for 5min (b), and 10min (c). The scan areas are 1 x 1 μ m^2.

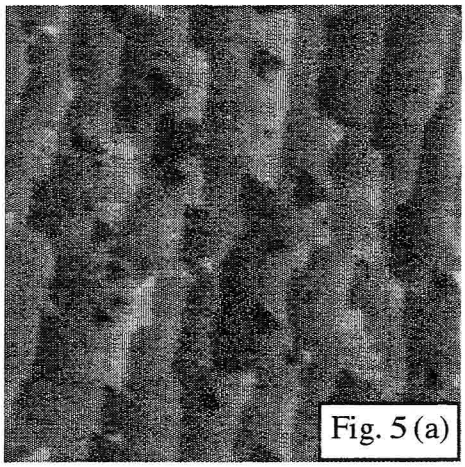

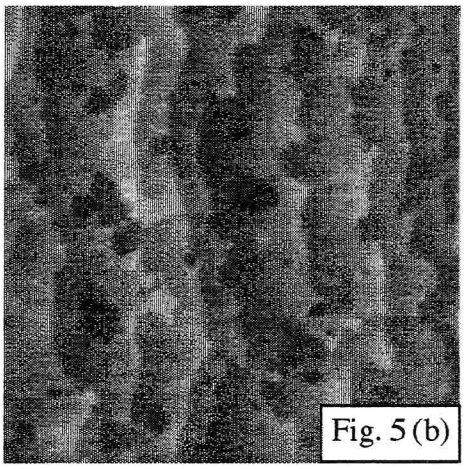

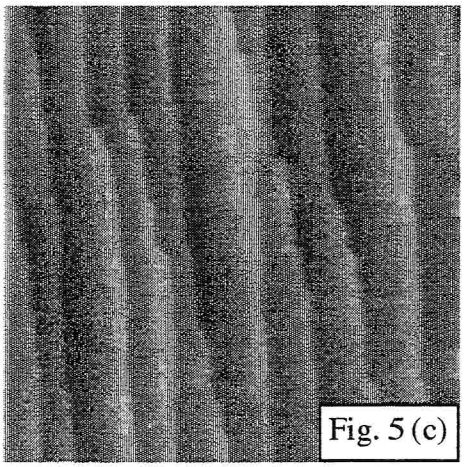

Fig. 5 AFM image of Si(111) treated with 2.5% NH_4OH bubbled with N_2 gas (DOC: 25 ppb) at room temperature for 1 min (a), 5 min (b), and 10 min (c). The scan areas are 1 x 1 μ m^2.

smaller than that after treatment with the air-saturated solution. The density of kinks also decreases with time; 2 x 10^{10} cm^{-2} for 1 min treatment, and 5 x 10^{9} cm^{-2} for 10 min treatment. Steps extended straightforwardly 100–200 nm. The flatness of Si(111) surface treated in this solution (Fig. 5(c)) is comparable to that treated in 40% NH_4F for 15 min.[7] Hence, the flattening rate of Si(111) in this solution is concluded to be almost as same as that in 40% NH_4F. The results shown in Figs. 4 and 5 indicate that oxygen in alkaline solution initiates etch pits.

To investigate the effect of dissolved oxygen in more detail, we investigated the surface morphology of Si(111) after treatment with 2.5% NH_4OH solution, from which dissolved oxygen is more effciently removed by the addition of sulfite ion (DOC:**5ppb**). Then, it was found that Si(111) can be atomically flattened within 1 min as shown in Fig. 6(a). The degree of the flatness of this surface (the density of etch pits is below 3 x 10^{9} cm^{-2}, the density of kinks is 5 x 10^{9} cm^{-2}) is almost as same as that of the surface treated with 2.5% aqueous ammonia for 10 min, where dissolved oxygen is removed by nitrogen gas bubbling (DOC:**25ppb**). In addition, the flatness of this surface is comparable to that treated with 40% NH_4F for 15min. Hence, the flattening rate of Si(111) is found to be larger than that in 40% NH_4F. The selectivity of the etching in this solution is almost as same as that in 40% NH_4F.

The flatness of the surface was improved by extending the treatment time (Figs. 6(a) and (b)) in the above solution. The density of etch pits on the surface treated with this solution for 10 min is below 1 x 10^{8} cm^{-2}, the density of kinks is 2.5 x 10^{9} cm^{-2}. These values indicate that this solution can produce the best surface among the above 2.5% NH_4OH solutions with higher dissolved oxygen concentration.

The point to be noted is that step bunching occured on the surface treated with the solution (DOC:5ppb) for 5 min (Fig. 6(b)) and 10 min (Fig. 6(c)). The reason for the occurrence of step bunching is the high etching rate of Si in this solution. This warrant can be supported by an experimental fact that the step bunching did not occur when the temperature of the solution was lowerd to 273 K (Fig. 7). Furthermore, step bunching did not occur when Si(111) surfaces were treated in 40% NH_4F and water. Etching rates of Si(111) in water and 40% NH_4F solutions are much smaller than that in 2.5% NH_4OH solutions, as will be shown in the later section (Chapter 4.3.3). The above results (Figs. 4-7) show that DOC is a critical parameter to control the flatness of Si(111) in alkaline solutions.

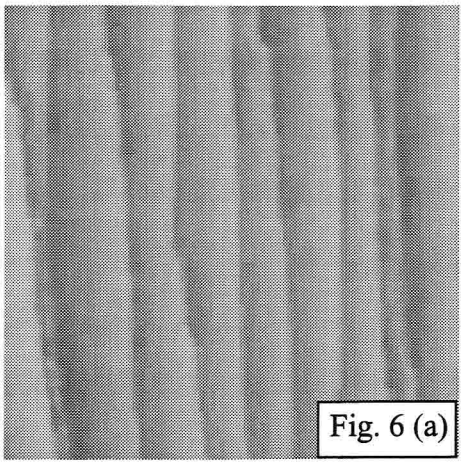

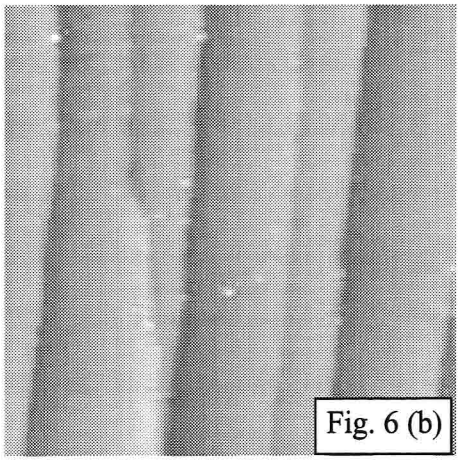

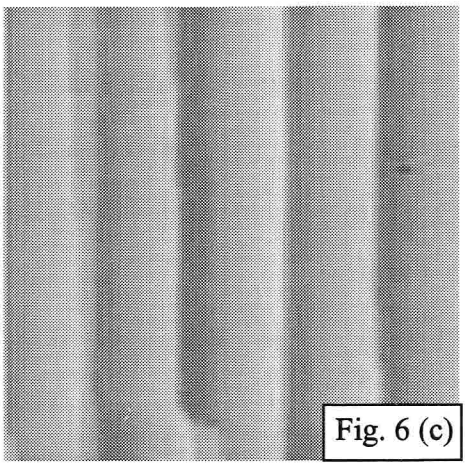

Fig. 6 AFM image of Si(111) treated with oxygen-free 2.5% NH_4OH (DOC : 5 ppb) at room temperature, for 1 min (a), 5 min (b), and 10 min (c). Dissolved oxygen is removed by the addition of sulfite ion. The scan areas are 1 x 1 μm^2.

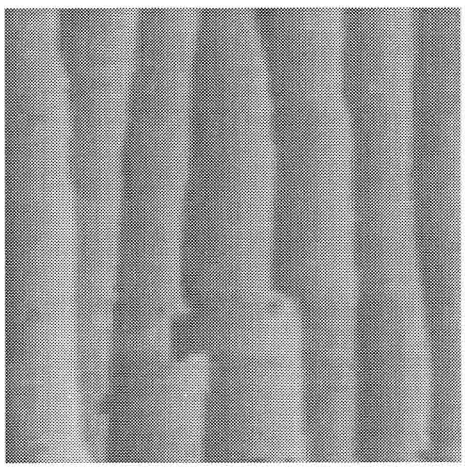

Fig. 7 AFM image of Si(111) treated with oxygen-free 2.5% NH_4OH (DOC : 5 ppb) at 0°C for 20 min. Dissolved oxygen is removed by the addition of sulfite ion. The scan areas are 1 x 1 μm^2.

FTIR measurements were conducted to investigate the termination of Si(111) surface treated with 2.5% NH_4OH with and without dissolved oxygen. For the measurements, silicon sample itself was used as a prism for internal reflection (100 times), and infrared light was p-polarized.

The sharp absorption band due to terrace monohydride indicates that Si(111) is atomically flattened in 2.5% aqueous ammonia, both with and without dissolved oxygen, as shown in Fig. 8. The full width at half maximum of the spectrum of Si(111) (2.8 cm^{-1}) treated with 2.5% aqueous ammonia with oxygen (DOC:**8 ppm**) is larger than that (2.3 cm^{-1}) treated with 2.5% aqueous ammonia without dissolved oxygen (DOC:**5 ppb**). According to the work about the linewidth of terrace modes on hydrogen-terminated Si(111),[17] the full width at half maxima of terrace mode is a good measure of the homogeneity of the surface. Hence, these FTIR spectra show that dissolved oxygen reduces the homogeneity, i.e., flatness of Si(111). This is in good agreement with the surface observations by AFM shown above.

To see the relation between dissolution process and flattening process, we measured the dissolution rate of Si(111) in 2.5% aqueous solutions with and without dissolved oxygen. The rate was determined from the analysis of H_2 molecules evolved during the dissolution of silicon, according to the following reaction[18]; $Si + 4H^+ \rightarrow Si^{4+} + 2H_2$

The amount of H_2 can be precisely measured by the use of gas chromatography. In our experiments, the detection limit of H_2 is about 0.1 n mol, equivalent to sub-monolayer amount of Si.

From the measurement of H_2, the dissolution rate of Si(111) in 2.5% aqueous ammonia containing dissolved oxygen (DOC:**8 ppm**) was determined to be 19.4. nm/min. In 2.5% aqueous ammonia without dissolved oxygen (DOC:**5 ppb**), the etching rate of Si(111) was determined to be 25.2 nm/min. It is now clear that dissolved oxygen impedes both flattening and dissolution process of Si(111) in aqueous ammonia solution as well as in NH_4F solution (Chapter 3).

The above results of the etching rates seem to be puzzling. One would expect that etching rate increases when the density of etch pits increases. However, this argument can stand only when the microscopic etching rate unchange by the existence of dissolved oxygen.

Our explanation for the effect of dissolved oxygen on the etching rates is as follows; The density of the etch pits on terraces is determined by two parameters. One is a step flow rate, the other is the nucleation rate of etch pits. Dissolved oxygen is assumed to affect both of these by initiating etch pits and decreasing the step flow rate. In the etching of Si(111) in weakly alkaline solution, the

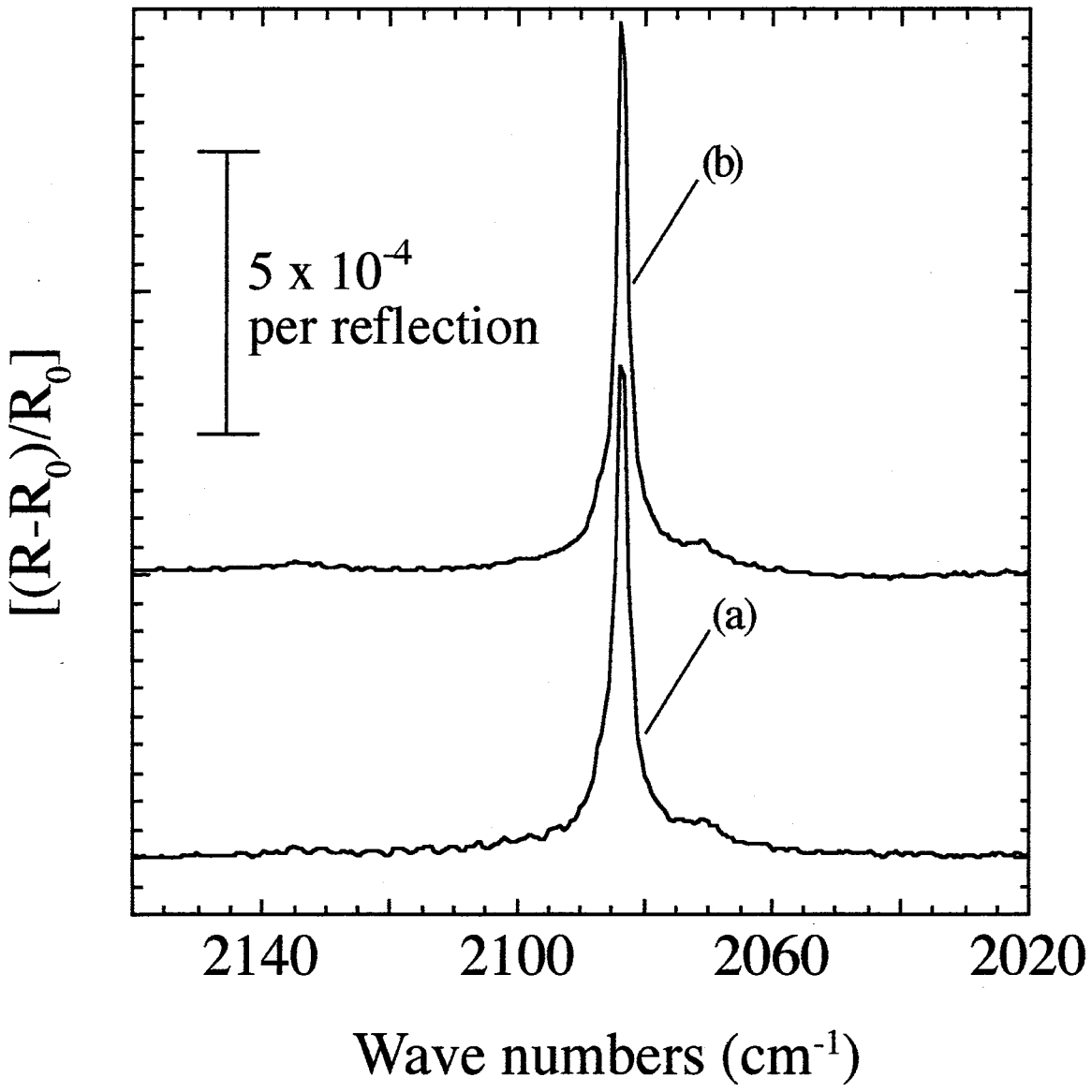

Fig. 8 ATR-FTIR spectra of Si(111) surfaces treated in 2.5% NH_4OH solutions with (a) and without (b) dissolved oxygen, respectively. Dissolved oxygen was removed by the addition of sulfite ion.

increase in step flow rate by removing oxygen is larger than an increase in etching rate due to the initiation of etch pits by the presence of dissolved oxygen. The decrease of step flow rate may be ascribed to the oxidation of kink sites by dissolved oxygen. This can be supported by the experimental fact that the etching rate of thermal oxide is smaller that bulk silicon in aqueous ammonia solutions.[19)]

The effect of dissolved oxygen onto surface morphology is less pronounced in weakly alkaline solutions than in water. In fact, Watanabe et al. showed that Si(111) become atomically roughened in water containing dissolved oxygen (DOC 4 ppm). On the other hand, our result showed that Si(111) can be atomically flattened in 2.5% NH_4OH solution containing dissolved oxygen. The ability of these etchants to etch oxide probably causes the difference in the flattening processes in the etchants. This reasoning can be supported by the previous results that, in weakly alkaline solutions, SiO_2 can be etched[19)], while SiO_2 cannot be easily etched in water.[20)]

4.3.1.3 Surface observations of Si(111) treated with strong alkaline solutions (pH=14)

The surface structure of Si(111) treated with strong alkaline solutions (pH=14) is very different from that treated with water (pH=7) and alkaline solutions (pH=12), as shown below.

Fig. 9 shows AFM images of Si(111) surfaces treated in 1M NaOH solution without dissolved oxygen for 1 min (Fig. 9 (a)) and 10 min (Fig. 9(b)). These images show that, in strong alkaline solutions, Si(111) surface cannot be atomically flattened even when dissolved oxygen is absent. This markedly contrasts with the results in the former section that Si(111) can be atomically flattened in weakly alkalien solutions without dissolved oxygen.

On the Si(111) surfaces treated with 1M NaOH solution, many etch pits exist and they increase in size with the treatment time. The shape of etch pits is almost hexagonal. According to the work of kinetic Monte Carlo simulation by Flidr et al,[14] the etching rate of monodydride step is estimated to be comparable to that of dihydride step, while, in 2.5% NH_4OH solution without dissolved oxygen, the etching rate of monohydride step is lower than that of dihydride step by two orders of magnitude. The density and size of the etch pits increased as the treatment time was extended.

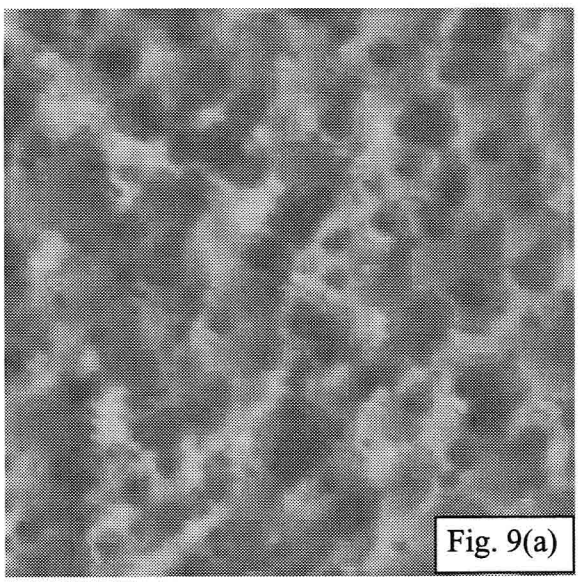

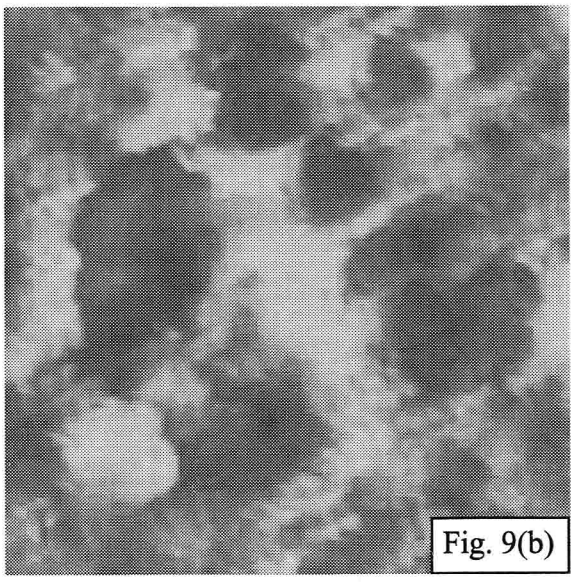

Fig. 9 AFM image of Si(111) treated in 1M NaOH at room temperature where dissolved oxygen is removed by the addition of sulfite ion (DOC: 5 ppb) for 1min (a) and 10min (b). The scan areas are 1 x 1 μ m^2. The samples used is n-Si(111) slightly misoriented in the direction of [11$\bar{2}$].

To investigate the difference in surface conditions treated with strong alkaline solution and that with weakly alkaline solution, FTIR measurements of the surface were performed. The spectra of Si(111) surface treated with 1M NaOH solution with and without dissolved oxygen for 1 min are shown in Fig. 10. There are three points to be noted. First, the spectra indicate that dissolved oxygen reduces the homogeneity of the surface. This is because the full width at half maxium (FWHM) of the terrace modes (2082.5 cm^{-1}) of the surface treated with 1M NaOH solution with dissolved oxygen (5.7 cm^{-1}) is larger than that treated with 1M NaOH solution without dissolved oxygen (4.3 cm^{-1}).[17]

Second, Si(111) treated with 1M NaOH solution is partially oxidized, because the peaks due to oxidized Si-H species in 2200-2300 cm^{-1} [21] are present. On the contrary, the surface treated with 2.5% NH_4OH solution Si(111) was not oxidized . The oxidized Si-H species can be reduced by removing oxygen, as shown in Fig. 11. Lewerenz et al. previously reported that Si(111) in NaOH solution is hydrogen-terminated, not oxidized.[22] Their result is contrary to our result. There is an evidence to support our observation. Baum et al. reported that the contact angle of silicon surface treated with 2M KOH is 62 degrees,[23] while above 80 degrees is the contact angle of silicon surface treated with fluoride-containing solutions.[24] These results about contact angle of the surface indicate that the degree of the hydrogen-termination of the surface treated with strong alkaline solutions is less that that treated with HF solutions.

Third, dissolved oxygen reduces the selectivity of the etching because removal of dissolved oxygen leads to an increase of the density of monohydride step and a decrease of the density of dihydride step, as seen in Fig. 11.

In conclusion, AFM and FTIR measurements of Si(111) surface showed that the surface condition of Si(111) after the treatment with strong alkaline solutions is different from those treated with weakly alkaline solutions. In the later section (4.3.3), it will be shown that the change of surface condition with pH strongly affects the etching process.

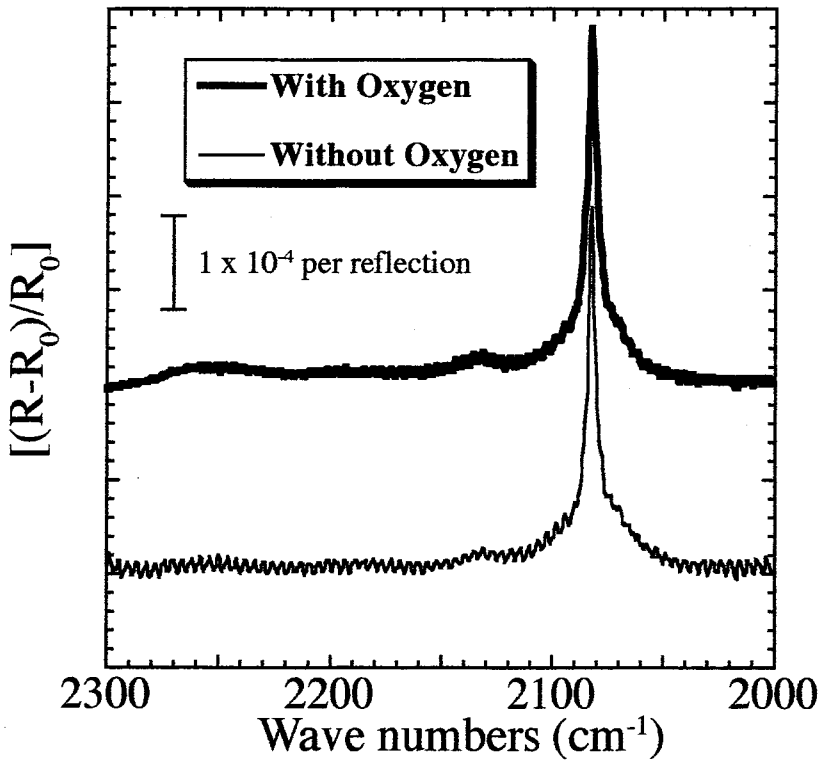

Fig. 10 ATR-FTIR spectra of Si(111) surfaces treated with 1M NH_4OH solution, with (bold line) and without (plain line) dissolved oxygen. Dissolved oxygen was removed by the addition of sulfite ion.

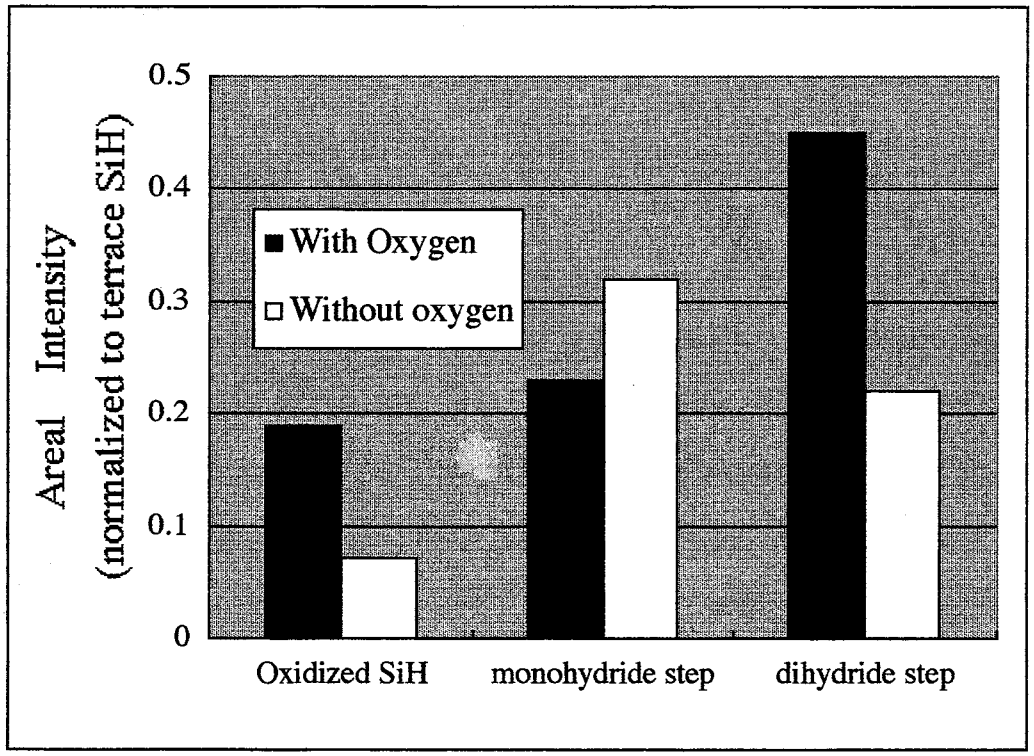

Fig. 11 Effect of dissolved oxygen onto surface species of Si(111) calculated from the ATR-FTIR spectra shown in Fig. 10. These areal intensities were nomalized to terrace Si-H intensities .

4.3.2 *In-situ obervation of the etching process of Si(111) in chemically deoxygentated water*

Time sequences of AFM images of the Si(111) surface observed by in situ AFM measurements in chemically deoxygenated water are shown in Fig. 12. To shorten the imaging time, the vertical scan range was restricted to one fourth of the horizontal scan range. Under the conditions, it took 12.5 s to take one image. On the Si(111) surface are seen atomically smooth terraces separated by the bilayer steps. A small particle (probably an impurity) seen at the center of the images was used to obtain a guide against thermal drift during AFM measurements. Using the guide, one can observe that steps flow slowly at an average rate of about 8 + 1 nm min^{-1}. This value is in good agreement with the etching rate estimated from the hydrogen evolution rate as will be shown in the following section. In the in situ AFM measurements, the surface structure of Si(111) may be affected by the laser beam of the AFM system, which cause photoetching. However, we think that the effect of photo-etching is very small, because the imaged area was shadowed by the monitoring tip. Furthermore, in the *in-situ* AFM measurements, we did not observed etch pits on the terraces, which were formed by the photoetching.

In situ AFM observation of Si(111) in water has been done by Ando et al. and reported that Si(111) surface is hardly etched. Their result is contrary to our result. This is probably because dissolved oxygen is not completely removed. Dissolved oxygen is very harmful to the dissolution of Si for the etching in water.[20] Our successful observation of step flow rate in water is ascribable to the utilization of sulfite as the chemical deoxygenator.

By observing the morphological changes, information on the dissolution process of the Si(111) surface in water can be obtained. On the images of Fig. 2, three representative structures of the steps are marked with A, B and C. Step A has no kinks, step B is connected with a pre-existing etch pit, and step C has kinks on it. The lowest flow rate is observed for step A, suggesting that the dissolution preferentially proceeds through kink sites and pits. This leads to flat surfaces. The similar behavior has been reported by Kaji et al. for the dissolution of Si(111) in fluoride containing solutions using *in situ* STM.[25] They estimated an average step flow rate of 15 nm min^{-1} for the mono-hydride step with kinks, which corresponds to step C in Fig. 2. In the recent paper,[26] Ye et al. reported that the step flow rate of monohydride step is 28 nm min^{-1}. The faster step flow rate in their measurements is ascribed to the effect of HF_2^- ions in solution. In addition, the etching in water is more selective than that in 40% NH_4F. The step flows faster in

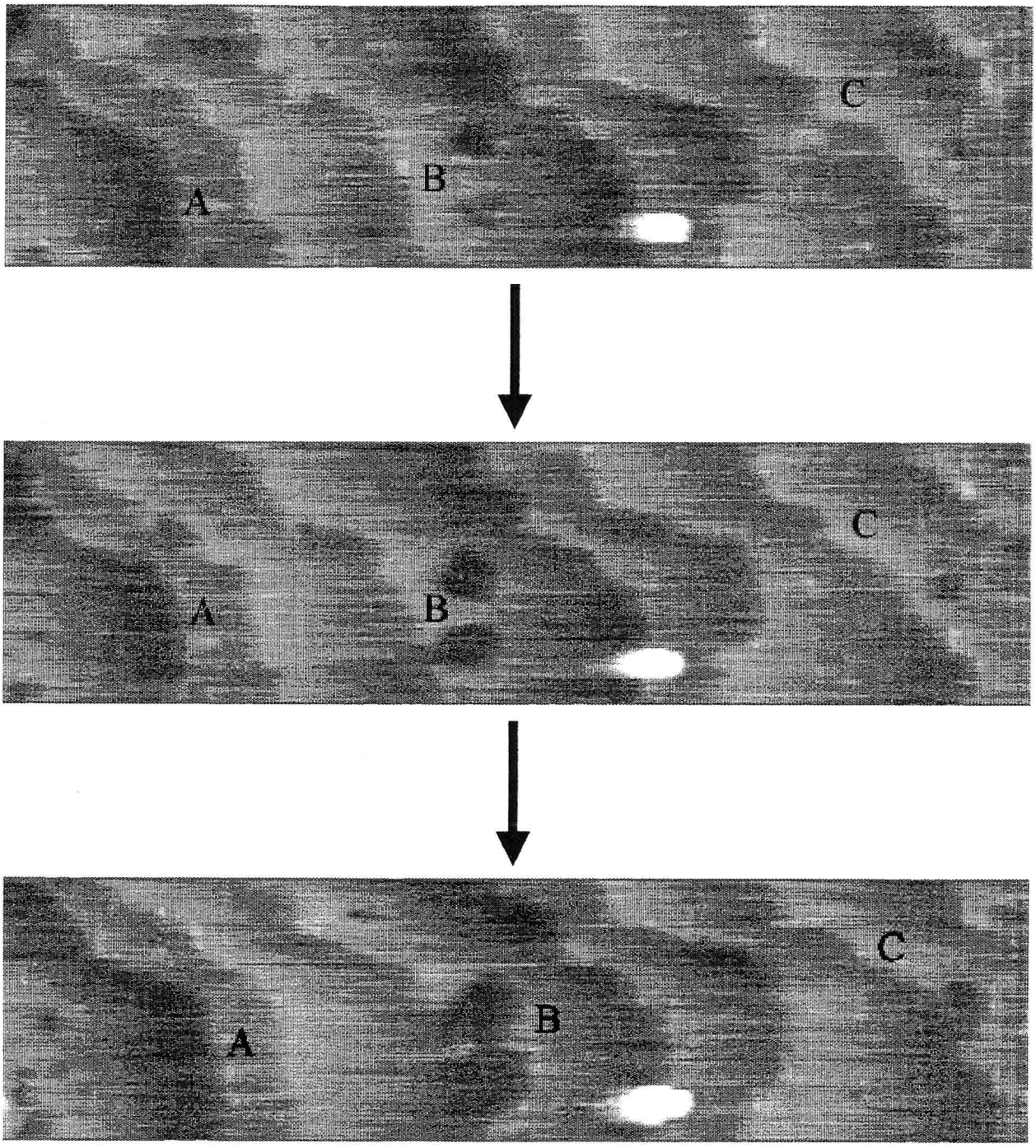

Fig. 12 Time sequences of images of the p-Si(111) surface in contact with water containing 0.05 mol/dm^3 ammonium sulfite. Si(111) surface was misoriented in the direction of [11$\bar{2}$] at an angle of 0.37°, and it was atomically flattened by 40% NH_4F, prior to the observation. The images are recorded every 25 s, at the scan rate of 10.2 Hz. The frames are 350 x 87.5 nm^2.

40% NH_4F than in water by a factor of 3, while the (macroscopic) etching rate in 40% NH_4F is higher than that in water by more than one order of magnitude. The higher etching rate compared with the step flow rate in 40% NH_4F solution is probably due to the formation of etch pits in 40% NH_4F at open circuit potential.[26] In fact, Ye et al. observed the etch pits formation on Si(111) surface

The step flow rate in water at pH 6.6 is slower than the rate reported in a 1 mol dm^{-3} NaOH solution by a factor of only 10,[6] although the concentration of OH^- differs by about 7 orders. The result suggests that pure water is a fairly good etchant if oxygen is removed, and that OH^- ion is not a etching species in water.

In summary, we succeeded in observing the *in situ* AFM images of the Si(111) surface while it is dissolving in oxygen-free water. The result is useful to deepen the understanding of the mechanism of wet etching and surface flattening processes of silicon, especially under the conditions free from the effects of oxygen.

4.3.3 *Effect of pH and dissolved oxygen onto etching of Si in the solutions without fluorine*

To establish the etching mechanism in the solutions with fluorine, I measured the pH dependence of the etching rate without dissolved oxygen (DOC: < 5 ppb). Figs.13 and 14 show the pH dependence of the etching rates of p- and n-Si(111) in the non-fluoride containing solutions without dissolved oxygen, respectively. Though the absolute values are a little different, the pH dependence of p- and n- Si(111) is quite similar and found that the pH dependences of the etching rates are different among three pH range, $6 < pH < 10$, and $10 < pH < 12$. I will, therefore, discuss the etching process in these three pH range, respectively.

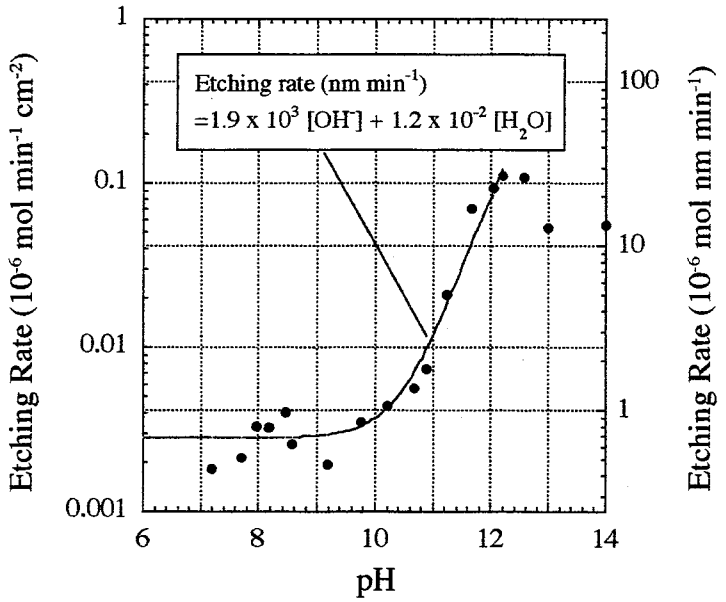

Fig. 13 pH dependence of etching rates of p-Si(111). Dissolved oxygen in the solutions was removed by the addition of sulfite ion.

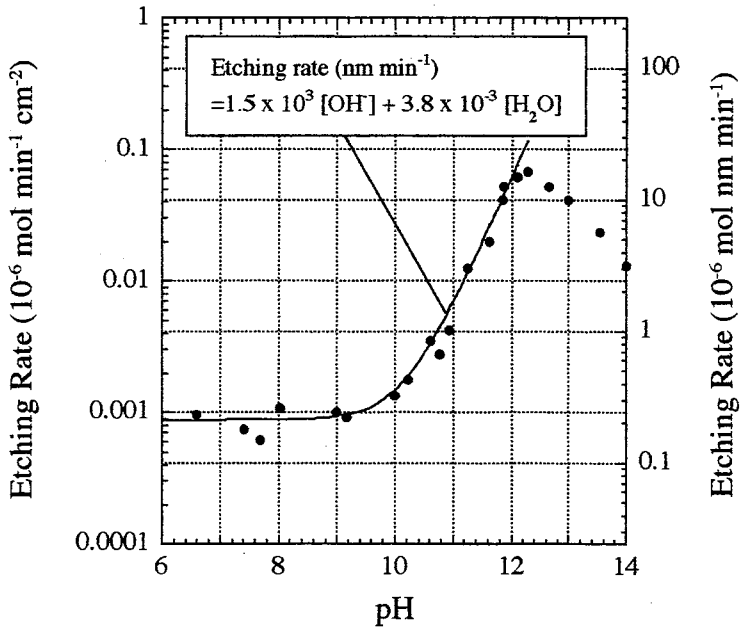

Fig. 14 pH dependence of etching rates of n-Si(111). Dissolved oxygen in the solutions was removed by the addition of sulfite ion.

In the pH range 6 to 10, the etching rate of Si(111) is almost constant. This result cannot be explained by the previous proposal for the etching mechanism of Si in water that OH^- is a main reactant in the etching of Si in water.[1), 11), 27)] It is now clear that H_2O, not OH^- ion, is responsible for the etching of Si(111) in this pH range.

Then, I made a new etching mechanism for the etching of Si(111) in this pH range (Fig. 15). In Fig. 15, the etching of dihydride (i.e. kink) is described because the etching of kink sites is predominant over the etching of other sites.[3), 6)] In our model, the reaction of H_2O with silicon atoms is supposed to be bimolecular nucleophilic substitution reaction via a five coordinated transition state, according to the works in the field of the chemistry of Si,[28)] and the rate determining step (RDS) is considered to be the reaction (1) in Fig. 15. In RDS, H_2O breaks a Si-Si backbond, not a Si-H bond, because the bond energy of Si-Si (226 kJ mol^{-1}) is much smaller than that of Si-H bond (318 kJ mol^{-1}).[29)] After the breakage of the Si-Si bond, OH^- is attached to the dihydride because the Si atom of dihydride is partly postively charged due to the difference in the electronegativity between Si (2.20) and H (1.90).[29)] Once the Si-OH bond is formed through the reactions (1), reaction (2) and (3) rapidly proceed. The reason for this is that oxygen must withdraw the electron from Si-Si back bond due to the large electronegativity of oxygen.

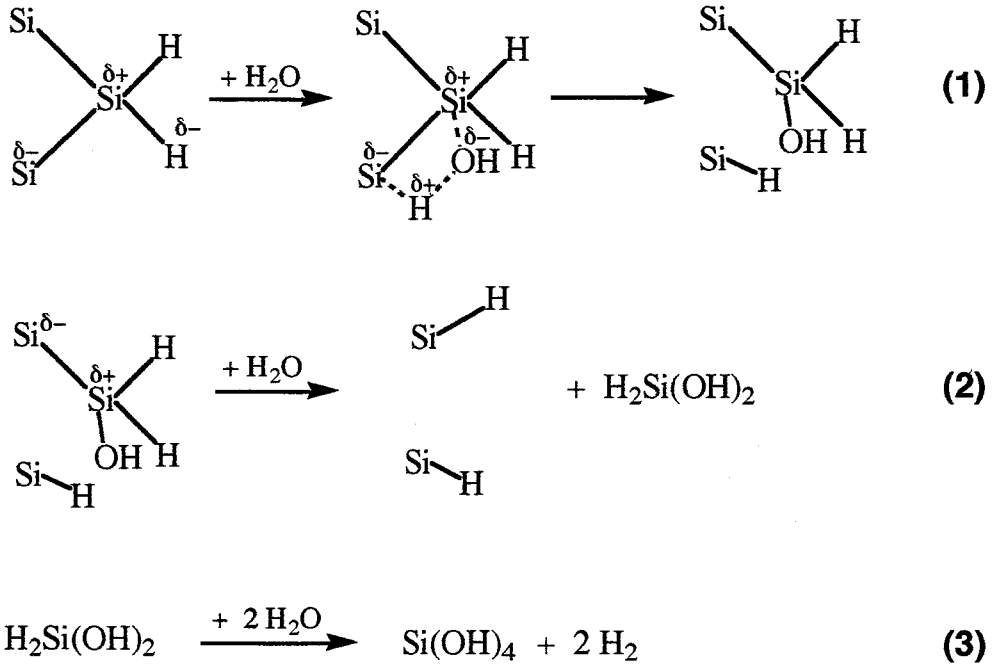

Fig. 15 The overall reaction scheme for the etching of Si in water. (In this reaction scheme, the etching of kink site (i.e. dihydride) are decribed.)

In contrast to the pH dependence in the pH range 6 to 10, the etching rate of Si(111) in the pH range from 10 to 12 is proportional to the first order of OH^- concentration. This indicates that OH^- ion is a major etching species in the pH range from 10 to 12.

Then, I made a reaction scheme for the etching of Si in this pH range (Fig. 16). Reactions (1) and (2) are assumed to be RDS, and OH^- is involved in RDS. In the reactions (1) and (2), OH- reacts with a Si atom so that Si-OH bond is formed and, simultanesouly the Si-Si back bond is broken. This is because the breakage of Si-Si bond is energetically more favorable that that of Si-H. On the contrary, Baum et al. proposed that, in RDS of alkaline etching, Si-H bond, in place of Si-Si bond, should be broken in the RDS, based on the their kinetic isotope experiment that the etching rate of Si in KOH is larger than that in KOD solution by a factor of 2.1 (its ideal value is 3.2).[30] To take their result into account, I proposed that the observed kinetic isotope effect is for the hydrogen evolution reaction from $H_2Si(OH)_2$ in the reaction (4). In general, hydrogen evolution reaction cannot proceed fast without catalyst such as Pt, Pd. In conclusion, reactions (1) and (2) as well as (4) are supposed to be RDS in alkaline etching of Si.

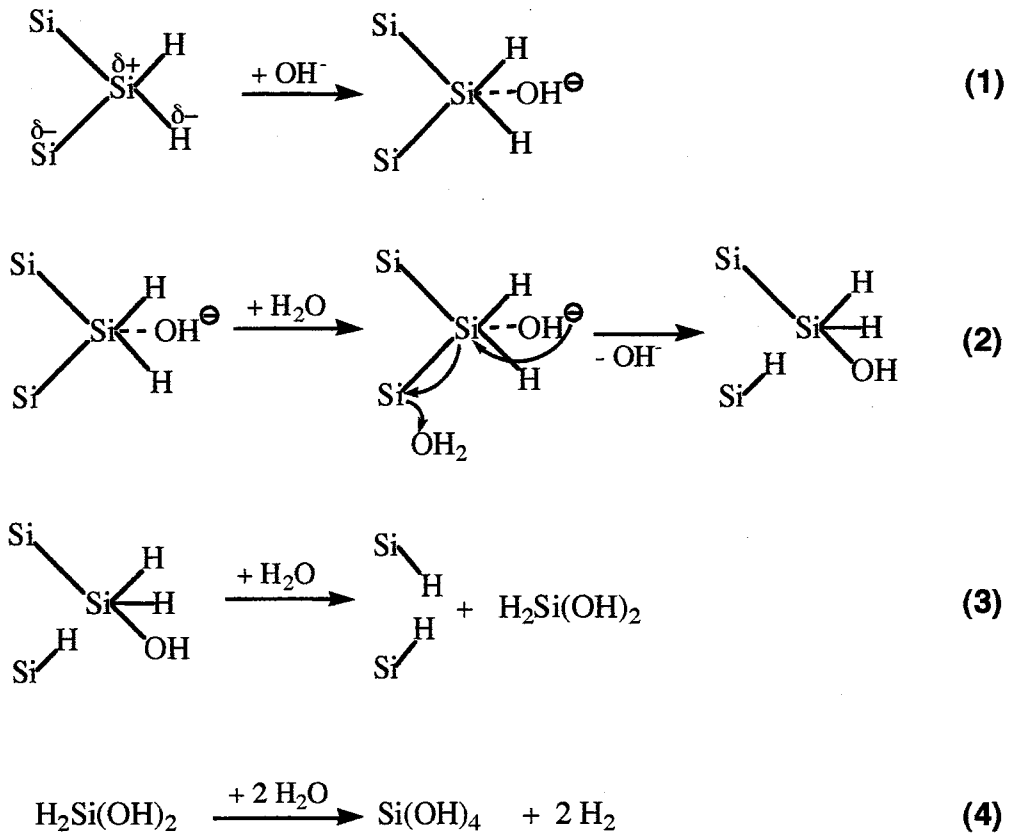

Fig. 16 The overall reaction scheme for the etching of Si in alkaline solutions. (In this reaction scheme, the etching of kink site (i.e. dihydride) are decribed.)

In the pH range from 6 to 12, we derived the equation for the etching rate of Si(111) with an assumption that etching rate of Si in water is propotional to the first order of [OH^-], as shown in the insets of Figs. 13 and 14:

Etching rate (nm min^{-1}) = 1.5 x 10^3 [OH^-] + 3.8 x 10^{-3} [H_2O] (p-Si(111))

Etching rate (nm min^{-1}) = 1.9 x 10^3 [OH^-] + 1.2 x 10^{-2} [H_2O] (n-Si(111))

From the coefficients in the above equations, one can see that the ability of H_2O to dissolved silicon is smaller than that of OH^- by about six orders of magnitude. This big difference in the ability to etch Si can be expalined by the difference in nucleophilicity of H_2O and OH^-. Ritchie et al. quantitavely investigated the effect of nucleophile on the reaction rate of bimolecular nucleophilic substitution (S_N2) of carbon. They revealed that the reaction rate with OH^- is larger than that with H_2O, by about six orders of magnitude. The work of Ritchie et al. strongly supports our etching mechanism of Si in water and alkaline solutions because, in many cases, the reaction of silicon is shown to be also S_N2 like carbon.

Unlike the pH dependence of the etching rate of Si in the pH range from 10 to 12, the etching rate in the pH range from 12 to 14 decrease with pH. The cause of decrease in etching rate in this pH range is due to the formation of $Si-O^-$ which can be formed above pH = 12 because the last pKa of $Si(OH)_4$ is 12.

The $Si-O^-$ plays two roles in the decrease of the etching of Si in the pH range above 12. First, the negative charge on increases the electron density of Si-Si backbond so that the rate of nucleoohilic attack of OH^- to Si-Si backbond is lower than that to Si-Si backbond to Si-OH. Second, $Si-O^-$ induces the formation of Si-O-Si which was supported by the FTIR observation of the surface in the previous section (4.3.1.3). The reaction scheme for the oxidation is shown in Fig. 17. The Si-O- do a nucleophilic attack to a adjacent a silicon atom. This can be suppored by the work by Holmes et al. for the condensation reaction of $Si(OH)_4$ that is initiated by OH^-. The reaction shown in Fig. 17 should mainly occur at dihydride sites. The reason for this is that OH^- can more easily attack Si atom at dihydride sites, and that $Si-O^-$ can more easily change its configuration to do the nucleophilic attack to the adjacent Si atom. The formation of Si-O-Si decreases the etching rate of silicon surface because it was shown that the etching rate of thermally grown SiO_2 is smaller than that of bare silicon, in alkaline solutions.[19] We have discussed the pH effect on the etching rate of Si and surface structures.

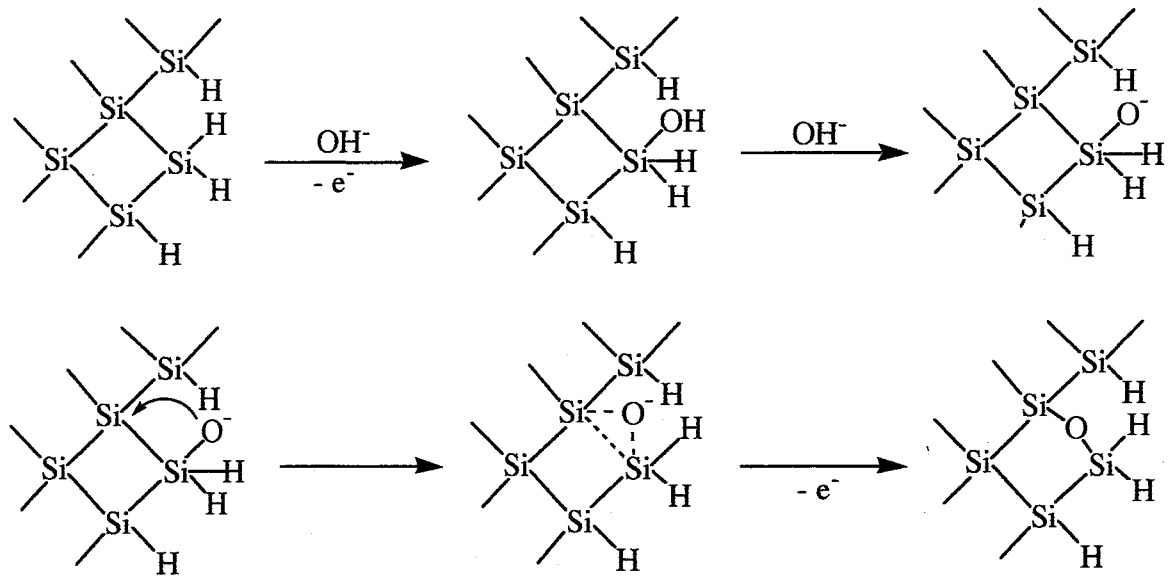

Fig. 17 The oxidation of Si(111) surface by OH^- ion in strong alkaline solutions. The reaction scheme is for the oxidation of kink sites where the oxidation more easily occurs.

Then, the effect of dissolved oxygen onto the etching process will be discussed here. In Fig. 18, the etching rate of Si(111) in the non fluoride-containing solutions in the pH range from 6 to 14 with and without dissolved oxygen. The figure clearly demonstrates that dissolved oxygen reduces the etching rate of Si(111) in the pH range from 6 to 14.

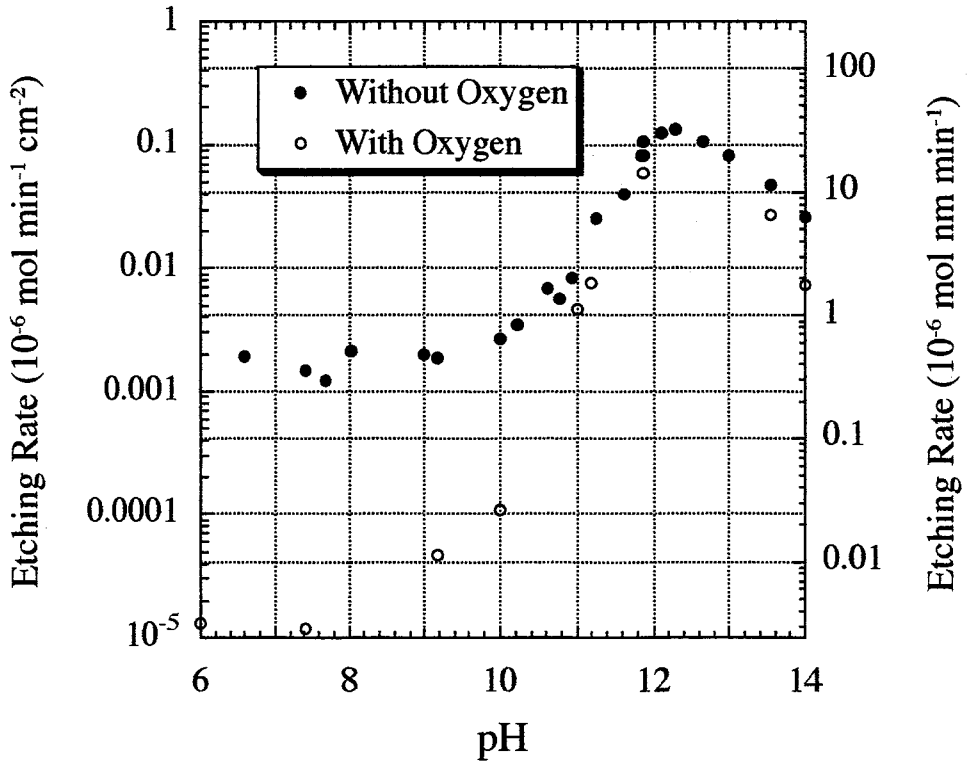

Fig. 18 Etching rate of p-Si(111) in the non fluoride-containing solutions with and without dissolved oxygen (Dissolved oxygen concentration is 8 ppm and below 5 ppb, respectively).

In the pH range from 6 to 10, the effect of dissolved oxygen is significant as shown in Fig. 18, compared with in the pH range above 10. The etching rate of silicon in water without dissolved oxygen is larger than that with dissolved oxygen by two orders of magnitude. The etching rate with dissolved oxygen is in good agreement with that reported by Morita et al.[19] The reason for the decrease of the etching rate by dissolved oxygen is that dissolved oxygen in water oxidized silicon surface. In fact, Morita et al. showed that in ultra pure water the rate of oxidation of silicon surface increases as dissolved oxygen increases.[20] Hence, oxidation of Si surface by dissovled oxygen is assumed to decrease the etching rate of Si in water. The reason for this is that the bond energy of Si-O-Si (368 kJ/mol) is much larger that that of Si-Si (226 kJ/mol), which should be broken during the etching. Besides, Watanabe et al.[4] clearly demonstrated that the flattening of Si(111) in water is prohibited by dissolved oxygen, and that the surface become oxidized in the presence of dissolved oxygen. From the results by Morita et al.[20] Watanabe et al.[4] and the result by us (Fig. 10), it can be concluded that dissolved oxygen in water affects both the flattening and etching of Si due to the low etching rate of SiO_2 in water.

In the pH range above 10 to 12, the etching rate of Si in the solutions with dissolved oxygen is proportional to $[OH^-]^2$. This is in good agreement with a recent work.[31] The etching rates of silicon in the solutions with dissolved oxygen approach that without dissolved oxygen with increasing pH from 10 to 12. This is because the concentration of OH^- become high enough to etch the oxide that decrease the etching rate of Si surface.

In the pH range above 12, the difference in the etching rates with and without dissolved oxygen increases with a increase in pH. This is due to the increases in the density of Si-O-Si. The increase in pH leads to the increase in the density of Si-O-Si bond by OH^- as shown above. The Si-O-Si bond is assumed to initiate further oxidation by dissolved oxygen because it gives a strain and polarization to adjacent silicon atoms.

4.4 Conclusion

In this chapter, I have discussed the etching mechanism of Si(111) in water and alkaline solutions. It was revealed that etching rate critically depends on two parameters, that is, pH and dissolved oxygen of the solutions of Si(111) surface. These two parameters also affect the morphology and composition of Si(111) surface. Based on the above results, I could present plausible mechanims for the etching of Si in water and alkaline solutions. In these solutions, the major etching speceis vary with pH of the solution. The results presented in this chapter can lead to the atomistic understanding of the etching of Si and the precise control of Si surface in ULSI processing, I believe.

[References]

1) G. S. Higashi and Y. J. Chabal: Handbook of Semiconductor Wafer Cleaning Technology, ed. W. Kern (Noyes Publications, New Jersey, 1993), p. 433.

2) S. A. Campbell, S. N. Port, and D. J. Schiffrin: Semiconductor Micromachining, Vol. 2, ed. S. A. Campbell and H. J. Lewerenz (John Wiley & Sons Ltd., Chichester, 1998), p. 1.

3) S. Watanabe, N. Nakayama, and T. Ito: Appl. Phys.Lett. **59** (1991) 1458.

4) S. Watanabe, Y. Sugita: Surf. Sci. **327** (1995) 1.

5) P. Allongue, H. Brune, and H. Gerischer, Surf. Sci. **275** (1992) 414.

6) P. Allongue, V. Costa-Kieling, and H. Gerischer, J. Electrochem. Soc. **140** (1993) 1009.

7) T. Komeda, K. Namba and Y. Nishioka: Jpn. J. Appl. Phys. **37** (1998) L214.

8) G. J. Pietsch, U. Köhler, and M. Henzler: J. Appl. Phys. **73** (1993) 4797.

9) P. Jakob and Y. J. Chabal: J. Chem. Phys. **95** (1991) 2897.

10) S. Watanabe, K. Horiuchi, and T. Ito: Jpn. J. Appl. Phys. **32** (1993) 3420.

11) K. Usuda and K. Yamada: J. Electrochem. Soc. **144** (1997) 3204.

12) A. Ando, K. Miki, T. Shimizu, K. Matsumoto, Y. Morita, and H. Tokumoto, Jpn. J. Appl. Phys. **34** (1995) 715.

13) A. Ando, K. Miki, T. Shimizu, K. Matsumoto, Y. Morita, and H. Tokumoto, in *Forces in*

Scanning Probe Methods, H.-J. Gütherodt, Editor, p. 537, Kluwer Academic Publishers, Netherlands (1995).

14) J. Flidr, Y.-C. Huang, T. A. Newton, and M. A. Newton, J. Chem. Phys. **108** (1998) 5542

15) C. P. Wade and C. E. Chidsey, Appl. Phys. Lett. **71** (1997) 1679.

16) H. Fukidome and M. Matsumura, Appl. Surf. Sci. **130-132** (1998) 146.

17) P. Jakob, Y. J. Chabal, and K. Raghavachari, Chem. Phys. Lett. **187** (1991) 325.

18) E. D. Palik, O. J. Glembocki, and I. Heard, Jr., J. Electrochem. Soc. **134** (1987) 404.

19) K. T. Lee and S. Raghavan, Electrochem. Solid State Lett. **2** (1999) 172

20) M. Morita, T. Ohmi, E. Hasegawa, M. Kawakami, and M. Ohwada, J. Appl. Phys. **68** (1990) 1272.

21) G. Lucovsky, Solid State Commun. **29** (1979) 571.

22) J. Rappich, H. J. Lewerenz, H. Gerischer, J. Electrochem. Soc. **141** (1994) L187

23) T. Baum, J. Satherley, and D. J. Schiffrin, Langmuir, **14** (1998) 2925.

24) Y. Sugita and S. Watanabe, Jpn. L. Appl. Phys. **38** (1999) 2427.

25) K. Kaji,S. L. Yau, and K. Itaya, J. Appl. Phys. **78**, 5727 (1995).

26) J. H. Ye, T. H. Bok, J. S. Pan, Sam. F. Y. Li, and J. Y. Lin, J. Phys. Chem. B **103** (1999) 5820.

27) K. Endo, K. Arima, T. Kataoka, Y. Oshikane, H. Inoue, and Y. Mori, Appl. Phys. Lett. **73** (1998) 1853.

28) Rober R. Holmes, Chem. Rev. **90** (1990) 17.

29) F. A. Cottons and G. Wilkinson: Advanced Inorganic Chemistry, A Comprehensive Text, 4th ed., Jonh Wiley & Sons, Inc., New York (1987).

30) T. Baum and D. J. Schiffrin, J. Electroanal. Chem. **436** (1997) 239.

31) K. Yamamoto, A. Nakamura, and U. Hase, IEEE Transactions on Semicoductor Manufacturing, **12** (1999) 288.

Chapter 5

General Conclusion

I have studied the mechanism of wet etching of silicon surface and how to control the surface structures of silicon on an atomic scale by wet etching. To characterize the reactions on the surface from viewpoints of chemistry and physics, (electro)chemical methods and surface analysis tools were used. In this way, I clarified unclear points which previous works only from a physical viewpoint did not, as below.

I have firstly studied etching mechanisms of Si in solutions with and without fluorine from the chemical viewpoint. For the etching in the solution with fluorine, I proposed a new etching mechanism that HF_2^- is a main reactant. Our proposal is more plausible than a previous proposal that OH^- is a common and main reactant in the solutions with and without fluorine. For the etching in the solution without fluorine, I clarified that OH^- is a main reactant only in alkaline solution, and that, in water, H_2O is a main reactant. Furthermore, it was revealed that the reactivity of the above reactants decreases in the order; $OH^- > HF_2^- >> H_2O$.

I have studied the surface morphology formed in the solutions to add the physical viewpoint onto the above study from the chemical viewpoint. It was revealed that the selectivity of the etchants to flatten Si(111) decreases in the order; water > NH_4F solution > alkaline solution. Further, two importants results on relative etching rates of microscopically different sites on the Si(111) surface were obtained as follows; First, the highest etching rate among the sites on the surface should be at dihydride-sites where monohydride steps are crossed each other. Second, the relative etching rates of terraces and mono- and dihydride steps can be controlled by pH, dissolved oxygen, and holes on the surface. An adjustment of these parameters enabled the formation of atomically straight dihydride steps on Si(111). This result may be useful for the formation of atomically flat Si(100) surface.

The results presented in this thesis will be useful for ULSI technologies of Si. For instance, the results can be applied for the precise control of RCA cleaning and the realization of the flattening of commercially important Si(100) surface. I believe the research with a chemical viewpoint should play a key role in a further progress on microtechnology of silicon, as well as other promising semiconductors, GaAs, SiC, and $SrTiO_3$.

List of Publication

[1] Michio Matsumura and Hirokazu Fukidome:

Enhanced Etching Rate of Silicon in Fluoride Containing Solutions at pH 6.4

J. Electrochem. Soc. **143** (1996) 2683-2686.

[2] Hirokazu Fukidome, Teruhisa Ohno, and Michio Matsumura:

Analysis of Silicon Surface in Connection with Its Unique Electrochemical and Etching Behavior

J. Electrochem. Soc. **144** (1997) 679-683.

[3] Hirokazu Fukidome and Michio Matsumura:

Electrochemical Study of Atomic-Flattening Process of Silicon Surface in 40% NH_4F Solution

Appl. Surf. Sci. **130-132** (1998) 146-149.

[4] Hirokazu Fukidome and Michio Matsumura:

A Very Simple Method of Flattening Si(111) Surface at an Atomic Level Using Oxygen-Free Water

Jpn. J. Appl. Phys. **38** (1999) L1083-1084.

[5] Hirokazu Fukidome, Michio Matsumura, Tadahiro Komeda, Kenji Namba, and Yasushiro Nishioka:

***In-situ* AFM Observation of Dissolution Process of Si(111) in Oxygen-Free Water at Room Temperature**

Electrochem. Solid-State Lett. **2** (1999) 393-394.

Acknowledgements

I would like to express my sincerest gratitude to Professor Michio Matsumura and Associate Professor Teruhisa Ohno for their guidance and encouragement during the work at Research Center for Photoenergetics of Organic Materials. I am grateful to Professor Yoshihiro Nakato, Professor Hikaru Kobayashi, Associate Professor Kei Murakoshi, Research Assistant Tetsushi Imanishi, and Research Assistant Noriko Wada for their kind advices and helpful discussions.

I would also express his thanks to the people who collaborated with him during the work; Mr. Maeda, Miss. Mizuta, Mr. Hirota, Mr. Sawada, and Mr. Fahd, and other students of Research Center for Photoenergetics of Organic Materials.

I would express my special thanks to the researchers at other research institutes in Japan; Dr. Namba, Dr. Komeda, Dr. Nishioka (Texas Instruments), Dr. Watanabe and Mr. Sugita (Fujitsu Laboratories) , Dr. Hara (Electrotechnical Laboratory), Mr. Harada, Dr. Niwa and Dr. Morita (Matsushita Electronics), Mr. Osada and Hanzawa (Morita Chemicals) for their valuable discussions, continuous encouragement, their supply of high-quality wafer and LSI-grade reagents.

I would like to express my hearty thanks to the researchers in foreign contries; Dr. Baum (Germany), Dr. Allongue (Pierre and Marie Curie University, Paris) and Dr. Chabal (Bell Laboratories, New Jersey) for their continuing interest, their valuable discussions. I will never forget good memories that I discussed my work with them in USA and Japan.

Lastly, but not least, I cannot help expressing my hearty thanks to my family for their assitance and continuous encouragement.

Then, I have just finished the thesis.

Hirokazu Fukidome

The Year 2000